SAHC

Earthquake-Induced Damage Assessment in an Historical Bell-tower Based on Long-term Dynamic Monitoring Data

Pier Francesco Giordano

Portugal | 2017

ADVANCED MASTERS IN STRUCTURAL ANALYSIS
OF MONUMENTS AND HISTORICAL CONSTRUCTIONS

Master's Thesis

Pier Francesco Giordano

Earthquake-Induced Damage Assessment in an Historical Bell-tower Based on Long-term Dynamic Monitoring Data

Universidade do Minho

UNIVERSITAT POLITÈCNICA DE CATALUNYA

Education and Culture

Erasmus Mundus

ADVANCED MASTERS IN STRUCTURAL ANALYSIS
OF MONUMENTS AND HISTORICAL CONSTRUCTIONS

Master's Thesis

Pier Francesco Giordano

Earthquake-Induced Damage Assessment in an Historical Bell-tower Based on Long-term Dynamic Monitoring Data

This Masters Course has been funded with support from the European Commission. This publication reflects the views only of the author, and the Commission cannot be held responsible for any use which may be made of the information contained therein.

Portugal | 2017

DECLARATION

Name:	Pier Francesco Giordano
Email:	pierf.giordano@gmail.com

Title of the Msc Dissertation:	Earthquake-induced damage assessment in an historical bell-tower based on long-term dynamic monitoring data
Supervisors:	L.F. Ramos, F. Ubertini
Year:	2016/2017

I hereby declare that all information in this document has been obtained and presented in accordance with academic rules and ethical conduct. I also declare that, as required by these rules and conduct, I have fully cited and referenced all material and results that are not original to this work.

I hereby declare that the MSc Consortium responsible for the Advanced Masters in Structural Analysis of Monuments and Historical Constructions is allowed to store and make available electronically the present MSc Dissertation.

University:	University of Minho
Date:	17/07/2017
Signature:	_____

This page is left blank on purpose.

Acknowledgements

Many people have been involved indirectly or directly in the realization of this thesis that could not be accomplished without their help. In particular, I would like to express my gratitude to:

- My supervisor, Professor Luís F. Ramos for addressing this work with enthusiasm and his precious advice;
- My co-supervisor, Professor Filippo Ubertini and Doctor Nicola Cavalagli for the hospitality received in the beautiful Perugia, for sharing with me their information about the bell tower of San Pietro, and the constant exchange of ideas;
- Doctor Maria Giovanna Masciotta for the kindness, the dedication, the continuous encouragement and the recommendations;
- PhD student Alban Kita for hospitality in Perugia and the help received during the in situ testing;
- PhD students Maria Pia Cocci, Alberto Barontini, Rafael Ramírez Álvarez de Lara and Engineer Georgios Marios Zarmpoutis for their help and interest;
- My friends and colleagues of SAHC and ELARCH for their continuous support and the good times in Guimarães. A special thank goes to Sonia Guerra Pinto and Luis Palomino;
- My friends and colleagues of SAHC, Angelique C. Kamsteeg and Angelo Leggio, that are always source of inspiration, even if distant;
- The local and visiting professors during my coursework in the Universitat Politècnica de Catalunya, in particular Professor Pere Roca and Professor Luca Pelà, for the great passion and knowledge that have shared with all students of SAHC;
- The SAHC consortium for providing me a scholarship to participate in the program;
- To my family for their unconditional support.

This page is left blank on purpose.

Abstract

San Pietro bell tower belongs to a monumental complex of exceptional historical, cultural and artistic value and it is considered one of the landmarks of Perugia. The preservation of this structure has been considered an essential issue over centuries and even more nowadays. For this reason, a permanent vibration-based structural health monitoring (SHM) system able to detect anomalies in the structural behavior by means of statistical process control tools has been installed in the tower. The SHM is based on the continuous identification of the natural frequencies of the bell tower and on the analysis of their variations. Environmental parameters, i.e. temperature and humidity, are monitored as well.

The aim of this work is to present the results of the most recent investigations carried out on the monument after 2016-2017 Central Italy earthquakes whose effects were perceived also in Perugia. In particular, visual inspection, Ambient Vibration Test (AVT) and sonic tests were performed. The visual survey allowed verifying the information about the monument and constituted the first step of the in-situ investigation. The objective of AVT was to detect any changes in the dynamic properties of the tower following the earthquakes as well as better characterize its mode shapes by means of a higher number of sensors. Twelve uniaxial piezoelectric accelerometers, placed at four different heights, were used. The results are compared with those of previous dynamic investigations. Sonic tests are carried out on the shaft of the tower in correspondence and their results of the test are used to characterize the materials of the monument.

Based on the material and geometrical survey, a Finite Element model of the tower was implemented. Following, a sensitivity analysis is executed with the purpose of evaluating the influence of material properties on numerical outcomes. The results of the sensitivity analysis are used for model calibration. The mechanical parameters of masonry are updated until the dynamic behavior of the model is consistent with the experimental data. Not only the natural frequencies are compared but also the mode shapes by means of the MAC values. The model is calibrated twice, considering the pre- and post- earthquakes conditions.

Furthermore, data related to natural frequencies and temperature are presented and the acquiring and processing methodology is described. The correlation between data is studied separately in pre- and post-earthquakes conditions. In particular, the correlation between natural frequencies themselves and between natural frequencies and temperature is investigated. The dependences of the dynamic parameters on the environmental factors is studied by means of AutoRegressive output with an eXogenous input (ARX) models. The comparison of results in pre- and post-earthquakes conditions allows detecting modifications in the structural behavior of the tower.

This page is left blank on purpose.

Resumo

A torre sineira de San Pietro pertence a um complexo monumental de excepcional valor histórico, cultural e artístico e é considerado um dos pontos de referência de Perugia, Itália. A preservação desta estrutura tem sido considerada uma questão essencial ao longo dos séculos e com mais peso no período atual. Por esta razão, foi instalado na torre um sistema permanente de monitorização da condição estrutural (SHM) baseado em vibrações, capaz de detectar anomalias no comportamento estrutural por meio de ferramentas estatísticas de controlo. O SHM é baseado na identificação contínua das frequências naturais da torre e na análise de suas variações. Os parâmetros ambientais, nomeadamente a temperatura e a humidade, também são monitorizados.

O objetivo deste trabalho é apresentar os resultados das investigações mais recentes realizadas no monumento após os recentes sismos no centro de Itália, cujos efeitos foram sentidos também em Perugia. Em particular, foram realizadas inspeções visuais, ensaios de Vibração Ambiental (AVT) e ensaios sónicos. A inspeção visual permitiu verificar a informação sobre o monumento e constituiu o primeiro passo da investigação in-situ. O objetivo da AVT foi detectar qualquer alteração nas propriedades dinâmicas da torre após os sismos, além de caracterizar melhor as suas formas modais através de um maior número de sensores. Foram utilizados doze acelerómetros piezoelétricos uniaxiais colocados a quatro alturas diferentes. Os resultados são comparados com os das investigações dinâmicas anteriores. Os resultados dos ensaios sónicos foram usados para caracterizar os materiais do monumento.

Um modelo de elementos finitos da torre foi construído com base no levantamento material e geométrico. A seguir, foi realizada uma análise de sensibilidade com o objetivo de avaliar a influência das propriedades materiais sobre os resultados numéricos. Os resultados da análise de sensibilidade foram utilizados para a calibração do modelo. Os parâmetros mecânicos da alvenaria foram atualizados até que o comportamento dinâmico do modelo ficou consistente com os dados experimentais. Não só foram comparadas as frequências naturais, com também as formas modais por meio coeficientes MAC. Finalmente, o modelo foi calibrado duas vezes, considerando as condições pré e pós-sismos.

Os dados de monitorização que relacionam as frequências naturais com as temperaturas foram apresentados, assim como a metodologia de aquisição e processamento de dados. A correlação entre os dados foi estudada separadamente nas condições pré e pós-sismos. Em particular, foram analisadaa a correlação entre as próprias frequências naturais e entre as frequências naturais e a temperatura ambiente. As dependências dos parâmetros dinâmicos nos fatores ambientais foram estudadas por meio de modelos ARX. A comparação dos resultados nas condições pré e pós-sismos permitiu a detecção de modificações no comportamento estrutural da torre.

This page is left blank on purpose.

Resumen

El campanario de San Pietro pertenece a un complejo monumental de excepcional valor histórico, cultural y artístico y es considerado uno de los edificios emblemáticos de Perugia. La preservación de esta estructura ha sido considerada como una cuestión esencial durante siglos pasados y más aún en la actualidad. Por este motivo, se ha instalado en la torre un sistema permanente de vigilancia de la salud estructural (SHM) capaz de detectar anomalías en el comportamiento estructural mediante herramientas estadísticas de control. El SHM se basa en la identificación continua de las frecuencias naturales del campanario y en el análisis de sus variaciones. También se controlan los parámetros ambientales, es decir, la temperatura y la humedad.

El objetivo de este trabajo es presentar los resultados de las investigaciones más recientes realizadas sobre el monumento después de los recientes terremotos en el centro de Italia cuyos efectos se perciben también en Perugia. En particular, se realizaron inspecciones visuales, pruebas de vibración ambiental (AVT) y pruebas sónicas. La inspección visual permitió verificar la información sobre el monumento y constituyó el primer paso de la investigación in situ. El objetivo de AVT fue detectar cualquier cambio en las propiedades dinámicas de la torre después de los terremotos, así como caracterizar mejor sus formas de modo mediante un mayor número de sensores. Se utilizaron doce acelerómetros piezoeléctricos uniaxiales, colocados a cuatro alturas diferentes. Los resultados se comparan con los datos obtenidos de las investigaciones dinámicas anteriores. Los resultados de la prueba sonica se utilizan para caracterizar los materiales del monumento.

Se implementó un modelo de elementos finitos de la torre sobre la base del levantamiento material y geométrico, con el cual se realiza un análisis de sensibilidad con el fin de evaluar la influencia de las propiedades de los materiales sobre los resultados numéricos Los resultados del análisis de sensibilidad se utilizan para la calibración del modelo. Los parámetros mecánicos de la mampostería se actualizan hasta que el comportamiento dinámico del modelo sea consistente con los datos experimentales. No sólo se comparan las frecuencias naturales, sino también las formas de modo mediante los valores MAC. El modelo se calibra dos veces, considerando las condiciones pre y post terremotos.

Además, se presentan datos relacionados con las frecuencias naturales y la temperatura y se describe la metodología de adquisición y procesamiento. La correlación entre los datos se estudia por separado en condiciones pre y post terremotos. En particular, se investiga la correlación entre las propias frecuencias naturales y entre las frecuencias naturales y la temperatura. Las dependencias de los parámetros dinámicos sobre los factores ambientales se estudian mediante la salida AutoRegressive con modelos de entrada eXógena (ARX). La comparación de los resultados en condiciones pre y post terremotos permite detectar modificaciones en el comportamiento estructural de la torre.

This page is left blank on purpose.

Riassunto

Il campanile di San Pietro fa parte di un complesso monumentale di eccezionale valore storico, culturale e artistico ed è considerato uno dei simboli di Perugia. La sua conservazione è stata una tematica di primaria importanza nei secoli passati e lo è a maggior ragione al giorno d'oggi. Per questo motivo, un sistema permanente di monitoraggio strutturale (SHM) a base vibrazionale è stato installato nella torre. Esso è in grado di rilevare anomalie nel comportamento della struttura mediante strumenti statistici di controllo. Il SHM si basa sulla continua identificazione delle frequenze naturali del campanile e sull'analisi delle loro variazioni. Anche parametri ambientali, quali temperatura e umidità, vengono monitorati.

L'obiettivo di questo lavoro è presentare i risultati delle più recenti indagini che sono state condotte sul monumento dopo terremoti dell'Italia Centrale del 2016-2017. In particolare, sono stati effettuati: ispezione visiva, prove ambientali di vibrazione(AVT) e prove soniche. L'ispezione visiva ha permesso di avvalorare le informazioni sul monumento e costituisce il primo passo dell'indagine in situ. Le finalità delle AVT sono molteplici, in particolare individuare eventuali cambiamenti nelle proprietà dinamiche della torre a seguito dei terremoti così come di caratterizzare meglio le sue forme modali con un numero maggiore di sensori. Sono stati impiegati dodici accelerometri piezoelettrici uniassiali, posizionati a quattro diverse altezze. I risultati sono stati confrontati con quelli delle precedenti indagini dinamiche. Per quanto riguarda i test sonici, i risultati sono stati utilizzati per caratterizzare i materiali che del monumento.

Sulla base delle suddette indagini si è costruito un modello ad Elementi Finiti della torre. Una volta ottenuto il modello, si è eseguita un''analisi di sensibilità allo scopo di valutare l'influenza delle proprietà di materiali sui risultati numerici. I risultati dell'analisi di sensibilità sono poi utilizzati per la calibrazione del modello. I parametri meccanici della muratura vengono aggiornati finché il comportamento dinamico del modello non è coerente con i dati sperimentali. Non solo le frequenze naturali vengono confrontate, ma anche le forme modali tramite i valori MAC. Il modello viene calibrato due volte, considerando le condizioni pre- e post-terremoti.

Inoltre, vengono presentati i dati relativi a frequenze naturali e a temperature e viene descritta la metodologia di acquisizione e di elaborazione. La correlazione tra i dati viene studiata separatamente prima e dopo lo sciame sismico. In particolare, viene analizzata la correlazione tra frequenze naturali e tra frequenze naturali e temperatura. Le dipendenze dei parametri modali sui fattori ambientali sono studiati per mezzo di modelli "Auto Regressive output with an eXogenous input (ARX)". Il confronto dei risultati nelle condizioni di pre- e post-terremoti consente di individuare eventuali modifiche nel comportamento strutturale della torre.

This page is left blank on purpose.

Table of Contents

1. Introduction

1.1 Motivation for Structural Health Monitoring

Historical masonry constructions are susceptible to damages related to the effects of soil settlements, weathering, human actions, deformations, material degradation and exceptional events. In particular, in seismic countries like Italy, the vulnerability of cultural heritage with respect of earthquake is one of the major concern. Maintenance and conservation are an expensive duty for the owner and the availability of automated methods of damage assessment is definitely attractive. The aim of Structural Health Monitoring (SHM) is to give, on continuous basis, a diagnosis of the state of a structure, at the level of constituent materials, different elements, and the assembly of them. The possibility of recording and processing data over time allow detecting the occurrence of damages as well as providing a prognosis about their evolution. In the field of heritage structures, SHM systems are related to both dynamic (e.g. natural frequencies) and static parameters (e.g. inclinations of pillars). In all cases, environmental sensors are indispensable to distinguish the alterations in the structural behavior due to exogenous agents (e.g. environmental action) from alterations due to endogenous agents (i.e. occurrence of damages). The dynamic monitoring allows to estimate and track the modal properties of the structure by measuring its vibrational response in operational conditions, under the effect of wind, traffic, and micro tremors. The observation of static parameters, such as deformations, strains, tilts, and displacements complement the Structural Health assessment.

1.2 Objectives and Methodology

The examined structure is the monumental San Pietro bell tower in Perugia, Central Italy. Starting from the year 2013, the bell tower has been object of dynamic investigations and numerical modeling by a team of researchers of the Department of Civil Engineering of the University of Perugia. The purpose of these studies was the installation of a permanent vibration-based structural health monitoring (SHM) system able to detect anomalies in the structural behavior by means of statistical process control tools such as control charts. The continuous system was activated in December 2014. The SHM is based on the continuous identification of the natural frequencies of the bell tower and on the analysis of their variations. The fluctuations of the modes are associate to daily and seasonal variations of environmental parameters and freezing conditions. A series of violent seismic events hit Central Italy in the period August 24th 2016 and January 18th 2017. Their effects were perceived also in Perugia, even if only minor damages occurred.

The objective of this work is to present the most recent investigations carried out on the monument. The results obtained will be used to detect any modifications in the structural behavior after the last earthquakes. Starting point is the collection of information of the structure, namely structural history and literature review. Any investigation on the monument depends on the accurate knowledge of this information. In situ investigation were carried out in May 2017 with the aim of corroborating the available information and gathering new one. The new study implied: (1) visual survey; (2) Ambient Vibration Tests (AVT); and (3) Sonic Test. In particular, the results of the AVT will be used to detect any changes in the dynamic properties of the tower following the 2016-2017 earthquakes as well as better characterize its mode shapes by means of a higher number of sensors. The results of sonic tests will be used to characterize the materials of the monument. Based on both old and new data, a numerical model of the tower will be implemented and tuned with the purpose of evaluating the influence of material properties on numerical outcomes. The mechanical parameters of masonry will be updated until the dynamic behavior of the model is

consistent with the experimental data. Not only the natural frequencies will be compared but also the mode shapes by means of the MAC values. The model will be calibrated twice, in pre-earthquakes and post-earthquakes conditions. Moreover, the data from continuous monitoring will be analyzed, i.e. natural frequencies and temperature. The results are useful to figure out which variables present the highest dependency and to detect any modifications is those relationships. Based on the correlation analysis, the dynamic response of the monument will be modelled by means of ARX models.

1.3 Organization of the thesis

The thesis is composed of eight chapters as follows:

- **Chapter 1** introduces the work and it is composed of motivations for SHM, the presentation of the case study, the objectives of the thesis, methodology, and the outline of the dissertation;
- **Chapter 2** presents the essential theoretical tools on which monitoring of historical masonry constructions is based. The first section introduces the chapter. The second section gives a general overview about the effects of earthquakes on masonry constructions, with a special focus on towers and bell towers. The structure and the function of Structural Health Monitoring systems applied to heritage constructions are described in the third part of the chapter. In particular, dynamic investigations techniques and the effects of environmental factors on the dynamic behavior are addressed in section fourth and fifth sections, respectively. The automated damage detection method is described in the sixth section. It was used during previous work on the studied bell tower. The following section concerns complementary nondestructive tools for SHM, such as sonic pulse velocity test and QMI method. The chapter ends with conclusions;
- **Chapter 3** presents the structural history of the monument, from the construction to the most recent restauration. The third part is devoted to describing the recent previous studies on the bell tower. First, the geometrical and material characteristics of the monument are delineated. The remaining section of the chapter illustrates: the dynamic characterization of the tower, the continuous structural health monitoring system, the monitoring data analysis, the numerical modeling. The collected data are used as starting point for the dissertation work and as comparison with the new results. Conclusions end the chapter;
- **Chapter 4** presents the new in situ studies that were conducted on San Pietro bell tower between the days 15th and 19th of May. They consist of visual inspection and survey of the metal structure, AVT, and sonic tests. The visual inspection is at the base of the MQI method that is applied on the masonry of the shaft. Moreover, the metal structure is studied, since it was neglected in previous studies. The constitutive elements are identified and the geometric survey is carried out and. The collected information allow evaluating the effect of this element on the tower. Conclusions are given at the end;
- **Chapter 5** presents the numerical modelling to San Pietro bell tower. A FE model with 3D elements is built in the software FX+ and the analysis is carried out with the software DIANA v.10.1. Structural eigenvalue analyses are performed. Following, a sensitivity analysis is executed. The results of the sensitivity analysis are used for model calibration. An additional topic of this chapter is the study of the influence of the metal structure on the dynamic properties of the bell tower by means of an additional numerical model. The chapter is ended with conclusions;
- **Chapter 6** presents the long-term monitoring data recorded in San Pietro bell tower and their preliminary elaboration. In the first section, the data related to natural frequencies and temperature are presented and

the acquiring and processing methodology is described. Then, the correlation between data is studied separately in pre- and post-earthquakes conditions. Finally, the dynamic response of the monument is modelled by means of ARX models.

- **Chapter 7** contains the main conclusions of the work and proposals for future studies.

This page is left blank on purpose.

2. State of the art

2.1 Introduction

Historical masonry construction are susceptible to damages related to the effects of soil settlements, weathering, human actions, deformations, material degradation and exceptional events. In particular, in seismic countries like Italy, the vulnerability of cultural heritage with respect of earthquake is one of the major concern. The maintenance and conservation are an expensive duty for the owner and the availability of automated methods of damage assessment is definitely attractive. These techniques allow the condition-based maintenance instead of the scheduled or breakdown operations. Typically, the monitoring of historical masonry structures can be divided in four steps: (1) data collection, including historical, geometrical, topographic and damage survey, materials characterization, numerical analysis; (2) health monitoring plan, consisting of localization of sensors (accelerometers, temperature and humidity sensors, etc.), data storage, study of the effects of environmental factors and damage triggering tools; (3) full scale survey after alarm triggering to confirm and locate damages, including dynamic survey with additional sensors; (4) local damage assessment by means of visual and complementary tests. [1]

The aim of this chapter is to present the essential theoretical tools on which monitoring of historical masonry constructions is based. Afterwards, the described techniques will be applied in the study of an historical bell tower. The structure of this chapter follows. The first section presents the chapter. The second section gives a general overview about the effects of earthquakes on masonry constructions, with a special focus on towers and bell towers. The structure and the function of Structural Health Monitoring (SHM) systems applied to heritage constructions are described in the third part of the chapter. In this context, SHM systems are related to both dynamic and static parameters. In all cases, environmental sensors are indispensable to distinguish the alterations in the structural behavior due to exogenous agents from alterations due to endogenous agents (i.e. occurrence of damages). In particular, dynamic investigations techniques and the effects of environmental factors on the dynamic behavior are addressed in section fourth and fifth sections, respectively. An automated damage detection method is described in the sixth section. It was used in previous work on the studied bell tower. The following section concerns complementary nondestructive tools for SHM, such as sonic pulse velocity test and QMI method. The chapter ends with conclusions.

2.2 Seismic behavior of historic masonry structures and bell towers

Innumerable masonry constructions typologies exist worldwide and their characteristics can significantly differ. However, it is possible to recognize recurrent damage patterns after earthquakes. They can be grouped into two main categories according to the properties of the structure, namely first mode and second mode mechanisms [2]. The first type of damages occur when the building is not able to redistribute the seismic-induced solicitations among the different structural elements, which consequently behave in an independent way. This mechanism is mostly related to the out-of-plane behavior of masonry walls, with flexural behavior and overturning. Nevertheless, it can also involve the in-plane response of structural elements, especially in the case of walls with large aligned openings or in presence of architectural elements such as arches and vaults. First mode mechanisms are due to deficiencies in connections between orthogonal walls and between walls and floors. Typical features of historical buildings, such as continuous transformations and existing damages, generate discontinuities in the masonry that promote a non-

unitary behavior of the structure and partial collapses characterized by loss of equilibrium. Good connection between perpendicular walls and between walls and floors, as well as presence devices such as tie rods, allow the collaboration among the various components of the structure. In this way, it is possible to make greater use of in-plane strength and stiffness of masonry walls. Second mode mechanisms are related to this type of performance in which the "box-like" behavior is established. However, the observation of the seismic performance of existing masonry buildings showed that rarely their behavior is characterized by a global response. The local mechanisms, in which portions of walls (macro-elements) lose their equilibrium, rotating or sliding, are much more frequent. In such mechanisms, the rigid displacements are widely prevalent on the displacement associated to deformations. [3] It is important to emphasize that the activation of a rigid mechanism is possible only in case of masonry of good quality. Otherwise, the mechanism may be preceded by the disintegration of the material, as often happens in the case of multi-layers masonry with bad connection between leaves [4].

In the case of tower and bell towers (Figure 2-1), the seismic performance depends on some specific factors that characterize the structure, expressly: slenderness, degree of connection between walls, action of shorter adjacent buildings, protruding elements (such as spire, bell-gable, and battlements), and presence of existing damages. Slenderness is a very variable parameter in historical towers. They can be considered massive constructions when limited height and thick walls characterize them. Otherwise, they can be schematized as one-dimensional structures, with cantilever behavior, when they show high level of slenderness. Good connection between walls allows the bell tower to respond as a single structure, with stiffness associate to the whole section, and not as a set of separate elements. The traditional techniques to ensure monolithic behavior are good interlocking between perpendicular walls, use of confining devices and tie rods, and construction of well-fixed floors. The presence of shorter buildings in contact with the bell tower has a great influence on its seismic performance. They limit the slenderness of the tower and constitute stiffening bodies that cause localized concentration of stresses.

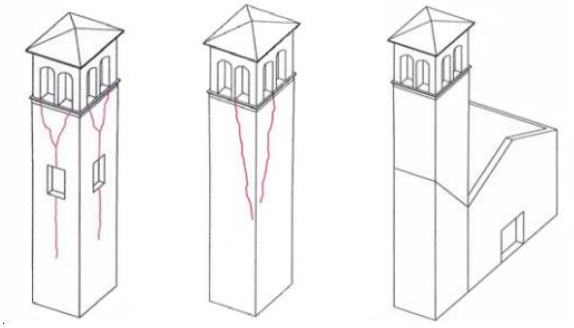

Figure 2-1 Common collapse mechanisms of bell towers [4]

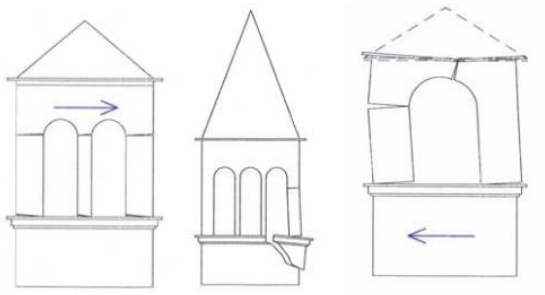

Figure 2-2 Common collapse mechanisms in belfries [4]

The belfry is one of the most delicate parts of a bell tower (Figure 2-2). Indeed, large openings and thin, slightly loaded columns that are very prone to shear failure and sliding in case of earthquake usually characterize it. Similar consideration are valid for any protruding element located at the top of the bell tower. In addition, the seismic motion amplifications that occur at the top of the bell-tower must be taken into consideration. During an earthquake, similar belfry suffer different damages depending on the interaction between seismic input, soil, basement and shaft [5].

2.3 Structural Health Monitoring systems applied to heritage constructions

The aim of Structural Health Monitoring (SHM) is to give, on continuous basis, a diagnosis of the state of a structure, at the level of constituent materials, different elements, and the assembly of them. In fact, the action of aging, environmental factors, and exceptional events such as earthquakes may alter the regular structural behavior. The possibility of recording and processing data over time allow detecting the occurrence of damages as well as providing a prognosis about their evolution. [6] SHM is a very multidisciplinary field, in which several skills (e.g. civil and electronic engineering, seismology, and computer science) and institutions collaborate together [7]. Moreover, it changes the organization of the maintenance activities by replacing planned and periodic actions with performance-based maintenance. From the economic point of view, structures with SHM system have constant maintenance costs and reliability, whereas structures without SHM system are characterized by increasing maintenance costs and reduction in reliability with time [6].

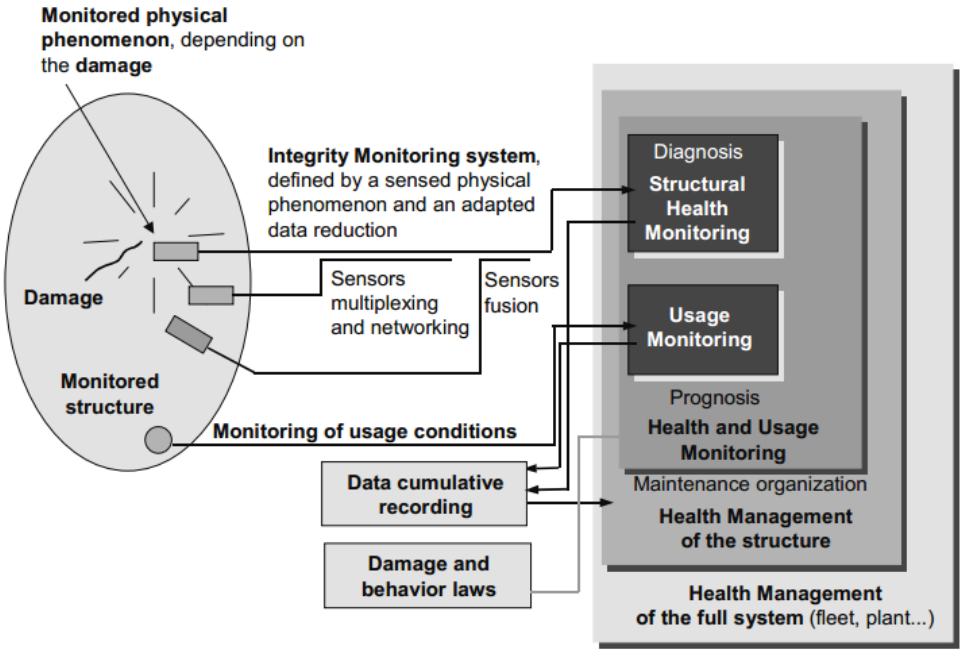

Figure 2-3 Principle and organization of a SHM system [6]

The structure of a typical SHM system follows (Figure 2-3). The first part is the Integrity Monitoring system, which is defined by the monitored physical phenomenon and by the physical phenomenon that the sensor measures to generate the signal sent to the acquisition and storage sub-system. A group of equivalent sensors form a network. Usually, several networks are created in order to combine different types of data. The Integrity Monitoring system receives the information and uses it, together with those previously recorded, to produce a diagnostic. The Usage Monitoring system records the operational performance of the structure. The information provided by the Integrity and Usage Monitoring systems, together with the implementation of damage and behavior models, permit to provide the prognosis and indications about the health management of the structure. SHM systems can be related to specific portions of the structures. When combined allow the heath management of the entire system. Working SHM system simpler than the one above described are possible too [6].

In the field of heritage structures, SHM systems are related to both dynamic and static parameters. In all cases, environmental sensors are indispensable to distinguish the alterations in the structural behavior due to exogenous agents (e.g. environmental action) from alterations due to endogenous agents (i.e. occurrence of damages). The dynamic monitoring allows to estimate and track the modal properties of the structure by measuring its vibrational response in operational conditions, under the effect of wind, traffic, and micro tremors. Automated procedures for modal parameters estimation, mostly based on the Stochastic Subspace Identification (SSI) method, are indispensable to reduce the data processing time. The observation of static parameters, such as deformations, strains, tilts, and displacements complement the Structural Health assessment [8].

At the state of the art, SHM systems are only able to alert the occurrence of damage and eventually localize it but they do not provide sufficiently accurate information about the extent and the type of damage. These methods, which can only inform whether the damage is present or not in the whole structure, are called Global Heath methods. Other types of investigations are necessary to precisely localize the damage and characterize it. These second category of techniques are called Local Heath monitoring methods [9]. Local methods include visual inspections or NDT [1].

SHM is particularly indicated in the case of cultural heritage, where the need of minimum intervention often limit the range of usable techniques for structural characterization. Moreover, SHM may be used as control tool during and after the completing of consolidation works to assess the evolution and the effectiveness of the interventions. Within the methodology proposed by ICOMOS/ISCARSAH in “Recommendations for the Analysis, Conservation and Structural Restoration of Architectural Heritage” [10], made of (1) anamnesis, (2) diagnosis, (3) therapy and (4) control, SHM is the main support of phases (2) and (4). [8]

2.4 Dynamic investigations on historical structures

2.4.1 Objectives

Historical structures can be object of two groups of dynamic investigations, which are indeed interconnected operations: (1) dynamic identification and (2) dynamic monitoring. Both activities have numerous aims. Dynamic identifications are performed in order to: (1) estimate the dynamic properties of the structures (natural frequencies, mode shapes, damping factors); (2) tune numerical models; (3) evaluate the level of interconnection between the different parts of the construction; (4) identify critical structural weakness; (5) investigate the relations between major damages and overall structural response; (6) assess the effectiveness of repairing operations by studying the dynamic parameters before and after the interventions; (7) monitor the state of the structure before (diagnosis) and after the intervention (post-intervention control); (8) to select the optimal configuration of permanent sensors. Dynamic monitoring, not only allows to evaluate the modal characteristic of the structures and to calibrate numerical model, but also permit to achieve to following objectives: (1) follow the evolution with time of the modal parameters; (2) study the influence of environmental action; (3) capture the structural behavior in concomitance of exceptional events (earthquakes); (4) monitor the state of the structure during strengthening operations; (5) implement a long term maintenance program [11] .

2.4.2 Equipment

The tools for in situ modal identification can be divided in three groups, namely: (1) excitation mechanisms, (2) response transducers, and (3) data acquisition system [12].

Shakers, impulse hammers, and drop weight systems are the excitation mechanism used commonly in civil engineering. Shakers can transmit large forces and are mostly used to investigate the stationary dynamic behavior of structures. Usually, the use of shakers is expensive and implies limitations in the use of the structure. Three types of shakers exist, i.e. mechanic, electro-hydraulic, and electro-magnetic shakers. Hammers are used with light/medium structures, e.g. in the fields of mechanical engineering, and provide accurate results. The characteristics of the impulse depend on the mass of the head, the type of tip, and the velocity of the impact. A sensor measures the impact forces. The drop weight method is similar to the hammer one, but allow a better control of the test and to apply higher energy. A excitation mechanism is not always necessary, as in the case of Ambient Vibration Test (AVT), where the structural response is measured in service conditions [12].

Response transducers are devices able to convert a physical quantity into proportional electric signals that are sent to the data acquisition system. In civil engineering structures, response transducers based on accelerations, i.e. accelerometers, are preferred for practical reasons. Common types of accelerometers are piezoelectric accelerometers, piezoresistive and capacitive accelerometers, and force-balance accelerometers [12].

The Data AcQuisition system (DAQ) registers the signals in discrete time domain. Typically, the data received must be conditioned before they can be process to obtain the desired modal information. For instance, a low-pass filter must be used to eliminate components of the signal with frequency higher than a certain minimum value close to the Nyquist frequency (anti-aliasing filter). In fact, two signals at high and low frequencies respectively can produce the same registered signal. The Nyquist frequency is defined as the maximum frequency value beyond which the signal contents cannot be correctly represented in discrete form. Once the signal has been acquired, digital computer processing is needed [12].

2.4.3 Identification techniques

General classification

Several identification methods to determine the modal parameters of a structure are available. They can be classified in three groups: (1) input-output techniques, in which the input excitation is controlled and the structural response is measured; (2) output-only techniques, in which only the response is measured; (3) free vibration techniques, in which an initial deformation is imposed in the systems and then it is quickly released. Input-Output techniques aim at estimating the Frequency Response Function (FRF) or the Impulse Response Functions (IRF), either in the time of in the frequency domain. This class of methods can be classified according to the type of formulation, number of degree of freedom, type of estimates and number of inputs and outputs. Output-only identification techniques, also called Operational Modal Analysis (OMA), allow measuring the modal properties of a system under ambient or operational conditions. They are particularly useful in the case of large civil engineering structures, in which the application of artificial input may be complex. Output-only algorithms are classified according to the type of data they use, i.e. frequency or time domains. Frequency domain methods are

computationally simpler than time domain methods but have difficulty in identifying natural frequencies close in value. In general, there is no absolute best modal identification method. In general, the most suitable one will depend on the specific type of application [12]. In this section, special attention is given to two well know Output-only dynamic identification techniques, namely: Frequency Domain Decomposition (FDD) method and Stochastic Subspace Identification (SSI) method. The former is a frequency domain method, the latter a time domain one. Anyway, before starting describing the methods, the definition of FRF is given.

Frequency Response Function (FRF)

For a Multiple Degree of Freedom System, the Frequency Response Function (FRF) is a complex function defined in the modal space as ratio between the spectrum of the response $Q(\omega)$ and the spectrum of the excitation force $P(\omega)$:

$$H(\omega) = \frac{Q(\omega)}{P(\omega)} \qquad 2\text{-}1$$

Theoretically, it is possible to compute the FRF, $H_{(i,j)}(\omega)$, once the response time history $y(t)$ in the i degree of freedom and the excitation time history $u(t)$ on the j degree of freedom are recorded:

$$H_{(i,j)}(\omega) = \frac{Y_i(\omega)}{U_j(\omega)} \qquad 2\text{-}2$$

where $Y_i(\omega)$ and $U_j(\omega)$ are the Fourier transform of the response and of the excitation signals, respectively. In practice, because the data are discrete in time with spacing Δt, the FRFs are computed as estimation of real values by means of the relations (the superscript ^ indicates estimate):

$$\widehat{H}_{(i,j)}(\omega) = \frac{\hat{S}_{(i,j)}(\omega)}{\hat{S}_{(j,j)}(\omega)} \qquad \text{and} \qquad \left|\widehat{H}_{(i,j)}(\omega)\right|^2 = \frac{\hat{S}_{(i,i)}(\omega)}{\hat{S}_{(j,j)}(\omega)} \qquad 2\text{-}3$$

where $\hat{S}_{(i,j)}(\omega)$ are the cross-spectra density functions between the excitation and the response, and $\hat{S}_{(i,i)}(\omega)$ and $\hat{S}_{(j,j)}(\omega)$ are the Power Spectra Density (PSD) functions of the response and of the excitation, respectively,

In the context of output-only techniques, the excitation is considered as a stationary Gaussian white noise stochastic process in a specific frequency interval. Therefore, the PSD function $\hat{S}_{(j,j)}(\omega)$ is considered as constant C and the second relation given in Eq. 2-3 becomes:

$$\left|\widehat{H}_{(i,j)}(\omega)\right|^2 = \frac{\hat{S}_{(i,i)}(\omega)}{C} \qquad 2\text{-}4$$

This means that the measured response y_k includes the contributions from three different sources: (1) the ambient forces, (2) the structural system and (3) the noise signals from other sources. If the assumption of white noise is not satisfied, the dominants components of frequencies associated to the input are identified in the response [12].

Frequency Domain Decomposition (FDD) technique

The basic assumptions behind the FDD method are two: (1) the resonance frequencies are well spaced in frequency and (2) the response of the system is controlled by the resonant mode shape in proximity of the resonant frequency, thus the contribution of the other modes is negligible. The method implies the Singular Value Decomposition (SVD) of the response spectral density matrix, expressed as:

$$S_y(\omega_k) = \Psi_{\mathrm{k}} \Lambda_{\mathrm{k}} \Psi_{\mathrm{k}}^{\mathrm{H}} \qquad 2\text{-}5$$

where Λ_{k} is the singular values diagonal matrix and Ψ_{k} is an orthogonal complex matrix containing the mode shape vectors. Then, the resonant peaks and the corresponding mode shape are selected by means of the coherence function $\gamma^2(\omega)$ between the response measured in two points, y_i and y_j, which is given by:

$$\gamma_{i,j}^2(\omega) = \frac{\left|\hat{S}_{y(i,j)}(\omega)\right|^2}{\hat{S}_{y(i,i)}(\omega)\hat{S}_{y(j,j)}(\omega)} \qquad 2\text{-}6$$

The coherence function ranges between zero and one and express the linearity between the measured signals and the existence of a global mode shape. High values of this function denote a strong relation between signals. The FDD method is relatively easy to apply but it meets difficulties in recognize resonance frequency with similar values [12].

Stochastic Subspace Identification (SSI) technique

The implementation of the SSI method is not trivial and requires more processing time than the FDD method. However, it permits estimating the modal parameters with great resolution. The method aims at fitting the raw times series of recorded data (data-driven Stochastic Subspace Identification, SSI-data) to a mathematical model based on the State-Space Formulation of dynamic systems. The model is defined by parameters that can be adjusted to minimize the error between the measured structural response and the predicted behavior. One of the main goal of the method is to compute the state matrix A and the output matrix C that contain the modal information needed. In general, similarly to other time domain methods, the SSI method can be formulated in a generalized form as an innovation state space formulation:

$$\begin{aligned} \hat{x}_{t+1} &= A\hat{x}_t + Ke_t \\ y_t &= C\hat{x}_t + e_t \end{aligned} \qquad 2\text{-}7$$

where the A-matrix presents the physical information, the C-matrix extracts the information that can be observed in the system response and the K-matrix presents the statistical information.

The definition of the correct number of parameters is an important aspect of the process. Indeed, a small number does not allow to model correctly the structural behavior, whereas a big number of parameters may induce large statistical uncertainties in the model. [12]

2.4.4 Modal Assurance Criteria (MAC)

The Modal Assurance Criterion (MAC) is one of the most famous tools for the quantitative comparison of modal vectors. It is used as Mode Shape Correlation Constant to measure the accuracy of the recognized mode shapes. Indeed, it is recommended comparing: (1) measured mode shapes and vectors determined by analytical models, (2) estimations of the same test modal vector identified from different excitation locations, (3) estimations of the same modal vector recognized from different identification techniques; and, (4) single mode shape before and after a modification in the structure. For complex mode of vibration, the MAC is computed as:

$$MAC(r,q) = \frac{\left|\{\psi_A\}_r^T \{\psi_X\}_q^*\right|^2}{(\{\psi_A\}_r^T \{\psi_A\}_r^*)(\{\psi_X\}_q^T \{\psi_X\}_q^*)} \quad 2\text{-}8$$

where $\{\psi_X\}_q$ is the eigenvector defining the complex damped mode of vibration, $\{\psi_A\}_r$ is the eigenvector defining the complex damped mode of vibrations, $\{\psi_X\}_q^*$ is the complex conjugate of $\{\psi_X\}_q$, $\{\psi_X\}_q^T$ is the transpose of $\{\psi_X\}_q$, $\{\psi_A\}_r^*$ is the complex conjugate of $\{\psi_A\}_r$, $\{\psi_A\}_r^T$ is the transpose of $\{\psi_A\}_r$.

The MAC ranges between zero and one. Low values mean no consistent correspondence whereas values close to unit show a consistent correspondence. However, the MAC can only show consistency, not validity. It is not able of distinguishing between systematic errors and local discrepancies. Moreover, it cannot recognize if the vectors are orthogonal or incomplete [13].

2.5 Monitoring analysis and environmental effects removal

The environmental parameters, such as temperature, ice, and humidity, demonstrated to have strong influence on the dynamic response of historical structures. [1] [11] [14] [15] These factors are expected to affect the stiffness and the boundary conditions of the system. In the case of masonry, humidity may have impact on the mass of the constructions. In addition to this, also the loading conditions are known to alter the dynamic behavior.

In the field of AVT and OMA, the environmental and loading effects should be taken into account and modeled independently of the method applied to estimate the modal properties, i.e. frequencies, modes of vibration, and damping. The model should indicate the correlation between the environmental and loading conditions and the dynamic response of the structure in order to allow the detection of damages [12].

2.5.1 Correlation coefficient

The first step in modelling the influence of exogenous factors is to study the correlation between parameters. It can be computed by means of the correlation coefficient, r_{xy}, or its square, R_{xy}^2, that is also referred as coefficient of determination. The correlation coefficient is given by:

$$\hat{r}_{xy} = \frac{\hat{R}_{xy}}{\hat{\sigma}_x \hat{\sigma}_y} \quad 2\text{-}9$$

where $\hat{R}_{xy}$ is the estimated covariance, which is expressed as:

$$\hat{R}_{xy} = \frac{1}{N-1}\sum_{k=1}^{N}(x_k - \bar{x})(y_k - \bar{y}) \quad 2\text{-}10$$

and $\hat{\sigma}_x$ and $\hat{\sigma}_y$ are the estimated standard deviations, which are expressed as

$$\hat{\sigma}_x = \sqrt{\frac{1}{N-1}\sum_{k=1}^{N}(x_k - \bar{x})^2} \quad \text{and} \quad \hat{\sigma}_y = \sqrt{\frac{1}{N-1}\sum_{k=1}^{N}(y_k - \bar{y})^2} \quad 2\text{-}11$$

The absolute values of r_{xy} can varies between zero and one. Values close to one indicates strong correlation between the two series of data. If the correlation is small, the complexity of the environmental filter can be reduced. [12]

2.5.2 Linear regression

A simple way to model the relation between environmental and modal parameters is the linear, or multi-linear, regression by means of the least squares method. Using this approach, the estimated response, $\hat{y}_k$, (e.g. the resonant frequencies) is given by:

$$\hat{y}_k = a_0 + a_1 u_{1,k}^{env} + a_2 u_{2,k}^{env} + \cdots + e_k \quad 2\text{-}12$$

where $u_{i,k}^{env}$are the environmental effects, a_i are model coefficients that can be determined by the least square method, and e_k are the residuals, that can be expresses as:

$$e_k = y_k - \hat{y}_k \quad 2\text{-}13$$

If necessary, polynomial or non-linear regressions can be adopted to increase the model efficiency. All these models are referred as static because they are not able to consider the thermal inertia of the structure, which significantly influences the dynamic response of structures. Other types of models, such as autoregressive models or dynamic models, are able to deal with this additional property [12].

2.5.3 ARX models

One example of dynamic models is the AutoRegressive output with an eXogenous input (ARX) model. The response in the instant k depends on the input for the same instant and on the evolution of the previous input and output. The estimated response is given by:

$$\begin{aligned}\hat{y}_k + a_1 y_{k-1} + \cdots + a_{na} y_{k-na} \\ = b_1 u_{k-nk}^{env} + b_2 u_{k-nk-1}^{env} + \cdots + b_{nb} u_{k-nk-nb+1}^{env} + e_k\end{aligned} \quad 2\text{-}14$$

where a_1 is the coefficient for the autoregressive part, b_1 is the coefficient for the exogenous part, na and nb are the autoregressive and the exogenous order, respectively, nk is the number of delays from input to output, and e_k is the unknown residuals. Usually, the ARX is defined according to the selected parameters na, nb and nk [12]. Finally, the selection of the best model is based on quantitative quality criteria, such as the Normalized Root Mean Squared Error (NRMSE), the Mean Squared Error, Final Prediction Error (FPE) [16].

2.6 Automated damage detection

In the field of permanent vibration-based SHM system, an automated damage detection methodology has been recently proposed by Ubertini et al. [17] [18]. It has two main purposes: (1) to remove the effects of the environmental factors from the identified frequencies and (2) to detect any changes in the dynamic parameters that may indicate the occurrence of structural damages. A fully automated SSI technique is used to extract the modal parameters from AVT. Then, the Multivariate Linear Regression (MLR) and Principal Component Analysis (PCA) techniques are combined and applied to model the environmental effects. Finally, a Novelty Analysis technique, based on control charts, is used for damage detection.

The quantities used for damage identification are contained in the residual error matrix, E, defined as:

$$E = Y - \hat{Y} \qquad 2\text{-}15$$

where Y is the $n \times N$ observation matrix (n is the number of identified frequencies and N is the number of observation) and $\hat{Y}$ is the $n \times N$ matrix of independently estimated modal frequencies by means of statistical models. In normal conditions, the matrix E contains the residual variance associated to errors in dynamic identification and to un-modeled exogenous phenomena. If damage occurs, it affects the matrix Y and it induces changes in the distribution of E. Thanks to its properties, the residual error matrix is used in Novelty Analysis to compute the T^2-statistic, which is given by:

$$T^2 = r\left(\bar{E} - \bar{\bar{E}}\right)^T \Sigma^{-1} \left(\bar{E} - \bar{\bar{E}}\right) \qquad 2\text{-}16$$

where r is a integer factor called group averaging size, $\bar{E}$ is the mean of the residuals in the subgroup of the last r observations, $\bar{\bar{E}}$ and Σ are the mean values and the covariance matrix of the residuals, respectively, estimated during the so-called *training period* in which the structure is considered in healthy conditions. The values of T^2 must be contained between statistically fixed control limits. A value of the statistical distance that is positioned outside those limits is called outliner. The limits of T^2 are defined by zero and the value corresponding to a cumulative frequency of 95% in the training period. In such a way, there is the 5% of probability to observe an outliner in healthy conditions. Contrariwise, this probability is greater than 5% if damage occurs.

2.7 Tuning of numerical models

The realization of reliable Finite Element (FE) models for historical masonry building is anything but trivial. The difficulties are related to the accurate representation of materials, geometry, and boundary conditions between the structural elements. The model calibration is aimed at creating a more accurate representation of the structure by

reducing the discrepancies between the outputs of the FE model and experimental data. The calibration process consists in modifying the parameters of the model until satisfactory results are obtained [19].

Model correlation is based on experimental investigations, namely: (1) visual analysis; (2) static tests; or (3) dynamic tests. Visual analysis is the oldest and simplest method and it is based on the localization of cracks in the real structure which are compared to numerical estimates of tensile areas. The method is susceptible to significant errors due to the difficulty in inspecting hidden parts of the structure or in the case of differential settlements or long-term creep phenomena. Static methods concern destructive and non-destructive static tests on scale laboratory models of portion of the real structure. Quantities, such as stresses, strains, and deflections are measured under controlled loading. In this way, it is possible to study the structural behavior under loads regimes that could not be applied on the actual structure, i.e. up to the failure. Nevertheless, it is difficult to study properly the global behavior of buildings. Dynamic experiments deal with the modal parameters of the structures and can be applied to both scaled laboratory models and existing structures. Controlled laboratory tests provide more accurate results because they are mostly immune to environmental effects. As for in-situ dynamic tests, the natural frequencies are considered the most suitable comparative feature for calibration because of their sensitivity to structural changes [19].

The selection of correct comparative factors and the calibration of right parameters determine the success of model tuning. The comparative factors must be of good quality and quantity. The calibration parameters must be chosen according to both parameter uncertainty and parameter sensitivity. The parameter uncertainty is determined by test on materials or by experience. The parameters sensitivity can be studied by means of sensitivity analysis. It is used to determine the changes in the model results due to a unit change in the input. Therefore, it allows selecting the most influential parameters. After that, the model calibration consists in updating the calibration parameters. The calibration parameters are strictly related to the type, quantity and quality if comparative features. For instance, calibration based on the modal parameters are useful to determine mass and stiffness of the structure, but do not provide direct information about the nonlinear behavior and ultimate capacity [19].

Various types of calibration approaches exits. They can be classified in deterministic models and stochastic models. Deterministic models assume that the model parameters are exact and known with certainty. Two common deterministic calibration methods are the manual calibration and the automated calibration. Manual calibration is mostly guided by engineering judgment but can be effective when the inaccurate parameters are not correlated. In automated calibration, parameters are modified by means of automated calibration algorithms, such as the Inverse-Eigen-Sensitivity (IES) method and the Douglas-Reid (DR) method. The implementation of stochastic models allows going beyond the limit of the deterministic approach by reaching a statistical correlation between the experimental data and the numerical results [19].

2.8 Complementary nondestructive tests for SHM

In relation to historical structures monitoring, NDT are useful in two cases: (1) before the implementation of a SHM system, when data about the structure are collected, and (2) in the last phase, once the occurrence of damage has been confirmed, to better characterize it. Those methods are particularly indicated in investigating heritage buildings when the need of minimum intervention must be satisfy. [1]

Several NDT are available, such as thermovision inspection and sonic, ultrasonic, and radar methods. Most of them come from other fields of research or were originally developed for other modern materials, such as concrete or steel. Due to the high heterogeneity of masonry, the majority of NDT can provide only qualitative data about the properties of this complex material. The best solution to very complex problem is the use of different and complementary techniques. However, the interpretation and harmonization of the results may be challenging. [20]

Due to the high number of variables that characterize masonry constructions, the accurate evaluation of the mechanical properties of this material and of its ultimate load can be achieve by mean of in situ tests. However, only qualitative method can be used when destructive techniques are not feasible, as in case of historical constructions. The Masonry Quality Index (QMI) is an innovative method that allow to estimate the mechanical properties of masonry by means of visual inspection, taking into account seven parameters and they compliance with the “rule of art”.

2.8.1 Sonic Pulse Velocity Test

Sonic Pulse Velocity Test the most commonly used wave transmission technique to investigate masonry. It is a suitable NDT to obtain qualitative information about masonry, such as internal structure of walls, damages, effectiveness of injections, and estimation of elastic properties. The method is based on the generation of a mechanical pulse in the sonic frequency range by percussion (hammer) and its collection through a receiver (unidirectional accelerometer) which can be located in different positions. The difference between the signal emitted and received can provide information about the medium it went through. Among the several parameters that characterized each wave (velocity, energy and wavelength), velocity is the property most often used in sonic testing. This velocity, $v(m/s)$, can be determined once the travel time, $t(s)$, and distance between transmitter and receiver, $d(m)$, are known. [21]

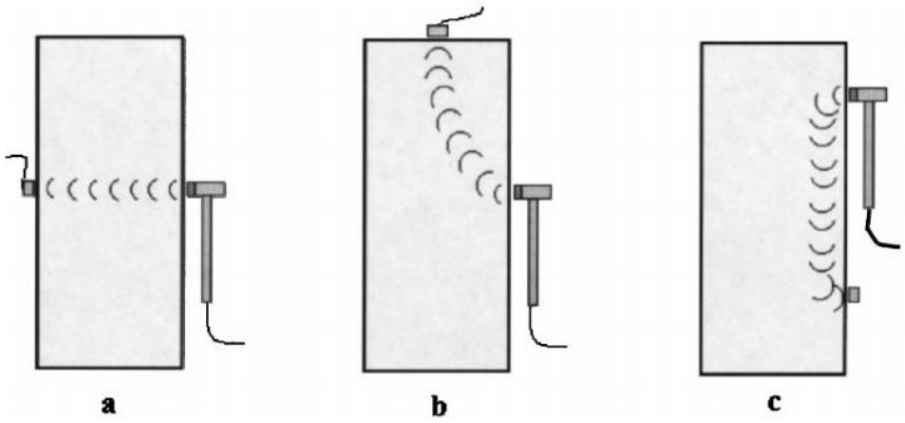

Figure 2-4 Transmission modes for sonic wave tests: a) direct, b) semi-direct, c) indirect [22]

Voids, boundaries and detachments in the materials have strong impact on the wave behavior. Sonic waves cannot pass through an air gap and therefore they have to find a path around the cavity. As a result, inhomogeneous materials show low values of wave velocity. On the contrary, compact and homogeneous materials present high values. The computed velocity is the average of the local velocities along the trajectory of the wave. Thus, it is not possible to detect the exact localization and the extent of any possible discontinuity. The transmission configuration

for sonic wave tests can be classified in direct, semi-direct or indirect according to the relative position between the impact area and the receiver. The result of the sonic test are usually represented as spatial velocity maps which allows a simple evaluation of the relative interior condition of the masonry element [22]. It is important to highlight that the wave velocity is a characteristic parameter for each masonry typology. Therefore, generalizations are not feasible [20].

The obtained results can be correlated with the compressive strength and the elastic properties of masonry. For instance, in the case of homogeneous material, analytical relations exist between the velocity of waves, the Young's modulus, E, the Poisson's ration, υ, and the density, ρ:

$$V_p = \sqrt{\frac{E(1-\upsilon)}{\rho(1+\upsilon)(1-2\upsilon)}} \qquad V_r = \frac{0.87+1.12\upsilon}{1+\upsilon}\sqrt{\frac{E}{\rho}\frac{1}{(1-2\upsilon)}} \qquad 2\text{-}17$$

where V_p and V_r are the velocities of elastic compression waves, P, and surface Rayleigh waves, R, respectively. The former can be measured by means of direct sonic test, the latter using the indirect test.

2.8.2 Masonry Quality Index (MQI)

The Masonry Quality Index (MQI) method can be used to estimate the mechanical properties of masonry [23]. Seven parameters are considered, namely stone/brick mechanical properties (SM), unit dimensions (SD), unit shapes (SS), wall leaf connections (WS), horizontal bed joint characteristics (HJ), vertical bed joint characteristics (VJ), and mortar mechanical properties (MM).

Each parameter is evaluated according to the "rules of the art" (it can be fulfilled, F, partially Fulfilled, PF, or not Fulfilled, NF) and a numerical value is assigned to it. Thus, the MQI is calculated by means of the following expression:

$$MQI = SM \times (SD + SS + WC + HJ + VJ + MM) \qquad 2\text{-}18$$

For the same wall, the MQI can have three different values depending on the loading condition: vertical loading (V), horizontal in-plane loading (I), horizontal out of plane loading (O). In case of fulfillment of all parameters, the MQI is equal to 10 for al loading conditions. In relation of the MQI computed, the masonry is classified in three categories: Category A (good behavior of masonry), Category B (behavior of average quality of the masonry), Category C (inadequate behavior of masonry). Finally, experimental curves allow to correlate the values of MQI to the mechanical parameters of masonry.

2.9 Conclusions

In this chapter, a state of the art about monitoring of historical masonry based on automated methods of damage assessment was presented. The addressed subjects cover: the effects of earthquakes on masonry constructions, the organization and the function of Structural Health Monitoring systems applied to heritage constructions, the

dynamic investigations techniques, the effects of environmental factors, an automated damage detection method, and some complementary nondestructive tools for SHM.

The seismic behavior of historical masonry buildings depends on specific factors, such as masonry quality and degree of connection between structural elements. Either a global “box-like” behavior or local mechanisms can be observed after earthquakes according to the intrinsic characteristics of the structure. In particular, in the case of tower and bell towers, the seismic performance depends on some specific factors, such as: slenderness, degree of connection between walls, action of shorter adjacent buildings, protruding elements, and presence of existing damages.

The action of aging, environmental factors, and exceptional events such as earthquakes may alter the regular structural behavior. The aim of Structural Health Monitoring (SHM) is to give, on continuous basis, a diagnosis of the state of a structure, at the level of constituent materials, different elements, and the assembly of them. These techniques allow the condition-based maintenance instead of the scheduled or breakdown operations with relative economic benefits. At the state of the art, SHM systems are only able to alert the occurrence of damage and eventually localize it but they do not provide sufficiently accurate information about the extent and the type of damage.

In the context of SHM, dynamic identification and monitoring techniques have great importance because their large application fields. In particular, dynamic identification allows to estimate the modal properties of structures and to calibrate numerical models; dynamic monitoring allows following the evolution with time of the modal parameters. Operational Modal Analysis (OMA), that allow measuring the modal properties of a system under ambient or operational conditions, are particularly useful in the case of large structures. Within OMA, Frequency Domain Decomposition (FDD) method and Stochastic Subspace Identification (SSI) method are the most common identification techniques.

The environmental parameters demonstrated to have strong influence on the dynamic response of historical structures. Temperature, ice, and humidity are expected to affect the stiffness and the boundary conditions of the system. In the case of masonry, humidity may have impact on the mass of the constructions. The loading conditions may alter the dynamic behavior as well. The relation between environmental factors and dynamic properties must be studied and modelled. This allows distinguishing alterations in the structural behavior due to exogenous agents from those due to endogenous agents.

NDT can be used to collect data about the structure and to localize and confirm the occurrence of damage. Those methods are particularly indicated in investigating heritage buildings when the need of minimum intervention must be satisfy. Several NDT are available, such as thermovision inspection and sonic, ultrasonic, and radar methods. However, due to the high heterogeneity of masonry, the majority of NDT can provide only qualitative data about the properties of this complex material. The use of different and complementary techniques is considered the best approach.

3. Case study: San Pietro bell tower

3.1 Introduction

The structure examined in this work is the monumental San Pietro bell tower in Perugia (Figure 3-1), the capital city of the Umbria region in central Italy. This Benedictine abbey was erected in the year 996 on the former Episcopal Church of the city. It lies on top of Calvary Mount, which is located in the south area of the city. The abbey is one of the oldest and most prestigious of central Italy and its bell tower is considered one of the landmarks of Perugia. Nowadays, the San Pietro complex includes the basilica, three cloisters, the bell tower and several buildings that embody the monastery, the Faculty of Agriculture, and the seismic observatory "Andrea Bina".

Figure 3-1 North-West side of the bell tower

This chapter aims at presenting the case study and it is organized as follows. The first section introduces the chapter. The second part addresses the structural history of the monument, from the construction to the most recent restauration. The third part is devoted to describing the recent previous studies on the bell tower. First, (1) the geometrical and material characteristics of the monument are delineated. Any investigation on the monument depends on the accurate knowledge of this information. The remaining section of the chapter illustrates: (2) the dynamic characterization of the tower; (3) the continuous structural health monitoring system; (4) the monitoring data analysis; and (5) the numerical modeling. The collected data are used as starting point for the dissertation work and as comparison with the new results. Conclusions end the chapter.

3.2 Structural historic survey

According to the ICOMOS/ISCARSAH recommendation [10], "The purpose of the historical survey is to understand the conception and the significance of the building, the techniques and the skills used in its construction, the subsequent changes in both the structure and its environment and any events that may have caused damage". Moreover, "Knowledge of what has occurred in the past can help to forecast future behaviour and can be a useful indication of the level of safety provided by the present state of the structure. History is the most complete, life-size, experimental laboratory". Extensive researches were conducted in various historical archives of Perugia [24]. More specifically, the data was collected in the archive of San Pietro [25], the archive of the Foundation for Agricultural Education [26], and in the archival library of the Commission for the Architectural and Landscape Heritage of the Umbria region in Priori Palace [27]. Valuable support for the study were the chronicles of the abbots who have ruled throughout the history of the Monastery [28].

3.2.1 Ancient times: from the construction to the 19th century

The primeval structure may have been erected on a Roman tomb where the sarcophagi of two emperors may still be present [29]. The first historical evidence about the bell tower is a document dated from 1286 in which the production of a bell for the abbey is mentioned. In 1347, a document refers to a plot of land sold to obtain the necessary funding to repair the bell tower.

Figure 3-2 Ancient representations of the bell tower: a) Register of Collegio del Cambio, by Matteo di Ser Cambio, 1377; b) fresco in Priori Palace, by Benedetto Bonfigli, 1455-1479; c) painting of Perugia, by Gaspar Van Vittel, early 18th century

Substantial modifications in the structure were carried out at the end of the 14th century. In 1387, the abbot Francesco Guidalotti ordered the demolition of the cusp and part of the belfry in order to transform the bell tower into a defensive tower and the monastery into a fortress. A few years later, in 1393, pope Boniface IX ordered a

further lowering of the belfry to better utilize the tower for defense purposes. The tower remained in this condition for more than half a century.

The reconstruction of the steeple began in 1463 at the behest of the new abbot D. Luca di S. Benedetto da Firenze. The project was commissioned to the architect Bernardo Gambarelli, called Rossellino, to which the actual aspect of the bell tower is attributed. The works were completed by master Giovanni di Betto, in 1468. In Figure 3-2, some ancient representations of the bell tower are reported.

Figure 3-3 Reparation brickwork

Figure 3-4 Tie rods in the shaft

Figure 3-5 Tie rods in the belfry

Figure 3-6 Detail of metal confinement

In the course of the centuries, the bell tower has undergone numerous repair interventions (Figure 3-3) following damage caused by earthquakes and, especially, lightning. The chronicles refer to collapses and damages caused by lightning and related restoration works in the years 1481, 1498, 1569, 1574, 1592, 1616, 1618, 1640, 1667, 1674, 1730, 1778, and 1787. Worthy of note are the works of restoration executed between the years 1498 and 1514, which were assigned to master Biagio Allovigi. In addition to repairing the damages caused by lightning, the master built the masonry vault above the bells (before there was a timber floor) and started the construction of the internal stairs. At the end of the work, a ball and a golden cross were placed on top of the cusp. Around the year 1730, metal tie rods were inserted in the structure, at various heights and positions, see Figure 3-4 and Figure 3-5. These elements were replaced several times during the history of the bell tower. In 1753, the steeple was confined

with the metal strips that are still visible nowadays, see Figure 3-6. At that time, the bell tower was showing worrying longitudinal cracks in the shaft, due to past lightning and earthquakes.

Curious is the intervention on the cusp in 1778, aimed at prevent damage caused by lightning, suggested by the professors of Physics at the University of Perugia. They thought that the conical shape of the bell would attract lightning, and therefore suggested to truncate the cusp. To re-establish the equilibrium, they overlapped some blocks of stone, and an old mill wheel. The fall of those masses, October 30, 1787, caused even more damage. The intervention was therefore useless. In 1788 one of the earliest modern protective lightning rods was installed on the tower. It was designed by Fonda delle Scuole Pie, professor of Experimental Physics at the University La Sapienza of Rome. The device proved to be effective and neither the tower nor the rest of the complex suffered from lightning in the decades that followed.

The available sources do not report any significant structural works during the 19th century.

3.2.2 Recent times: from the 20th century to the last restauration

In the last century, three large structural interventions were carried out on the monument. Between the years 1929 and 1933, the metal frame supporting the four bells was realized under the supervision of architect Arnolfo Bizzarri (Figure 3-7).

Figure 3-7 Bells supported by the metal structure

Figure 3-8 Concrete elements supporting the lateral arches of the demolished vault

The intervention was considered necessary to limit the oscillations caused by the ringing of the bells, but turned out to be rather invasive. The construction of the frame implied the destruction of the last portion of the stairs in the shaft and of the vault underneath the belfry. Moreover, it was necessary to consolidate the masonry arches that used to support the removed parts, see Figure 3-8. The strengthening was urgently performed casting concrete elements. The metal frame is directly supported by the walls of the shaft (in which penetrates through the whole thickness) is 9 meters high, and weights roughly 5500 kg. Evidently, the installation of the bell support determined radical changes in the internal structure of the steeple. In conjunction with this work, the top of the spire was stabilized and a new lightning protection system was installed. In addition, the metal ladder leading up to the cusp was built and some tie rods were replaced.

In 1951, a thorough inspection of the tower was performed by engineer Sisto Mastrodicasa. Globally, the structure was appearing in good condition with the exception of the basement, in which crushing signals could be observed. It was established the infilling of the access door with similar bricks using the "scusi-cuci" technique and cement grout injections. In conjunction with these works, the circular hole present at the center of the basement vault was created in order to allow the pass through of building materials.

Due to the 1997 Marche-Umbria earthquake, the monument underwent various damages that were repaired in 2002. The direction of the works was entrusted to architect Francesco Ventura and to engineer Riccardo Vetturini. The intervention was made with modern techniques and materials according to the observation of the crack pattern, and on the identification of damages and failure mechanisms. Carbon and glass fibers impregnated with epoxy resin and FRP bars were massively used to strengthen the cusp and the belfry. Regarding the cusp, the carbon fibers were applied in two perpendicular directions: longitudinally, to prevent rotation of the element, and radially, to prevent its opening. The horizontal confining fibers were fixed both on the exterior and on the interior surface. The two layer were connected by means of aramid bars. A framework of horizontal and vertical carbon fibers impregnated with epoxy resin was also applied in the belfry, see Figure 3-9.

Figure 3-9 Application of FRP materials during the last restauration works [30]

Figure 3-10 Confining elements in double-arched windows

Carbon bars were inserted in the six pillars and in the thin columns of double-arched windows in correspondence of the carbon bands. Drilling and insertion of carbon bars were also performed in proximity of the anchorages of the tie rods to restore their effectiveness. The base, the columns and the capitals of the double-arched windows were confined with glass fibers and titanium alloy elements, see Figure 3-10. The intervention on the bell tower was completed with the consolidation and the finishing of the surfaces. Additional information on this restauration work can be found on the personal webpage of engineer Vetturini [30].

3.2.3 2016-2017 Central Italy earthquakes

On August 24, 2016, at 3.36 am, a magnitude 6.0 earthquake strikes the Central Italy, affected the territories of Abruzzo, Lazio, Marche and Umbria. Thousands of people were involved in the event that caused 299 victims, many injured and serious damage to the territory. On 26 and 30 October, 2016 new violent earthquakes hit Central Italy, in particular the border between Umbria and Marche. The seismic event of October 30 - magnitude 6.5 - was

the strongest in Italy in the last thirty years: the number of evacuated people, as well as the damage, grow exponentially. There are no victims. In the second half of January, 2017 as the earthquake-related activities were continuing, the Civil Protection System faced an exceptional bad weather, that was affecting heavily Abruzzo, Lazio, Marche and Umbria. Rescue operations were numerous and complex: recovery and rescue of people in isolated fractions, reinstatement of road, infrastructure and essential services heavily compromised by heavy snow. The territory is already severely challenged when, on January 18, 2017 four earthquakes of magnitude higher than 5.0 hit again the areas of central Italy, particularly the Lazio and Abruzzo Regions. A few hours after the tremors, an avalanche overwhelmed and destroyed the Rigopiano Hotel, located on the slopes of Gran Sasso, in the province of Pescara. Rescue operations lasted for an uninterrupted period of eight days and eight nights, and made it possible to save eleven people. The events of January caused 34 victims, of which 29 in Rigopiano [31].

From 24 August 2016 to 13:00 on June 15, 2017, 70,328 Earthquake traced back to the sequence of Central Italy (Amatrice-Norcia-Visso) were recorded, about 240 earthquakes per day [32]. The most relevant seismic events that hit the area are displayed in Figure 3-11.

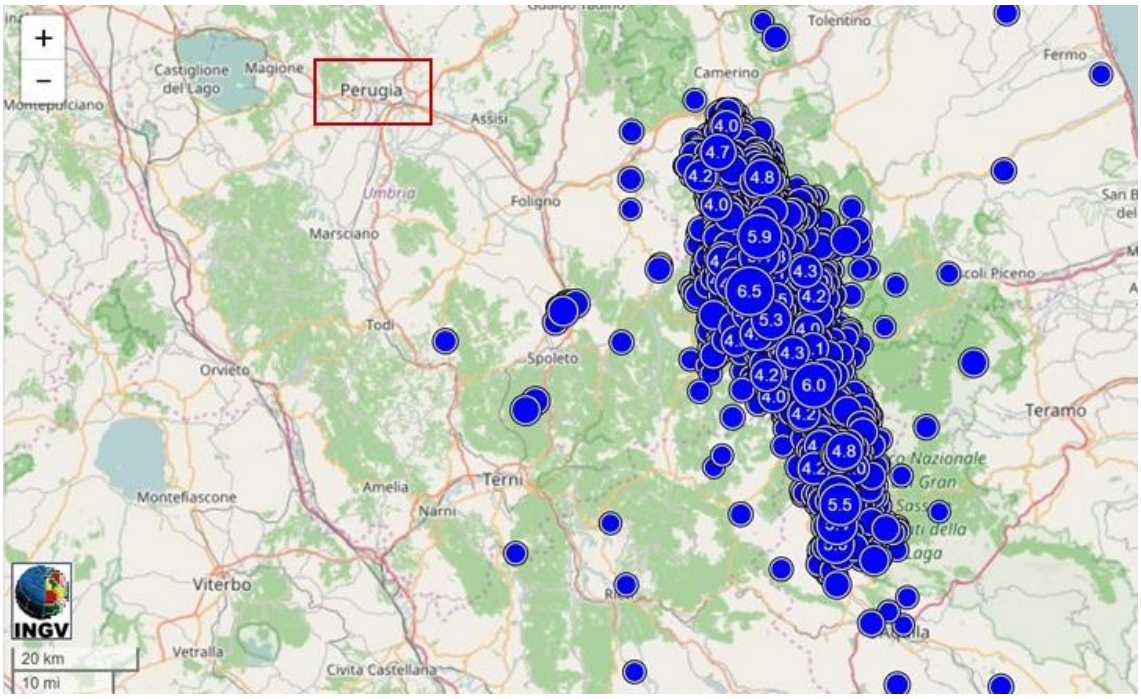

Figure 3-11 Map of seismic events located by the National Seismic Network from August 24, 2016 in the Central Italy area (magnitude greater than or equal to 2.5) [32]

3.3 Previous studies

Starting from the year 2013, the bell tower has been object of dynamic investigations and numerical modeling by a team of researchers of the Department of Civil Engineering of the University of Perugia. The purpose of these studies was the installation of a permanent vibration-based structural health monitoring (SHM) system able to detect anomalies in the structural behavior by means of statistical process control tools such as control charts. Ambient Vibration Testing (AVT) and Operational Model Analysis (OMA) were conducted under natural (ambient or

operational) excitation and the modal parameters were estimated from output-only data. The information collected was used to identify the baseline dynamic properties (lowest natural frequency, modal damping ratios, and mode shapes of the structures) as well as establish the best configuration for the installation of the continuous monitoring system. The continuous system was activated in December 2014. The dynamic parameters are strongly affected by the environmental conditions (such as temperature, humidity, presence of ice) and therefore statistical methods were used to remove the part of variance in the data associated to these phenomena. In addition, based on the experimental results, the vulnerability assessment of the monument was implemented through the calibration of finite element models.

3.3.1 Geometrical and material surveys

Detailed architectural survey data were collected by architect Ventura for the 2002 consolidation works (Figure 3-12). However, they are related only to belfry and cusp. Complementary information about the shaft can be found in other studies [24]. The tower is 61.45 m height and can be subdivided in four main parts: (1) basement; (2) shaft; (3) belfry; and (4) cusp. Concerning materials of the monument, they are rather inhomogeneous. The walls of the bell tower are made of three-leaf masonry with rubble-core. The external and internal layers are of stones and brick elements of variable dimensions disposed in a quasi-orderly manner. Various types of stones were used, namely grey travertine, white limestone and pink “Assisi” limestones.

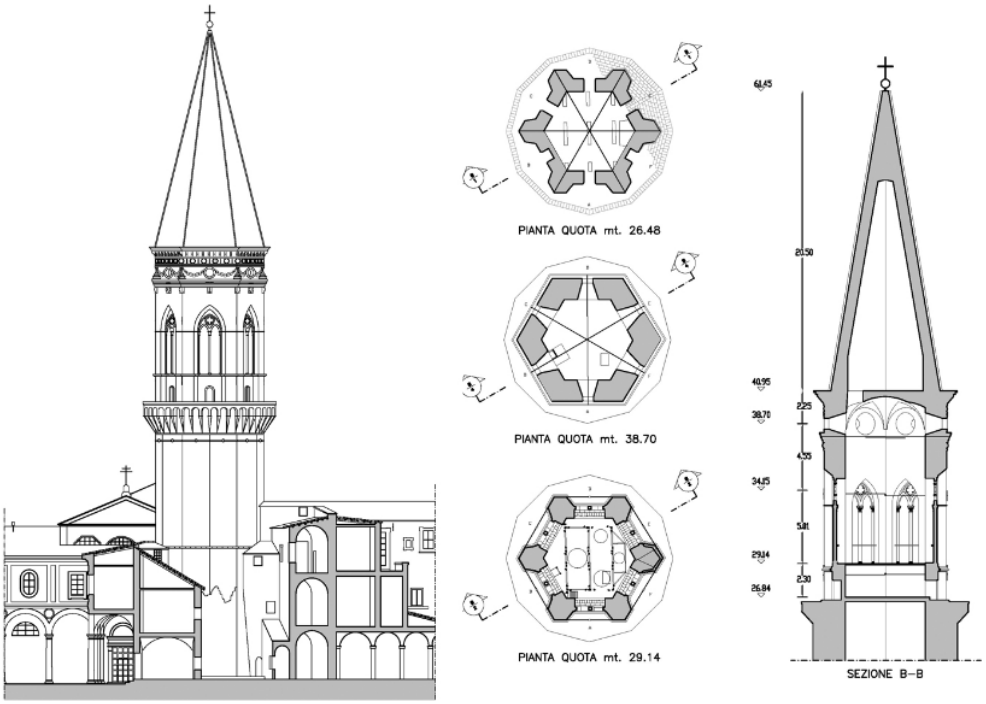

Figure 3-12 Plan and elevation of the bell tower [30]

The basement is visible from the outside and looks solid and massive. It has a truncated dodecagonal pyramid shape and a height of 8 m. It is characterized by massive stone walls, with thickness ranging roughly from 2 m to 3.5 m. The structure is visible from an external courtyard and from inside the monastery. In its interior, the basement consists in a semispherical dome of 6m diameter. The external leaves of the basement are made of irregular travertine blocks.

Figure 3-13 Basement of the tower

Figure 3-14 Interior of the shaft: partially demolished masonry stairs, lower part of the metal structure, room of the clock's mechanism

The shaft rests on the basement, at 4.5 m of height from the ground, has a dodecagonal cross section, and reaches a height of 26.84 m. The average thickness of the walls is 1.8m. Externally, it is divided into three sections by belt courses, placed in correspondence with the original floors. The outer leaf is made of limestone blocks and brick insertions. Inside, the structure is particularly complex, but it can be subdivided in two spaces. The lower room consists in a second hemispherical vault. Here, there are the signs of two old entrances: the opening closed in 1951, which leaded to the monastery and a more ancient one that leaded to the exterior of the complex. In addition, there are a window and a slit on the walls. It is possible to enter this room and the basement through two distinct doors. The only passage between them is the opening realized during the 1951 works. Clockwise stairs lead to a narrow counterclockwise flight of stairs, which leads to the next floor. The second room is located at a height of 11.6 m and occupies the remaining volume of the shaft. It is possible to enter there directly from the second floor of the monastery. The internal structure is rather irregular. In correspondence of the access door, masonry stairs develop counterclockwise around the walls of the shaft. They are supported by a series of arches their width is between 0.50 to 0.75 m. Under the stairway, an arched window faces north. The final portion of the staircase was demolished to allow the construction of the metal structure. It starts at a height of 22.8 m and it extends for 9 m up to the belfry. Recently, two timber floors were constructed to allow easy access to the belfry. At 23.6 m, the remains of the demolished vault are visible. Starting from this height, the interior structure of the shaft assumes a hexagonal shape, whereas are the exterior it remains dodecagonal. The materials used for the internal structure are strongly inhomogeneous. The walls are mostly made of limestone masonry, arches and vaults are made of bricks, some concrete elements are present as well.

At 26.84 m, a 40 cm thick floor made of iron beams and masonry vaults separates the shaft and the belfry. At the exterior, decorative brackets mark the passage between the two bodies. The belfry has a hexagonal shape and extends up to a height of 40.95m. The thickness of the walls decrease to 1.2 m. A timber floor subdivides the belfry in two parts. The first one shows one opening (1.2 m high and 0.8 m in width) on each wall and a wooden ladder that leads to the second floor, where the metal structure ends and the bells are placed. Large mullioned windows characterized the upper part of the belfry. These windows are 5.6 m high and 2 m wide. Between them, large, approximately hexagonal pillars are present. They have slightly different dimensions. At the top of the belfry, at 40.95 m height, there are circular openings in correspondence of each window. At the same height, on the outside, carved eaves adorn the tower. The belfry is mostly made of travertine and brick masonry. The columns of the mullioned windows, capitals and other decorations are in travertine.

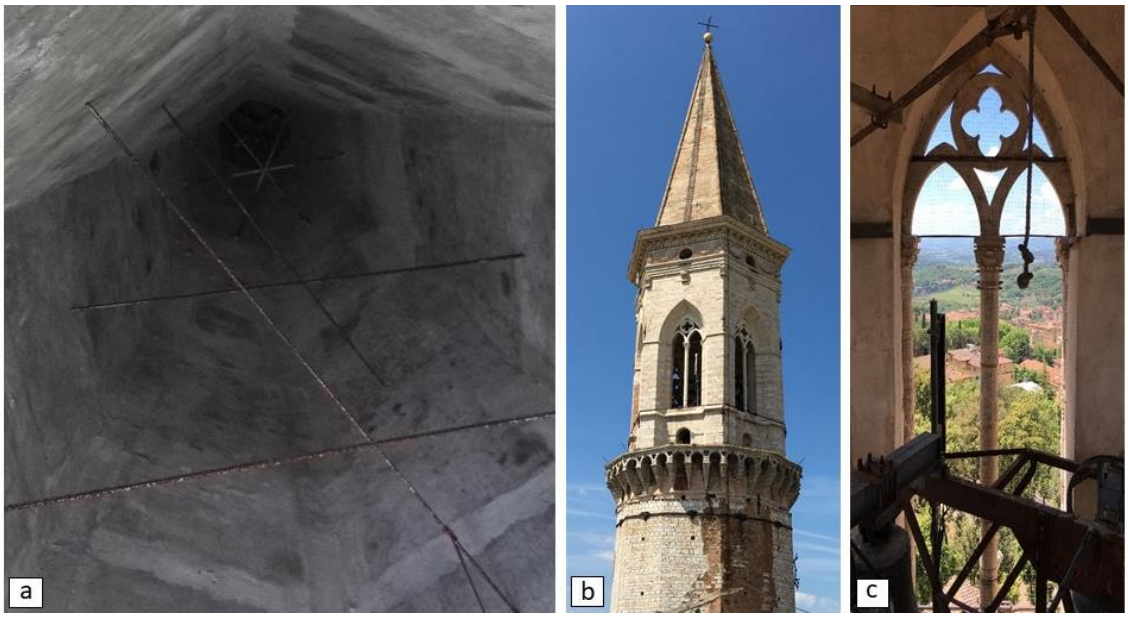

Figure 3-15 Belfry and cusp: a) interior of the cusp, b) north view, c) one of the mullioned window

A segmental dome closes the belfry and indicates the beginning of the cusp. A narrow aperture and a metal ladder allow reaching it. The cusp culminates the bell tower and extends up to a height of 61.45m. The cusp has the shape of a hexagonal pyramid. Its walls have a thickness of 1m. The last 6m are formed by a solid masonry block. The cusp is mainly made of travertine with an external layer of bricks. Some images of belfry and cusp are shown in Figure 3-15.

3.3.2 Nondestructive test

Direct pulse sonic tests have been carried out on the columns of the belfry during the 2002 consolidation works. The purpose was evaluating the effectiveness of the injections by comparing the mechanical properties of the masonry elements before and after the intervention. Two opposite sides of each column were investigated. The columns were accurately measured in order to compute the wave velocity. The grid of points examined had horizontal and vertical spacing of 20 and 25cm, respectively. The DAQ system was a seismograph PASI 24 bit. The signal was recorded at 62500Hz sampling rate and 32 ms time window. The sonic test was performed on all six columns in original conditions and only on columns A-B and E-F after the injection. Indeed, they are considered

representative elements of the belfry since they are made of limestone/travertine and bricks, respectively. The results showed different wave velocity according to the height of the column. Higher values, associable to better mechanical properties, are found in the lower parts. Lower values, associable to worst mechanical properties, are found in the upper parts. However, the computed velocities are lower than the expected values for undamaged masonry. The reason is attributed to the seismic action. The sonic test performed after the intervention showed that the average wave velocity increased, especially in areas that originally were showing poor mechanical characteristics. It proves the effectiveness of the injections. The results obtained are shown in Table 3-1. [24]

Table 3-1 Average results of Direct pulse sonic test

Side	Orientation	v_{mean} before intervention	v_{mean} after intervention	
A-B	North-Northeast	1165	1478	+21%
B-C	Northeast-Southeast	1533		
C-D	Southeast-South	2255		
D-E	South-Southwest	1547		
E-F	Southwest-Northwest	1650	1980	+28%
F-A	Northwest-North	2041		

3.3.3 Dynamic characterization of the tower

Several AVT were performed, in which the dynamic response of the bell tower in operational conditions were estimated. The information collected was used to identify the baseline modal parameters (lowest natural frequency, modal damping ratios, and mode shapes of the structures) as well as establish the best configuration for the installation of the continuous monitoring system. Here, the results of two AVT are reported.

The first AVT lasted for seven consecutive days (from 20 to 27) and was conducted in the month of December 2013. [33] [34] Five uniaxial accelerometers MEMS, model PCB 3711B112G, with sensitivity of 1V/g were used. They were placed at the base of the cusp, at an altitude of 40.8m. The data were acquired using a 24-channel system, model cDAQ-9188, with NI 9234 data acquisition modules (resolution of 24-bit, dynamic range of 102dB, and anti-aliasing filters). Data were recorded at 1653 Hz and down-sampled to 41.32 Hz before performing the modal identification. The levels of acceleration measured during operational conditions were very low. However, on December 22, at 11:06, a small earthquake occurred, (4.0 Richter magnitude, epicenter in the Gubbio's area). In addition, on the days 25 and 26, strong wind was observed. The modal parameters were extracted from two time windows of the signal: a 120s long window containing the earthquake-induced response (AVT1a) and a 15 minutes long window containing the wind-induced response (AVT1b). The data were processed with the commercial software ARTeMIS, using the Frequency Domain Decomposition (FDD) technique. Two lateral modes, indicated as Fx1 and Fy1, were identified from both series of data. An additional torsional mode, denoted as T1, was identified from the earthquake-induced response.

The most recent AVT (AVT2) was carried out on 16 February 2015 [17] [35] [36] [15]. Six uniaxial piezoelectric accelerometers, model PCB 393B12, with a sensitivity of 10 V/g, were used. They were placed at the level of the rigid diaphragms: three of them were placed at the base of the cusp (40.8 m) and other at the base of the belfry (29.1 m). The data were acquired using a 24-channel system, carrier model cDAQ-9184, with NI 9234 data

acquisition modules (resolution of 24-bit, dynamic range of 102 dB, and anti-aliasing filters) with a sampling frequency of 100 Hz. In this case, the main excitations on the structure were wind and micro vibration induced by vehicles traffic. The modal parameters were obtained from a 30 minutes long window of the signal. In this case, a fully automated Stochastic Subspace Identification (SSI) technique [18] was used. Seven mode shapes were identified, see Figure 3-16. The results of the AVT are shown in Table 3-2

Table 3-2 Results of dynamic investigations

Mode number	Frequency [Hz]			Mode Type
	AVT1a - Dec 2013	AVT1b - Dec 2013	AVT2 - Feb 2015	
I	1.437	1.402	1.449	Fx1
II	1.517	1.473	1.518	Fy1
III	-	4.197	4.342	T1
IV	-	-	4.575	Fx2
V	-	-	4.889	Fy2
VI	-	-	7.245	Fx3
VII	-	-	7.263	Fy3

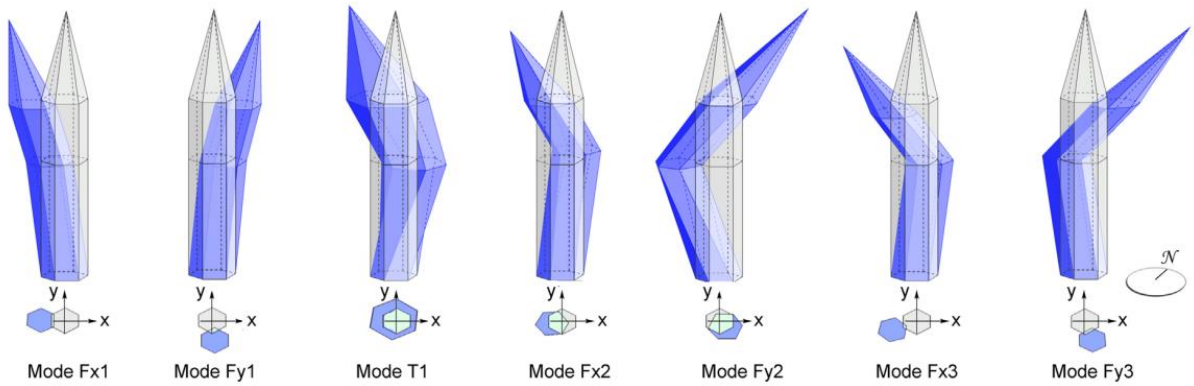

Figure 3-16 Identified mode shapes of the bell tower during AVT2 [35]

3.3.4 Continuous structural health monitoring

Monitoring system hardware

The dynamic monitoring of the bell tower started on December 9, 2014. [17] [35] [36] [15] The aim of the project was the automatic detection of any changes in the dynamic behavior of the structure by means of statistical process control tools of the identified modal frequency using automated OMA techniques. The continuous monitoring system is composed of several components: sensors, data acquisition system, data communication system, data processing system, and data storage system, see Figure 3-17. Three uniaxial piezoelectric accelerometers, with a sensitivity of 10V/g, and the data acquisition system are located at the base of the cusp. They are connected using short cables in order to reduce noises in the signal. The data acquisition system is the same described for AVT2. It is connected to a host personal computer (PC) placed in the shaft, below the belfry. A LabVIEW code,

implemented in the PC, is used for data acquisition and real time elaboration, such as amplitude and spectral plots. The data provided by the accelerometers are recorded at about 1600Hz, down-sampled at 100 Hz, and stored in distinct files of 30 recording minutes for automated modal identification. Various measures were taken to protect the equipment against lightning: the accelerometers are fixed to the masonry by means of a Plexiglas device; the short cable also avoid induced currents; the data acquisition system is placed inside a box that contains a protective system against overvoltage; a 30m long vertical fiber optic cable, which does not conduct induced currents, connects the data acquisition system to the computer. From the computer, the data are sent via internet to a remote server located in the Department of Civil Engineering of the University of Perugia. Here they are processed through a specific MatLab code. Since March 2015, environmental sensors were installed, model Tinytag from Gemini Data Loggers. They included eight temperature sensors (six dry bulb sensors and two surface sensors) and two humidity sensors. Environmental data are acquired each 30 minutes and registered by the sensors itself. The need to study the optimal configuration for the actual environmental monitoring system justified this high number of sensors. Currently, two permanently installed temperature sensors are present.

Health assessment methodology

The SHM is based on the continuous identification of the natural frequencies of the bell tower and on the analysis of their variations. [17] [35] [36] [15] It involves the following steps: (1) automated modal identification and modal tracking processes; (2) removal of environmental effects; (3) damage detection. The first step includes: (1) a pre-processing analysis to identify and correct anomalies in data; (2) detection and removal of vibrational data under the action of the swinging bells; (3) application of a low-pass filter and decimation of data to 40 Hz; (4) application of a fully automated SSI procedure [18]; (5) modal tracking of the estimated parameters based on similarity check. Then, a combination between the techniques of multivariate linear regression (MLR) and principal component analysis (PCA) is adopted to remove the environmental effects. Finally, the novelty analysis procedure is used for damage detection.

3.3.5 Monitoring data analysis

Frequency tracking

It is possible to carry out the modal tracking of five modes among the seven identified. [36] [15] The mode continuously recognized are the following: the first three modes (the bending modes f_{x1} and f_{y1} and the torsional mode f_{t1}) and the other two modes in the Y direction (f_{y2} and f_{y3}). Mode f_{x2} and f_{x3} are sporadically identified. The reason may be related to the low vibration levels of the bell tower in operational conditions, to wind directionally effects or to the presence of a single sensor along the x direction. The fluctuations of the modes are associate to daily and seasonal variations of environmental parameters and freezing conditions. Sensors included eight temperature sensors and two humidity sensors.

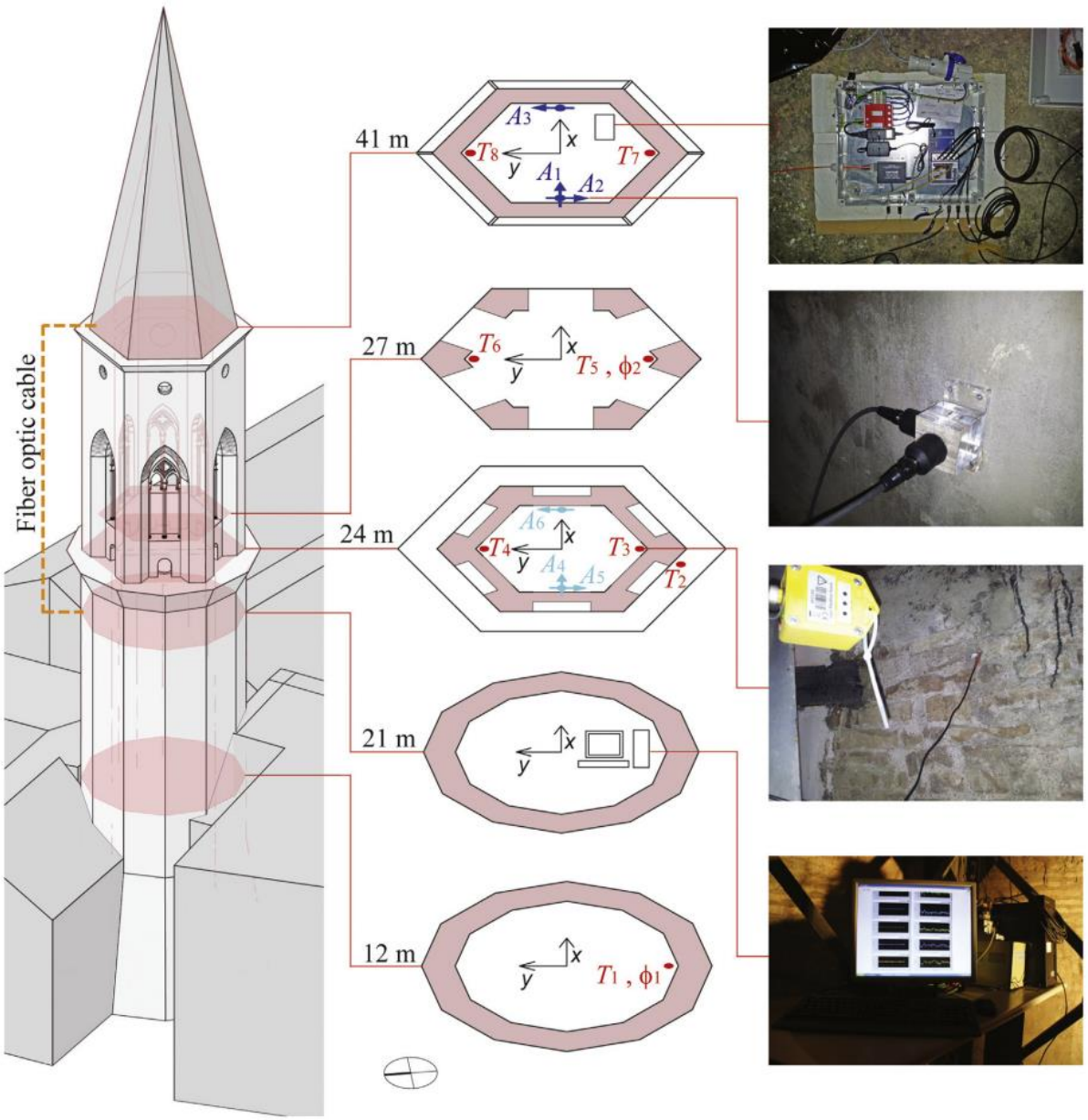

Figure 3-17 Sketch of the monitoring system with sensors positions and photo evidence of sensors on site and of data acquisition hardware (A, T and φ denote acceleration, temperature and humidity sensors, respectively). Acceleration sensors A1, A2 and A3 are used for permanent monitoring purposes, while sensors A4, A5 and A6 are only used in AVT [18]

Correlation analysis

Correlation analyses were carried out: between environmental parameters, between natural frequencies, and between environmental parameters and natural frequencies. [15] The study described in this paragraph take into account the data recorded in the period December, 2014 - September, 2015.

The results showed large degree of correlation between temperature data measured by different sensors. Within the shaft of the bell tower, air and indoor temperatures are highly correlated and numerically similar, no matter the orientation of sensors. Concerning the outdoor sensors, the location appears to be more important because of the

effect of solar radiation. Lower correlation coefficients are observed between indoor and outdoor temperature values recorded in different location of the structure. The correlation coefficients between temperature and air humidity data are low and sign-negative due to the reduction in air humidity with respect to increasing air temperature.

Large data correlation is observed between the natural frequencies of the modes f_{x1}, f_{y1} and f_{y2}. The torsional mode, f_{t1}, appears correlated only with mode f_{y3}, which, in turn, is somewhat correlated with the other modes.

With exception of the torsional mode, all the frequencies exhibit correlation with temperature data. This is attributable to the dependency of frequencies on environmental parameters. In general, with exception of mode f_{t1}, an increase in temperature determines an increase in natural frequencies. These results are in accordance with other literature studies and they can be explained with the closing of micro-cracks within mortar layers as a result of the thermal expansion of the material. As for the torsional mode, the negative correlations is attributed to the thermally induced loss of tension in fiber reinforcements and tie elements mounted during the 2002 strengthening works. By means of linear regression curves, it was demonstrated that a variation in the temperature of 10°C determines changes in the natural frequency values between 0.8 and 3.4%. Similar variations in natural frequencies are typical observed in structures that have suffered minor damages.

Noteworthy are the results obtained in freezing conditions. Abrupt increase in natural frequencies was noticed at the beginning of 2015 in concomitance with three consecutive days of negative temperatures. Moreover, contrarily to what observed in normal conditions, it was noticed that frequencies increase with lowering temperature under 0°C. This phenomenon is attributable to the formation of ice within the micro-pores of the masonry, which reasonably imply a stiffening of the material.

A significant remark is the following. Temperature data recorded by sensor T5 show the highest coefficients of correlation with the frequency values. Therefore, the sensor is placed in the best spot to install the permanent environmental data monitoring system.

3.3.6 Numerical modeling

Implementation and calibration of numerical models

Concurrently with the first dynamic investigations on San Pietro bell tower in 2013, numerical models of the structure were built using the Finite Element commercial software ABAQUS®. Hexahedral elements and a structured mesh were used in basement and in the shaft, whereas tetrahedral elements and a free mesh were used in the belfry and in the cusp. The constrains due to surrounding bodies were considered by inserting volume parts of them. A coarse mesh was used for those elements to limit the computational effort. All the parts were connected through internal tie constraints with a nod-to-surface formulation. For the sake of simplicity, local details, such as the steel structure or the brickworks insertion in the external layer of the shaft, were not taken into account. As for the mechanical characteristics of materials, the models were subdivided in three regions to which homogeneous orthotropic materials was assigned: basement and shaft, belfry, and cusp. The values were chosen in accordance with the Italian code for existing structures, see Table 3-3. [37] Linear modal analyses were performed with the numerical models. The results obtained were in good agreement with the experimental data (AVT1b) even if the

model was not tuned. In order to calibrate the numerical model (now on, they will be called Model 1 [33] and Model 2 [34], respectively), mode sensitivity analyses were carried out. The material properties of the update FE models are shown in Table 3-4.

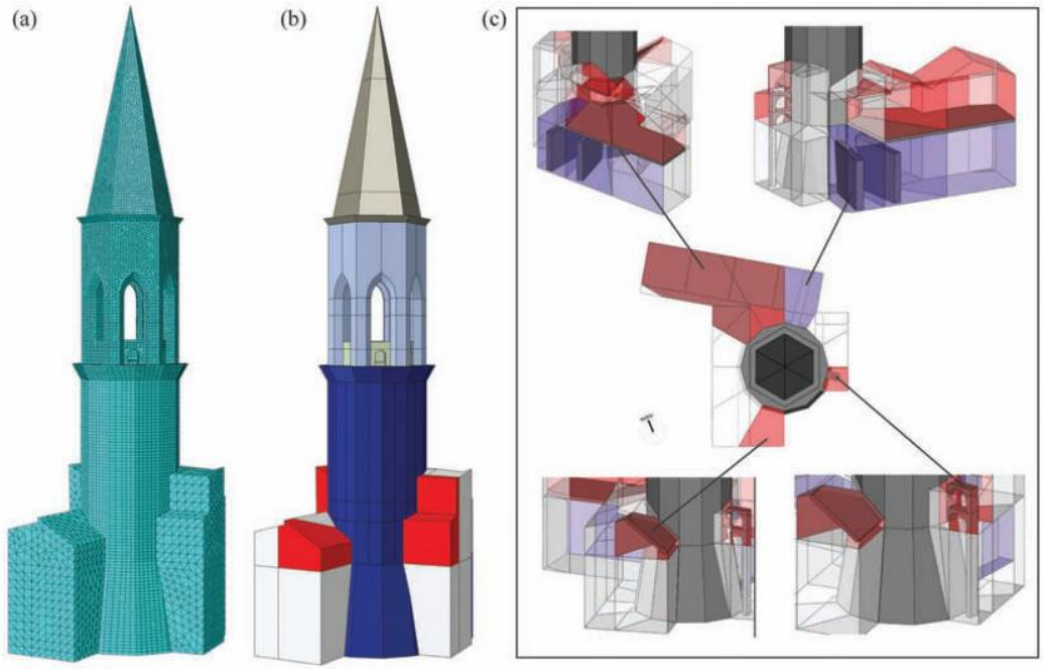

Figure 3-18 Image of the mesh used in the FE numerical model of the bell-tower. (b) Solid model of the bell-tower with material identification assigned to the different regions: the shaft, the belfry, the cusp and the neighboring buildings. (c) Particular of the structural restraints at the base of the bell-tower. [35]

Table 3-3 Initial mechanical properties of the orthotropic constitutive model

Structural element	Young's modulus [MPa]	Shear modulus [MPa]	Poisson coefficient
Basement and Shaft	4032	1238	0.25
Belfry	4032	1238	0.25
Cusp	1500	500	0.25

Table 3-4 Material properties of the update FE models – Model 1 and 2

Structural element	Young's modulus [MPa]		Shear modulus [MPa]		Poisson coefficient	
	Model 1	Model 2	Model 1	Model 2	Model 1	Model 2
Basement and Shaft	3883	5520	1238	1238	0.25	0.25
Belfry	4032	4032	1161	1161	0.25	0.25
Cusp	1500	1500	500	500	0.25	0.25

Similar models were built after the dynamic investigations of February 2015 (Model 3 [17] and Model 4 [35]). Also in these cases, modal sensitivity analyses and tuning operations were executed to in order to obtain more accurate representation of the real structure. The material properties of the update FE models are shown in Table 3-5. The model 4 is shown in Figure 3-18.

Table 3-5 Material properties of the update FE models – Model 3 and 4

Structural element	Young's modulus [MPa]		Shear modulus [MPa]		Poisson coefficient	
	Model 3	Model 4	Model 3	Model 4	Model 3	Model 4
Basement and Shaft	5450	5678	1238	1305	0.25	0.25
Belfry	2950	2800	1920	2847	0.25	0.25
Cusp	1500	1748	500	500	0.25	0.25

Damage sensitivity

More recent studies aimed to investigate the seismic vulnerability of the bell tower and the frequency sensitivities to damages. For that purpose, a damage pattern similar to the one caused by the 1997 earthquake was simulated. It implies cracks at the extremities of the columns of the belfry. The damage was modelled as a localized reduction in stiffness with the introduction of a damage parameter, d. It represents a reduction in the Young's and shear modulus as follow: $X_d = X_u(1-d)$, where X_u is the elastic moduli in the undamaged condition and X_d is the same quantity in the damaged condition. Two simulation were performed, using respectively Model 3 [17] and Model 4 [35]. As for the simulation with Model 3, the maximum damage parameter was assigned to one single column. The remaining columns were progressively less damaged with increasing distance. Zero damage parameter was assigned to the column opposed to the most damaged one. The results showed that the torsional mode is the most sensitive to damages. In particular, two damage scenarios were taken into account. A localized reduction of 8% of the stiffness (damage coefficient equal to 0.08) corresponds to a reduction to the torsional mode frequency equal to 0.5%. A localized reduction of 18% of the stiffness (damage coefficient equal to 0.18) corresponds to a reduction to the torsional mode frequency equal to 1.0%. The damage scenario are called respectively D1 and D2. Similarly, the damage conditions were simulated with Model 4. The maximum damage coefficient was assigned, in turn, to the six columns of the belfry. For each leading column, i.e. the column to which the maximum damage is assigned, four damage scenarios were considered, for a total al twenty four combinations. Also in this case, the torsional mode is the one that shows the higher sensitivity to damages: when $d = 0.3$, the frequency is reduced up to 2%.The first two modes undergo frequency variations of 1.3% and 1.4%, respectively.

3.4 Conclusions

San Pietro bell tower belongs to a monumental complex of exceptional historical, cultural and artistic value and it is considered one of the landmarks of Perugia. For this reason, the preservation of this structure has been considered an essential issue over centuries. The objective of this chapter was presenting this interesting case study, by providing information about its structural historical and the most recent studies carried out on the bell tower by researchers of the Department of Civil Engineering of the University of Perugia.

The structure has been subject to numerous repair interventions over time following damages caused by earthquakes and, especially, lightning. For this reason it presents several exterior masonry insertions and it was provided with several tie rods and metal confining elements. Particularly deleterious were the structural works carried out in the years1929-1933. They consisted in the construction of a metal frame supporting the four bells. This implied the destruction of the last portion of the stairs of the shaft and the vault underneath the belfry. Moreover, concrete was extensively used in order to consolidate the tower. The last restoration work were performed in the

2002 after the 1997 Marche-Umbria earthquake. New techniques and modern materials were used to repair and consolidate the tower. Several violent seismic events hit Central Italy starting from August 24th 2016. Their effects were perceived also in Perugia, even if major damages did not occur.

The investigations carried out since 2013 allowed installing a permanent vibration-based structural health monitoring (SHM) system able to detect anomalies in the structural behavior by means of statistical process control tools. Ambient Vibration Testing (AVT) and Operational Model Analysis (OMA) were conducted under operational excitation and the modal parameters were estimated from output-only data. The information collected was used to identify the baseline dynamic properties as well as establish the best configuration for the installation of the continuous monitoring system.

The SHM is based on the continuous identification of the natural frequencies of the bell tower and on the analysis of their variations. Environmental parameters, i.e. temperature and humidity, are monitored as well. In particular, it is possible to track five modes among the seven identified. Correlation analyses were carried out between environmental parameters and natural frequencies. With exception of the torsional mode, all the frequencies exhibit high correlations with temperature data. In general, an increase in temperature determines an increase in natural frequencies.

Concurrently with the first dynamic investigations on San Pietro bell tower in 2013, several FE numerical models of the structure were built in different occasions. After sensitivity analyses, the models were calibrated according to the experimental dynamic data. This allowed to update the material properties in order to obtain consistent results.

This page is left blank on purpose.

4. Inspection and Testing

New studies were conducted on San Pietro bell tower between the days 15th and 19th of May by the author of this thesis and researches of the University of Perugia. They consist of (1) visual inspection and survey of the metal structure, (2) AVT, and (3) sonic tests. The methodology used in the investigations as well as the results obtained are discussed in this chapter.

"Direct observation of the structure is an essential phase of the study, usually carried out by a qualified team to provide an initial understanding of the structure and to give an appropriate direction to the subsequent investigations." [10] The visual inspection is at the base of the MQI method that is applied on the masonry of the shaft. Moreover, the metal structure is studied, since it was neglected in previous studies. The constitutive elements are identified and the geometric survey is carried out. The collected information allow evaluating the effect of this element on the tower. AVT was also performed on the bell tower. The objective was to detect any changes in the dynamic properties of the tower following the 2016-2017 earthquakes as well as better characterize its mode shapes by means of a higher number of sensors. Twelve uniaxial piezoelectric accelerometers, placed at four different heights, were used. The results are compared with those obtained in the dynamic investigations of February 2015, which are also analyzed in the chapter. Sonic tests are carried out on the shaft of the tower in correspondence of: (1) interior stone masonry, (2) interior brick masonry, (3) exterior stone masonry, (4) exterior brick masonry. The results of the test are used to characterize the materials of the monument. In particular, information on the elastic moduli can be obtained. Conclusions are given at the end.

4.1 Visual survey

The visual survey allowed verifying the information about the monument and constituted the first step of the in-situ investigation. All the compartments of the bell tower were inspected, namely base, shaft, belfry and cusp. The visual inspection of the masonry of shaft allowed computing the MQI of its walls. Special attention was given to the metal structure, as no existing surveys were available. The following paragraphs of the chapter deal with these aspects. Furthermore, eventual damages caused by the last earthquake were examined.

Figure 4-1 Crack in the lower part of the belfry

Globally, the bell tower appears in good state of conservation from the structural point of view. Damages due to the last earthquakes are not clearly recognizable. Even the belfry, that typically is the most vulnerable portion of a bel tower, does not show evident criticalities. The reason may be attributed to the extensive insertion of FRP materials during the 2002 restauration. The only exception is constituted by some cracks that can be found in the lower portion of the belfry, in correspondence of the masonry arches above the six small windows, see Figure 4-1. As far as the maintenance status is concerned, the interior of the bell tower appears heavily dusty and unkempt even if this criticality does not affect the tower under the structural point of view. Moreover, the plastic anti-birds nets installed in proximity of openings start showing the first signs of degradations and the timber floor of the belfry appears rotten in certain points.

4.1.1 Masonry Quality Index

The masonry of the shaft is analized (Figure 4-2) with the MQI method. The brick masonry insertions are not taken into account. The seven parameters considered in MQI are analysed consistently with the indication provided in licterature [23]. The criteria for masonry assessment are shown in Table 4-1. The MQI evaluation is shown in Table 4-2.

Figure 4-2 Exterior masonry of the shaft

The mechanical parameters (compressive strength, shear strength and modulus of elasticity) of masonry are computed by means of experimental relationships as function of MQI values [21], according to the type of load (vertical, in-plane and out of plane). The results are shown in Table 4-3. The values obtained may be related to those corresponding to the masonry category “Dressed rectangular (ashlar) stone masonry” (Muratura a blocchi lapidei squadrati) found in the Italian code in Table C8A.2.1 [37], see Table 4-4.

Table 4-1 Criteria for the assessment of masonry parameters

Parameter	Outcome	Criteria
SM	F	Un-damaged elements or degraded/damaged elements <10%
SD	PF	Presence of more than 50 % of elements with large dimension 20–40 cm; co-presence of elements of different dimensions
SS	F	Barely cut stones or perfectly cut stones on both masonry leaves (predominant)
WC	NF	Small stones compare to wall thickness
HJ	F	Bed joints continuous
VJ	PF	Properly staggered vertical joints
MM	F	Good quality and non-degraded mortar, regular bed joint thickness or large bed joint thickness made of very good quality mortar

Table 4-2 MQI evaluation

Parameter	Vertical load	In-plane Load	Out of plane Load
SM	1	1	1
SD	0.5	0.5	0.5
SS	3	2	2
WC	0	0	0
HJ	2	1	2
VJ	0.5	1	0.5
MM	2	2	1
MQI	8	6.5	6
Category	A	A	B

Table 4-3 Computed masonry mechanical parameters

Shear strength (MPa)	Max	0.149	0.110	0.100
	Min	0.107	0.077	0.069
	Average	0.128	0.094	0.085
Elastic Modulus (MPa)	Max	3035	2375	2189
	Min	2202	1697	1556
	Average	2619	2036	1872
Compressive Strength (MPa)	Max	8.282	6.146	5.565
	Min	5.587	3.998	3.576
	Average	6.935	5.072	4.570

Table 4-4 Extract from Table C8A.2.1. of Circ. NTC08

Masonry typology	f_m (N/mm2)	τ_0 (N/mm2)	E (N/mm2)	G (N/mm2)	W (kN/m3)
	min-max	min-max	min-max	min-max	
Dressed rectangular (ashlar) stone masonry	6.0	0.090	2400	780	22
	8.0	0.120	3200	940	

4.1.1 Complementary geometrical surveys – metal structure

The metal structure is placed between the third portion of the shaft and the belfry and it is comprised of five two-dimensional sub-systems formed of several types of profiles. The structure is anchored to the tower only at its base by means of two sets of three perpendicular beams embedded in the shaft (Figure 4-4). Vertically, the structure is divided in four parts, identified by the floors that are placed in proximity of the horizontal beams (Figure 4-5). The lower floor is placed at a height of 9.5m with respect of the vault of the third portion of the shaft and it is made of timber. At the level of the second floor, also made of timber, the computer used for the continuous monitoring is positioned. The third floor is placed just below the small windows of the belfry and it made of concrete (Figure 4-6). It is not connected to the metal structure. In fact, the floor is perforated in proximity of each profile. The fourth floor is located at the level of the arched windows and it is made of timber. A waterproof layer applied on the floor protect the interior part of the belfry from the rain. The four bells are placed at the top of the structure (Figure 4-7). Eight principal types of metal profiles are identified, see Figure 4-3. Metal plates with different shapes and thickness are used in connections. They are joint with profiles by means of bolts (Figure 4-8). Additional elements constitute the oblique lateral supports (Figure 4-9). In general, the structure appears in good state of conservation. However, deformed and corroded elements are found. Some bolts are disintegrated by corrosion, see Figure 4-10. The estimated weight of the metal structure is 5,500kg, whereas the estimated weight of the bells is 4,500kg (10,000kg in total). The results are consistent with previous studies [24]. Additional details about the metal structure are provided in Annex 1.

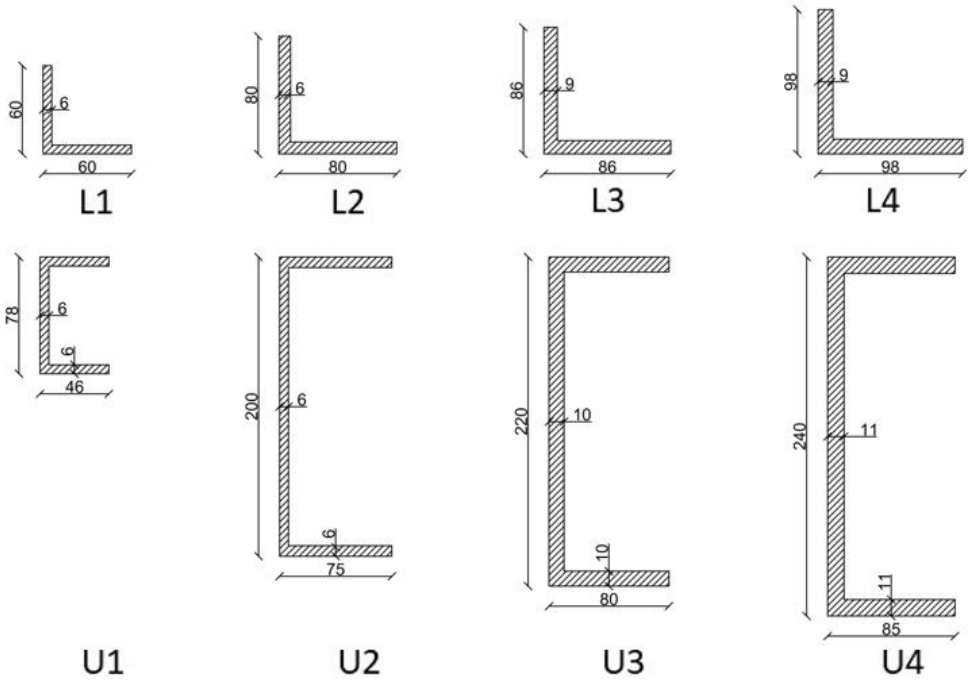

Figure 4-3 Principal metal profiles identified in the metal structure

Figure 4-4 Beams embedded in the shaft

Figure 4-5 First and second level of the metal structure

Figure 4-6 Concrete floor crossed by the metal structure

Figure 4-7 Upper part of the metal structure, in correspondence of the belfry, where bells are located

Figure 4-8 Example of connection between profiles

Figure 4-9 Example of oblique lateral support

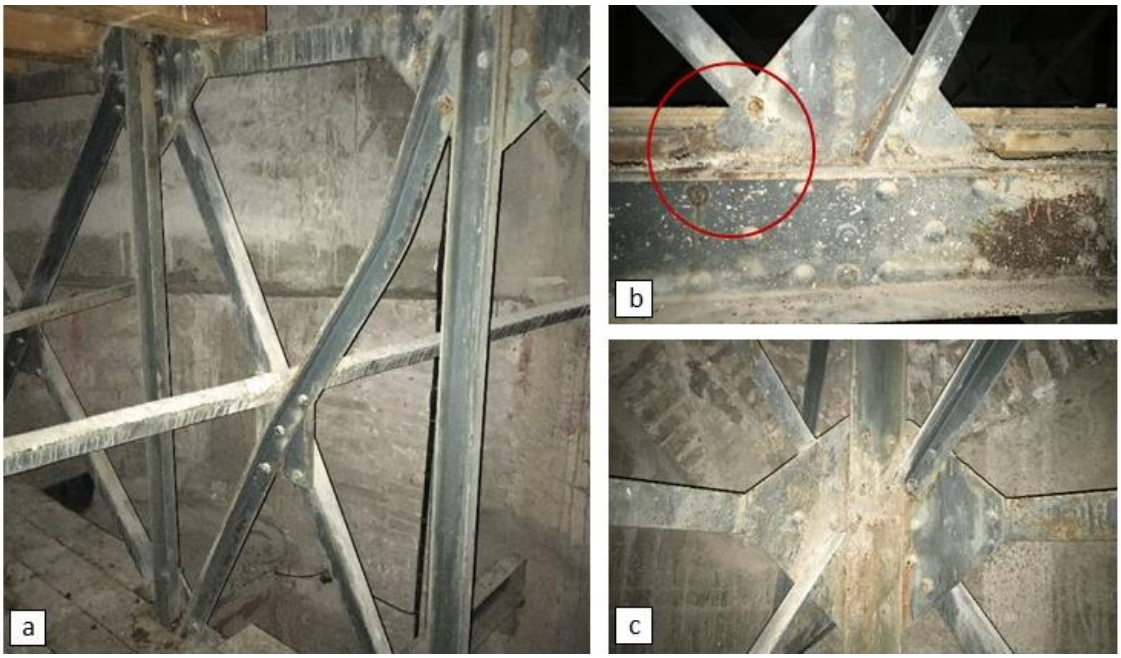

Figure 4-10 Metal structure decay: a) deformations, b) corrosion of connectors, c) corrosion of profiles

4.2 Experimental dynamic identification

In this chapter, data from AVT2 and from the most recent AVT (here called AVT3) are elaborated and the results compared. The former AVT was carried out before the 2016-2017 Central Italy earthquakes, the latter AVT was carried out in May 2017 after these seismic events.

4.2.1 AVT2 – Pre-earthquakes conditions

AVT2 was carried out on February 2015, see 3.3.3. Six uniaxial piezoelectric accelerometers were used in total. They were placed at two levels, at the height 26.8m, and 41m. At each level, three sensors were positioned, along the directions X, -Y and Y respectively. The additional accelerometer in direction Y was necessary to detect torsion modes. The layout of the sensors is shown in Figure 3-17. Data were processed with the software ARTeMIS 5.0 in which numerous Operational Modal Analysis estimator are available. In this study, the Enhanced Frequency Domain Decomposition (EFDD) and the Stochastic Subspace Identification – Principal Components (SSI-PC) are used, see Figure 4-11 and Figure 4-12. The results (natural frequencies, damping ratios and mode shapes) are considered cross-validated when the same modes are recognized with different identification techniques. Data belonging to a different time window was used with respect to the one used in previous works. Four modes are identified: the first two bending modes, f_{x1} and f_{y1}, the torsional mode, f_{t1}, and the other mode in the X direction, f_{x2}. Natural frequencies and relative damping ratios are shown in Table 4-5. MAC values between mode shapes are computed, see Table 4-6. The identified mode shapes are shown in Figure 4-13. Mode shapes obtained with the two different techniques appear quite similar since the MAC values are close to the unity. It was not possible to find all the seven modes found in previous studies. In particular, the third mode in X direction, f_{x3}, and the other modes in Y direction were not identified. The reason may be due to the different time window (excitation conditions) used or to the different dynamic identification techniques.

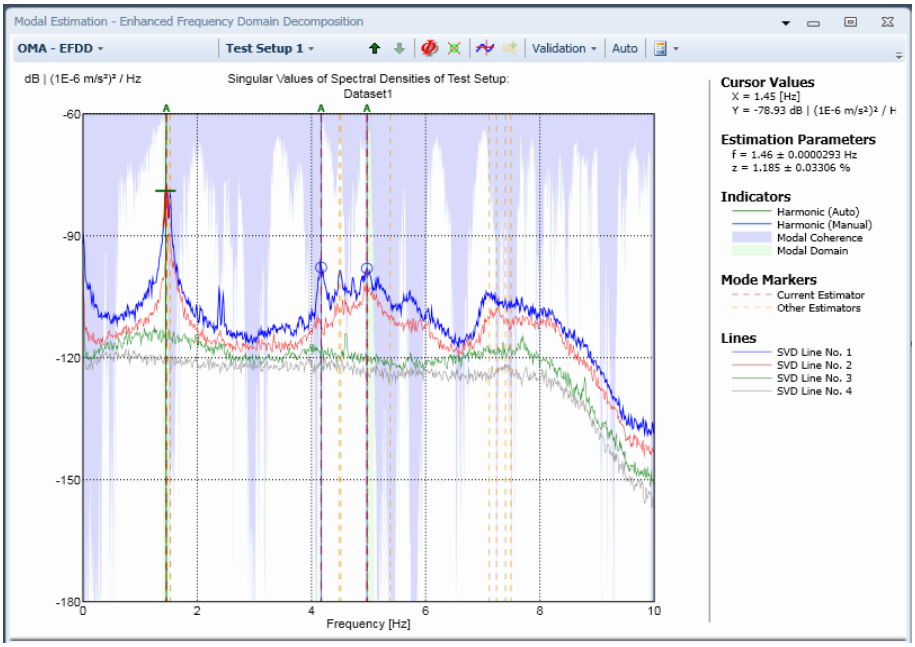

Figure 4-11 Typical results from EFDD

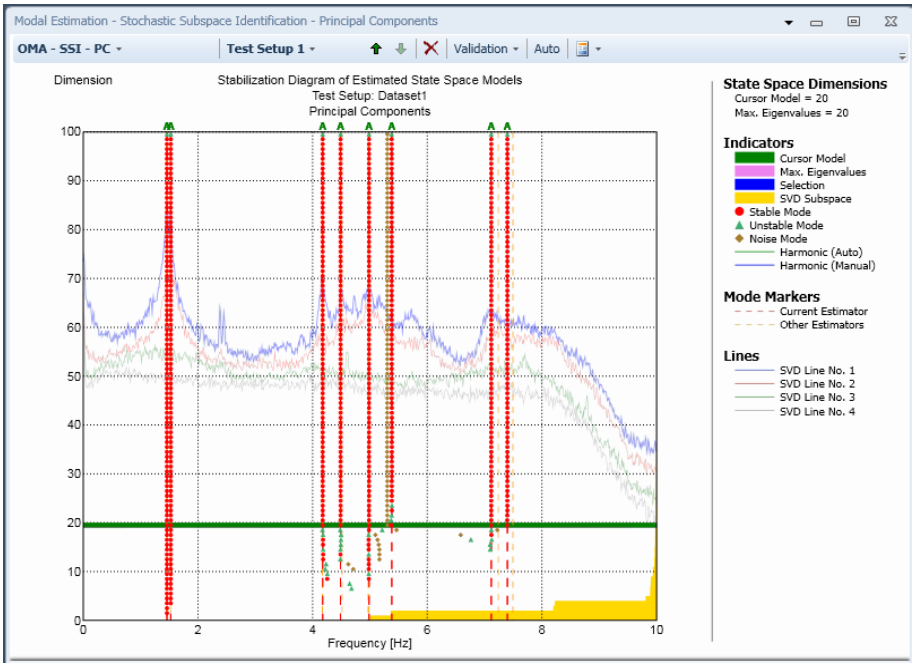

Figure 4-12 Typical results from SSI-PC

Table 4-5 AVT2 results: frequencies and relative damping

Mode number	EFDD		SSI-PC		Mode Type
	Frequency [Hz]	Damping [%]	Frequency [Hz]	Damping [%]	
I	1.458	1.131	1.455	1.014	Fx1
II	1.526	0.774	1.525	1.113	Fy1
III	4.357	1.217	4.376	2.560	T1
IV	4.617	0.171	4.620	3.136	Fy2

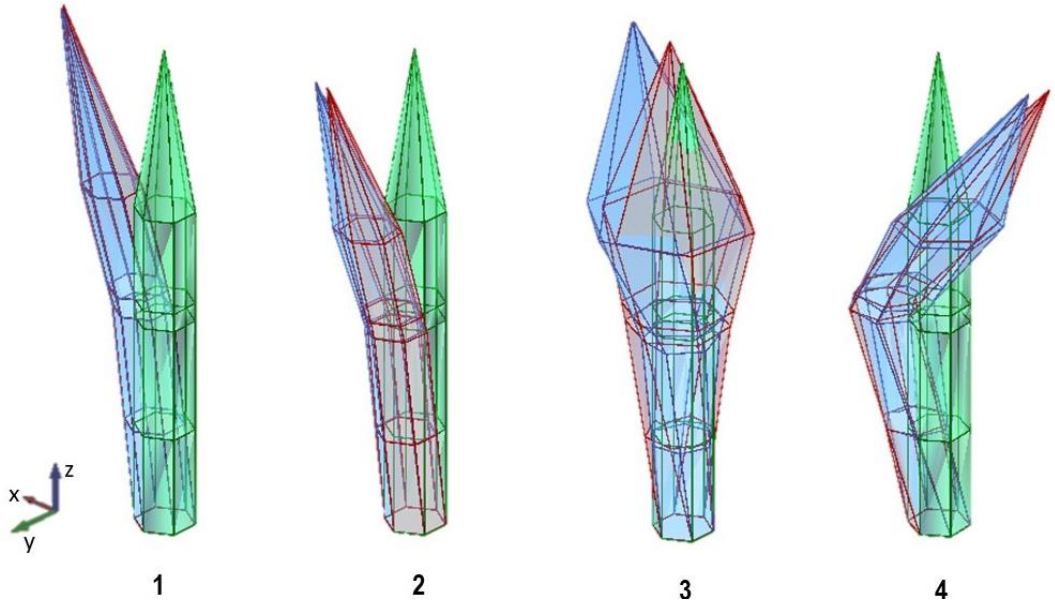

Figure 4-13 Identified mode shapes: undeformed structure in green, EFDD estimator in red, SSI-PC estimator in blue

Table 4-6 Scalar MAC between mode shapes

	EFDD	1.458 [Hz]	1.526 [Hz]	4.357 [Hz]	4.617 [Hz]
SSI-PC	1.455 [Hz]	0.999	0.013	0.082	0.065
	1.525 [Hz]	0.003	0.982	0.002	0.052
	4.376 [Hz]	0.035	0.010	0.979	0.355
	4.620 [Hz]	0.035	0.010	0.025	0.921

4.2.1 AVT3 – Post earthquakes conditions

On May 18th, a new AVT was carried out on San Pietro bell tower. The objective was to detect any changes in the dynamic properties of the tower following the 2016-2017 earthquakes as well as better characterize the mode shapes by means of a higher number of sensors. Twelve uniaxial piezoelectric accelerometers, model PCB 393B12, were used in total. They were placed at four levels, at the height of 21m, 26.8m, 29.1m, and 41m. At each level, three sensors were positioned, along the directions X, -Y and Y respectively. The additional accelerometer in Y direction was necessary to detect torsion modes. The data were acquired using a 24-channel system, carrier model cDAQ-9184, with NI 9234 data acquisition modules. The layout of the sensors is shown in Figure 4-14. Data were recorded for two hours and a half. The investigation was performed in a quite windy day (wind average velocity of 7 km/h [38]). Data from AVT2 are analysed with the software ARTeMIS with the same methodology described in the previous section. Six modes are found: the first three modes (the bending modes f_{x1} and f_{y1} and the torsional mode f_{t1}), the second mode in y direction, and the other two modes in the X direction (f_{x2} and f_{x3}). Natural frequencies and relative damping ratios are shown in Table 4-7. Furthermore, MAC values between mode shapes are computed, see Table 4-8. The identified mode shapes are shown in

Figure 4-15. The mode shapes obtained with the two different identification techniques appear quite similar since the MAC values are close to the unity. In this case, it was possible identifying a higher number of mode shapes with respect to those relative to AVT2. However, the third mode in y direction, f_{y3}, was not identified. The twelve

accelerometers used allowed to better estimating the mode shapes of the monument, especially as far it concerns the higher modes which result more complex to described.

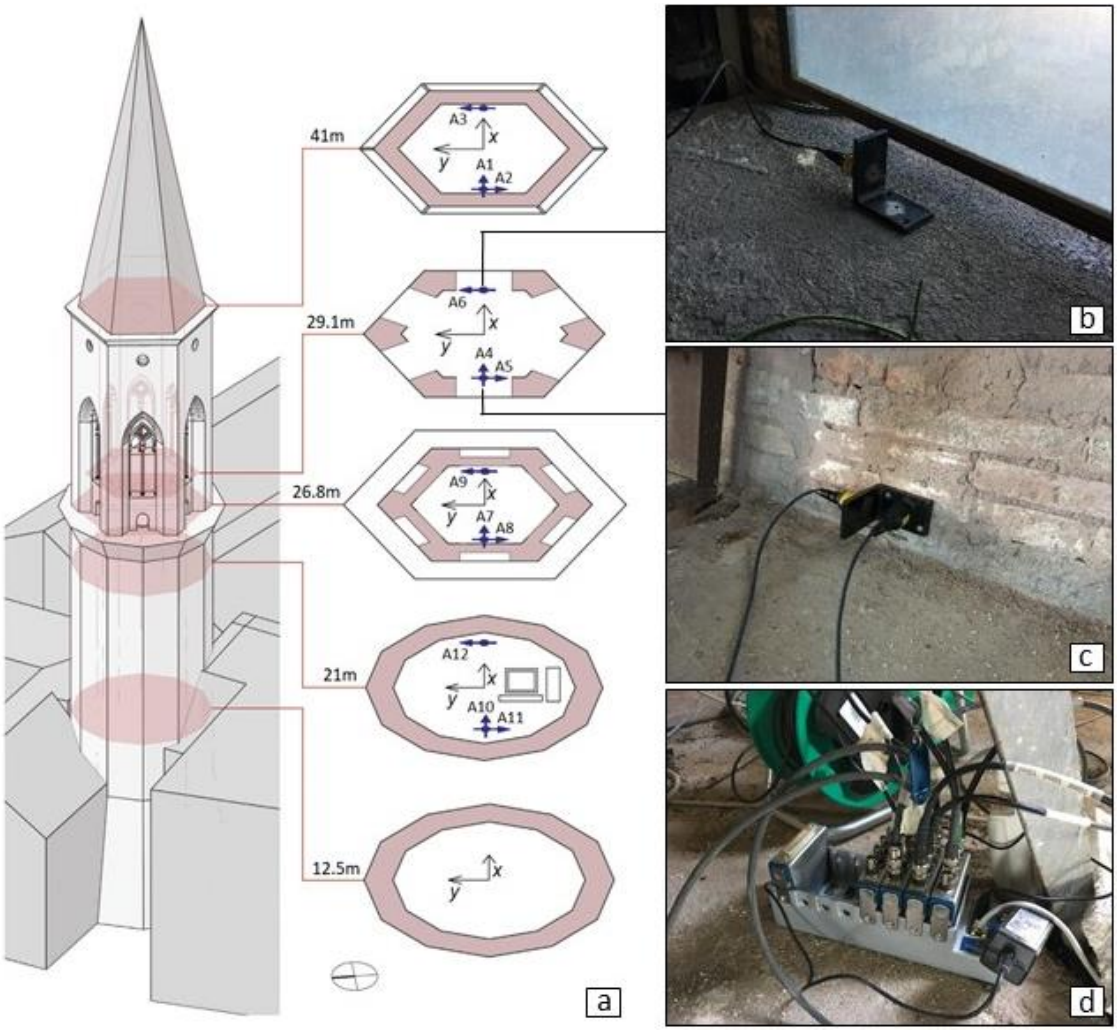

Figure 4-14 a) Localization of uniaxial accelerometers in the tower b) Accelerometer in Y-direction c) Accelerometers in X- and Y-direction d) Data acquisition system and cables.

Table 4-7 AVT3 results: frequencies and relative damping

Mode number	EFDD		SSI-PC		Mode Type
	Frequency [Hz]	Damping [%]	Frequency [Hz]	Damping [%]	
I	1.460	1.185	1.458	0.802	Fx1
II	1.526	0.488	1.526	0.730	Fy1
III	4.169	0.942	4.176	1.141	T1
IV	4.500	0.430	4.487	0.923	Fy2
V	4.972	1.219	4.983	2.218	Fx2
VI	7.252	0.056	7.116	2.223	Fx3

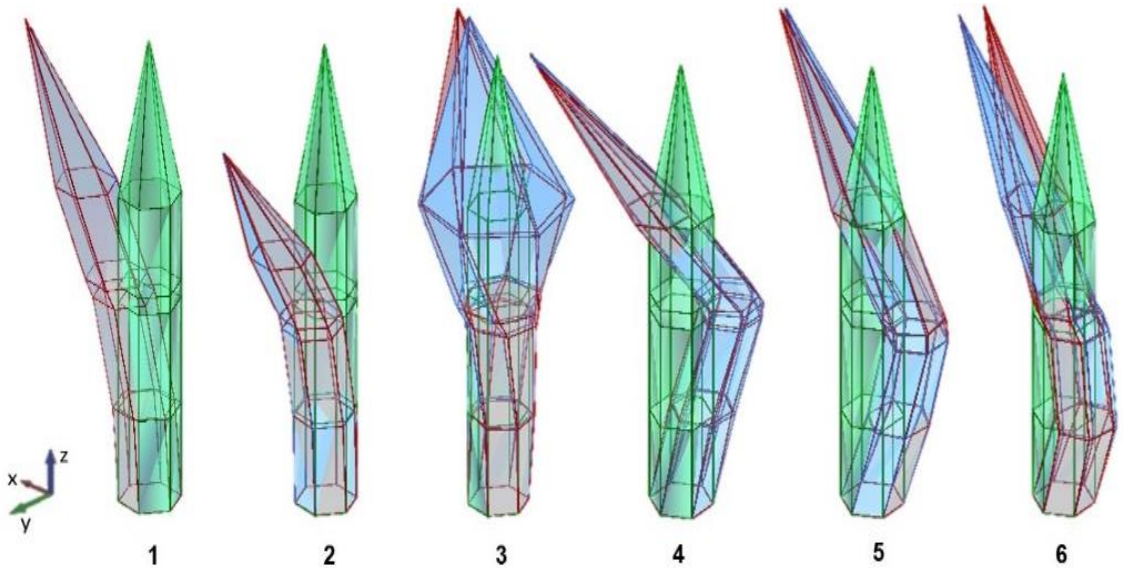

Figure 4-15 Identified mode shapes: undeformed structure in green, EFDD estimator in red, SSI-PC estimator in blue

Table 4-8 Scalar MAC between mode shapes

	EFDD	1.460 [Hz]	1.526 [Hz]	4.169 [Hz]	4.500 [Hz]	4.972 [Hz]	7.252 [Hz]
SSI-PC	1.458 [Hz]	0.999	0.003	0.011	0.007	0.009	0.352
	1.526 [Hz]	0.004	0.991	0.005	0.014	0.000	0.007
	4.176 [Hz]	0.012	0.008	0.944	0.016	0.032	0.097
	4.487 [Hz]	0.007	0.016	0.063	0.929	0.461	0.336
	4.983 [Hz]	0.008	0.001	0.082	0.539	0.993	0.507
	7.116 [Hz]	0.326	0.045	0.165	0.285	0.444	0.920

4.3 Result comparison

Data belonging to AVT3 allowed the estimation of a higher number of modes with respect to those identified after AVT2. The reason may be attributed neither to the higher number of sensor used in AVT3 or the higher level of excitation of the tower, since it was a quite windy day. As far as it concerns frequencies, the first two bending modes do not present significant changes. The first torsional mode and the second mode in X direction present more significant modifications. They may be caused by the occurrence of damages or by the effects of environmental factors. The mode shapes obtained in the two AVT are quantitatively compared by means of MAC, see Table 4-9.

Table 4-9 Result comparison by means of MAC values

Mode type	Frequencies [Hz] - EFDD		Δ(%)	MAC	Frequencies [Hz] – SSI-PC		Δ(%)	MAC
	AVT2	AVT3			AVT2	AVT3		
Fx1	1.458	1.460	+0.14	0.978	1.455	1.458	+0.21	0.987
Fy1	1.526	1.526	<0.01	0.969	1.525	1.526	+0.07	0.979
T1	4.357	4.169	-4.31	0.908	4.376	4.176	-4.57	0.738
Fy2	/	4.500	/	/	/	4.487	/	/
Fx2	4.617	4.972	+7.69	0.694	4.620	4.983	+7.86	0.818
Fx3	/	7.252	/	/	/	7.116	/	/

In general, the results show high values of MAC factors. This is even truer for the first two modes which present MAC close to unity. The mode shapes identified with the EFDD estimator and with the SSI-PC estimator are shown in Figure 4-16 and Figure 4-17, respectively.

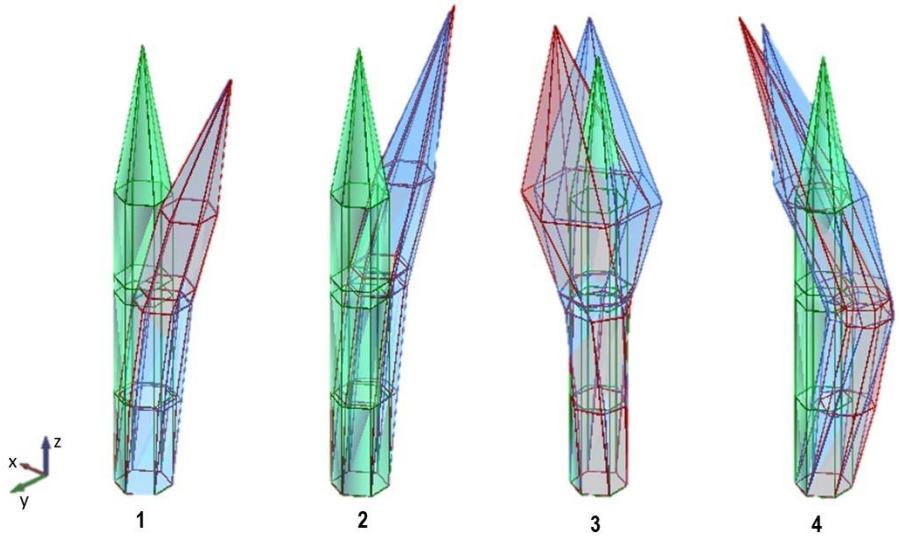

Figure 4-16 Identified mode shapes, EFDD estimator: undeformed structure in green, results from AVT3 in red, results from AVT2 in blue

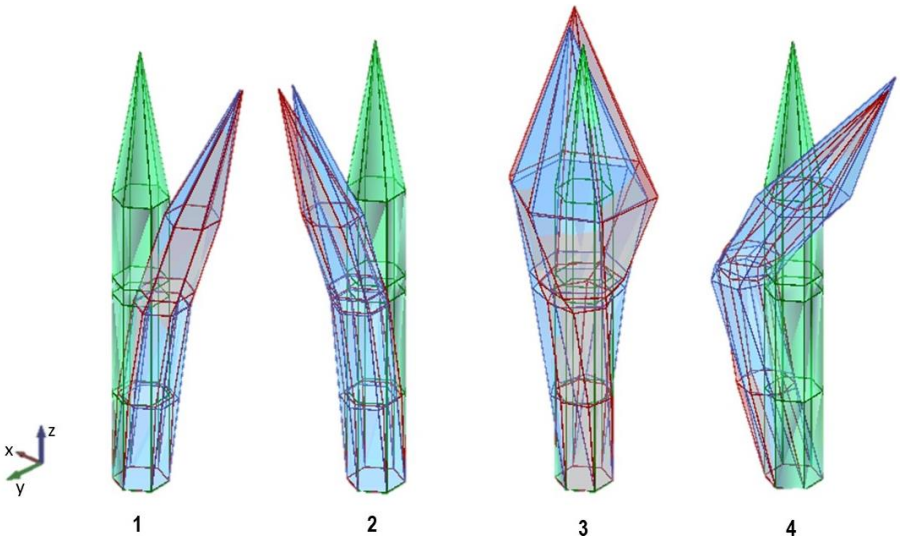

Figure 4-17 Identified mode shapes, SSI-PC estimator: undeformed structure in green, results from AVT3 in red, results from AVT2 in blue

4.4 Experimental sonic testing

Both indirect and direct sonic tests were performed to characterize materials. The indirect tests were carried out on the shaft in correspondence of: (1) interior stone masonry; (2) interior brick masonry; (3) exterior stone masonry; (4) exterior brick masonry. The direct tests were conducted in proximity of the entrance door and the window of the shaft, where both sides of the wall could be reached.

Figure 4-18 Equipment for sonic test: uniaxial accelerometer, hammer, ruler (from left to right)

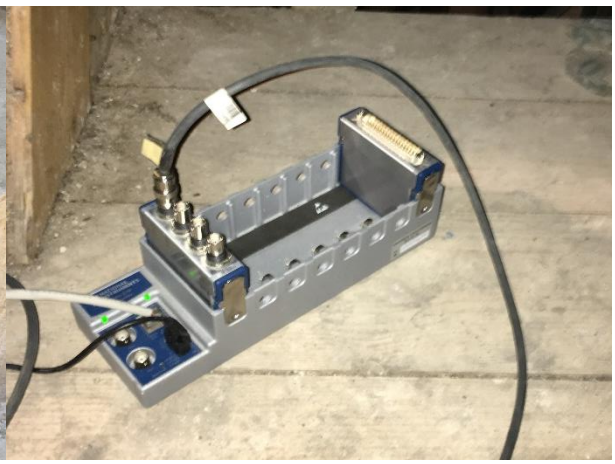

Figure 4-19 Acquisition system

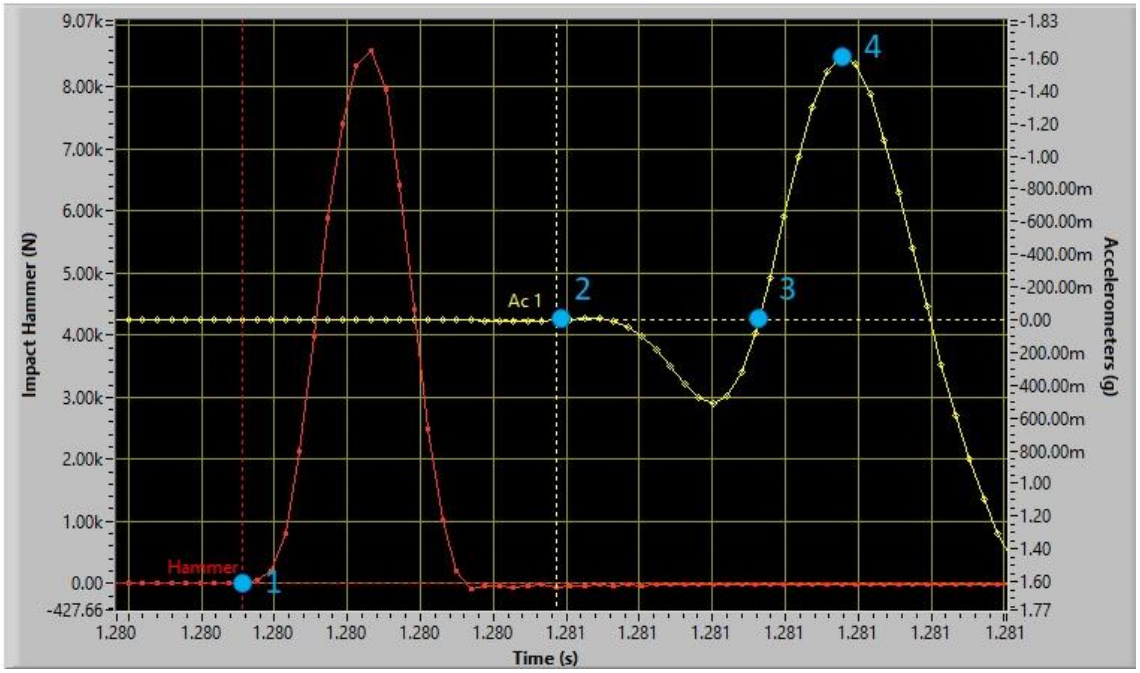

Figure 4-20 Typical sonic test result: the red curve corresponds to the signal of the hammer whereas the yellow one is the signal recorded by the accelerometer. Point 1: impact of the hammer. Point 2: P-waves arrival. Point 3: R-waves arrival. Point 4: R-wave maximum value

The equipment used consisted in hammer, accelerometer, DAQ system, personal computer, and relative cables, see Figure 4-18 and Figure 4-19. Data are acquired with a sampling frequency of 50,000 Hz. The software Sonic Acquier V1.6 and Sonic Analyzer V5 were used to acquire and analyze the data, respectively. It is worth noticing that the walls of the shaft are made of three leaves masonry. For this reason, the indirect sonic tests allow to characterize only exterior layers of the structure. The investigation is integrated with the direct sonic tests which provide additional information about the inner portion of the wall. The results are presented in the following paragraphs. In Figure 4-20 the typical output from a sonic test is shown. Once the distance between accelerometer and impact area of the hammer is assigned, the software allows to select the wave velocities moving the dedicated cursor to the point corresponding to P-waves and R-waves arrivals, respectively.

4.4.1 Material characterization – indirect tests

Interior stone masonry

The interior leaf of the shaft is made of homogeneous grey limestone masonry. The analyzed area is shown in Figure 4-21 and it is located in the lower part of the third division of the shaft. The test was performed in 4 points, roughly 20 cm apart. The distance assumed between accelerometer and impact area of the hammer is 0.6 m and 1.00 m. The results are shown in Table 4-10.

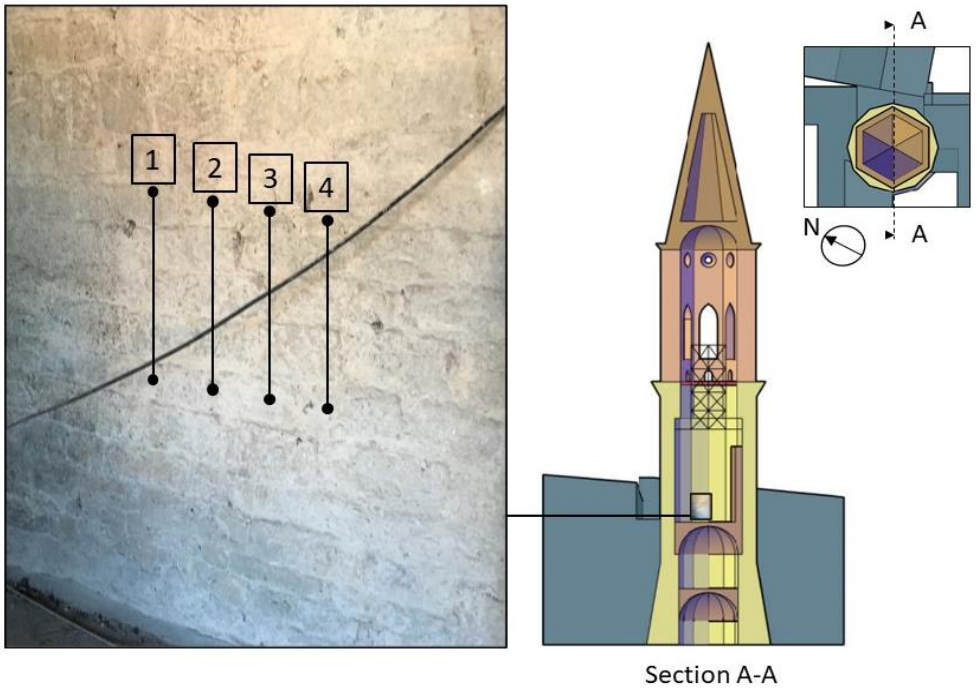

Figure 4-21 Interior stone masonry: investigated area and its localization in the bell tower

Table 4-10 Interior stone masonry: sonic test results – 0.60 m

Point	Mean velocity [m/s]		Coefficient of variation [%]	
	Wp	Wr	Wp	Wr
1	3070.6	1349.0	0.3	3.3
2	2736.0	1304.8	12.1	5.6
3	2650.4	1427.6	4.3	6.1
4	2814.6	1444.2	8.2	7.6
Average	2817.9	1381.4	9.3	7.2

Table 4-11 Interior stone masonry: sonic test results – 1.00 m

Point	Mean velocity [m/s]		Coefficient of variation [%]	
	Wp	Wr	Wp	Wr
1	3432.8	1408.4	6.9	3.6
2	3421.4	1378.4	4.2	4.1
3	3092.8	1326.8	6.3	2.7
4	3563.0	1384.8	3.4	2.8
Average	3377.5	1374.6	7.4	4.0

Interior brick masonry

The brick masonry stairs are studied (Figure 4-22). They allow to reach the metal structure and therefore the upper levels of the monument. The test was performed in 4 points, roughly 20 cm apart. The distance assumed between accelerometer and impact area of the hammer is 0.6 m. The results are shown in Table 4-12.

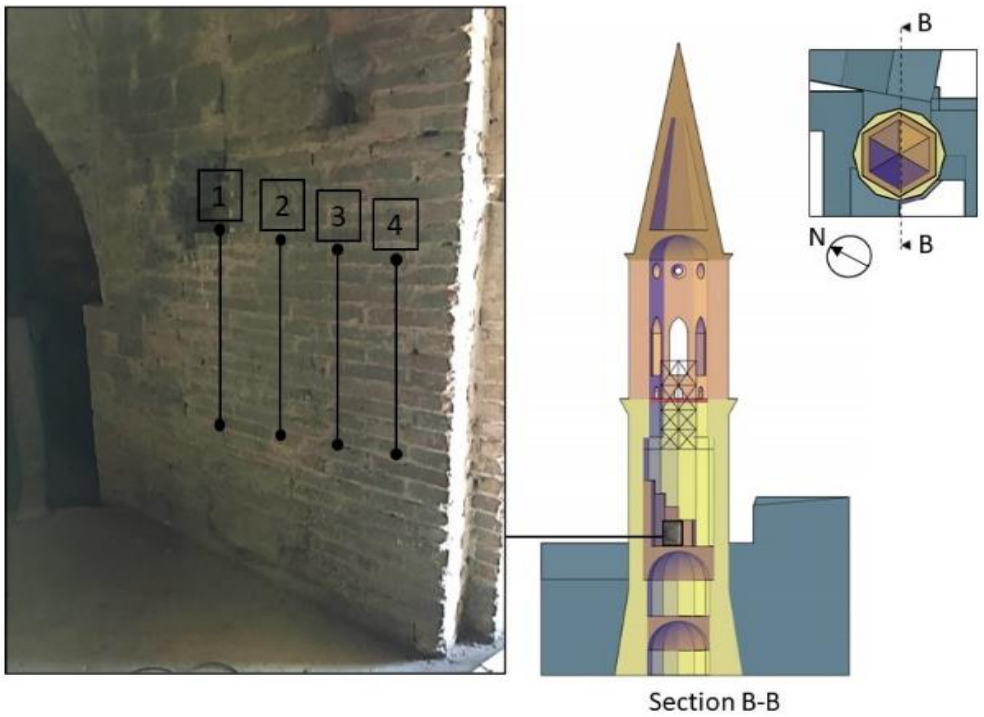

Figure 4-22 Interior brick masonry: investigated area and its localization in the bell tower

Table 4-12 Interior brick masonry: sonic test results

Point	Mean velocity [m/s]		Coefficient of variation [%]	
	Wp	Wr	Wp	Wr
1	1186	495.8	6.5	2.3
2	1234.4	489.2	6.4	2.2
3	1492.0	616.6	3.8	1.4
4	1600.4	598.8	2.0	4.5
Average	1378.2	550.1	13.4	10.9

Exterior stone masonry

The exterior leaf of the shaft can be reached in correspondence of the terrace adjacent to the entrance door of the tower. The masonry is made of grey and pink limestone. The analyzed area is shown in Figure 4-23. The test was performed in 3 points. Due to the morphology of the surface, it was not possible to execute the test at regular intervals. The distance assumed between accelerometer and impact area of the hammer is 0.6 m and 1.00 m. The results are shown in Table 4-13.

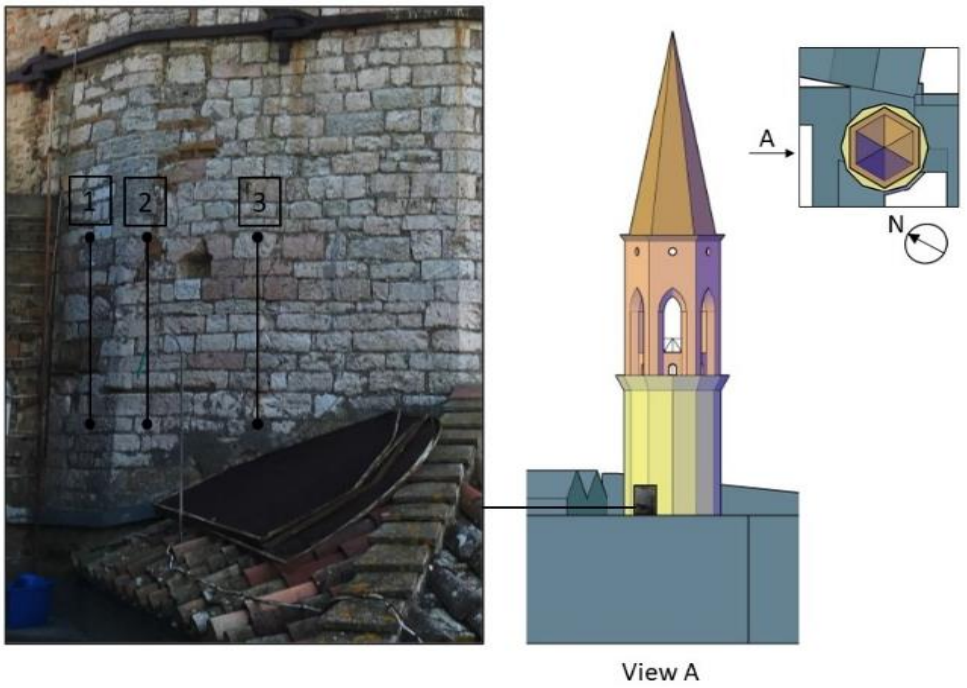

Figure 4-23 Exterior stone masonry: investigated area and its localization in the bell tower

Table 4-13 Exterior stone masonry: sonic test results – 0.60m

Point	Mean velocity [m/s]		Coefficient of variation [%]	
	Wp	Wr	Wp	Wr
1	2236.4	1052.6	6.8	3.3
2	2136.4	1173.4	3.4	2.8
3	2236.4	1364.0	6.9	6.1
Average	2203.1	1196.7	6.4	11.7

Table 4-14 Exterior stone masonry: sonic test results – 1.00m

Point	Mean velocity [m/s]		Coefficient of variation [%]	
	Wp	Wr	Wp	Wr
1	2701.4	1004.2	4.7	1.8
2	3327.8	1248.8	3.1	1.5
3	3208.0	1355.0	4.0	1.0
Average	3079.1	1202.7	9.6	12.3

Exterior brick masonry

A metal ladder placed on terrace adjacent to the entrance door of the tower allows accessing the roof of the monastery. Here, the exterior brick masonry can be reached and studied without scaffolding. The area analyzed is shown in Figure 4-24. Bricks were used in the past for reparation works. The test was performed in 3 points, roughly 20cm apart. The distance assumed between accelerometer and impact area of the hammer is 0.6m. The results are shown in Table 4-15.

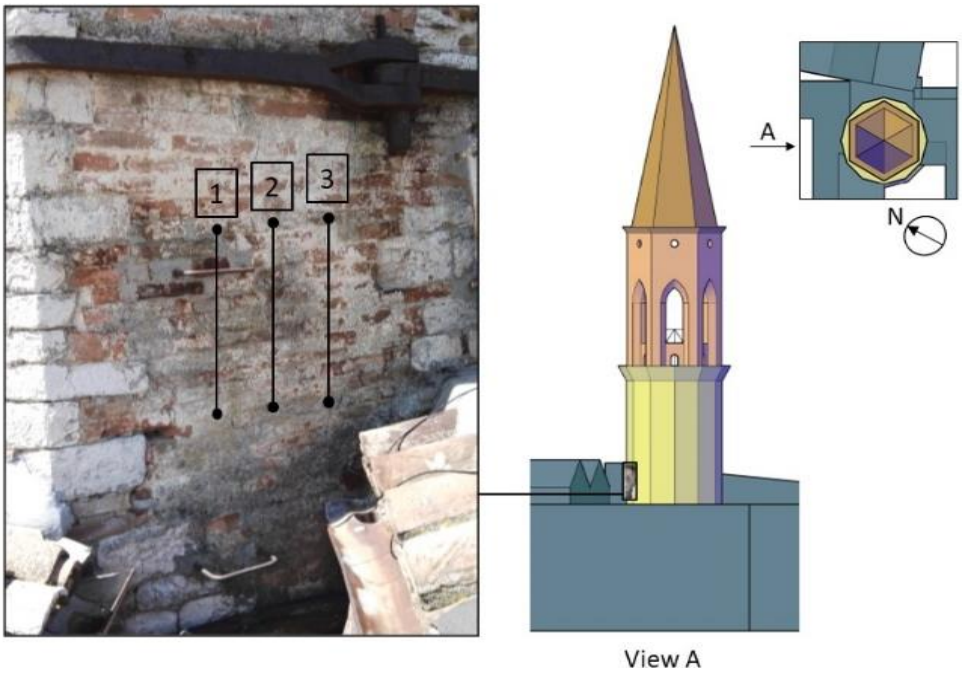

Figure 4-24 Exterior brick masonry: investigated area and its localization in the bell tower

Table 4-15 Exterior brick masonry: sonic test results

Point	Mean velocity [m/s]		Coefficient of variation [%]	
	Wp	Wr	Wp	Wr
1	1451.8	738.4	4.7	1.9
2	1074.4	533.6	1.7	0.8
3	1131	441.2	4.2	1.7
Average	1219.1	571.1	14.2	21.8

4.4.2 Material characterization – direct tests

Window

In proximity of the window of the shaft, which is located under the masonry stairs, it is possible to reach both side of the wall. Here, the thickness of the masonry is 1.35m. Due to the presence of a protection net against birds, the sonic test was performed only in one point, at a distance of 0.35m from the opening. The results are shown in Table 4-16.

Door

Additional direct tests were performed in proximity of the entrance door of the shaft. Two points were investigated, one on each side of the opening, respectively (see Figure 4-26). The thickness of the masonry is 1.40m. The sonic tests were performed at a distance of 0.70m from the opening. The results are shown in Table 4-17.

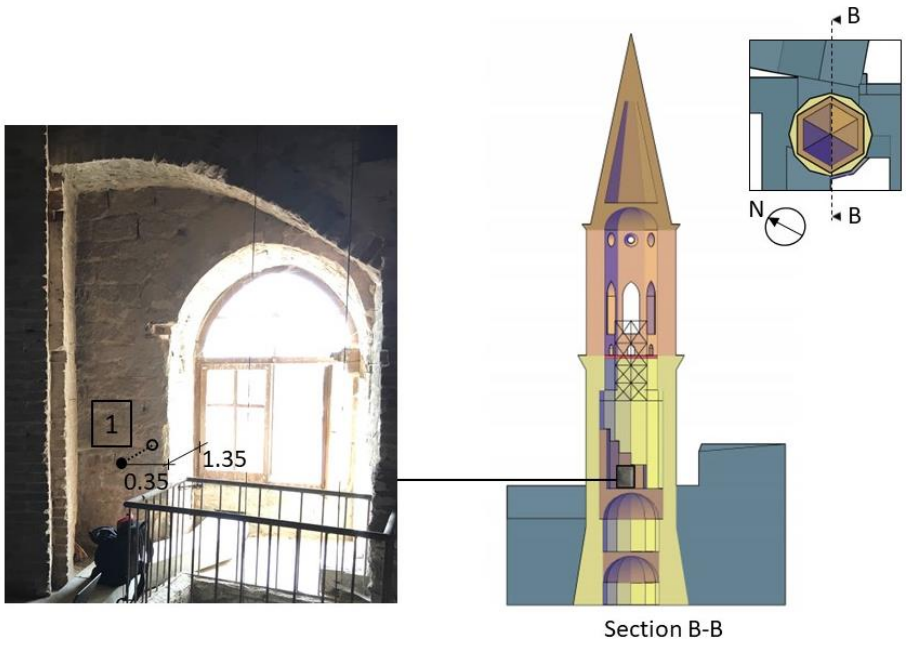

Figure 4-25 Window: investigated area and its localization in the bell tower

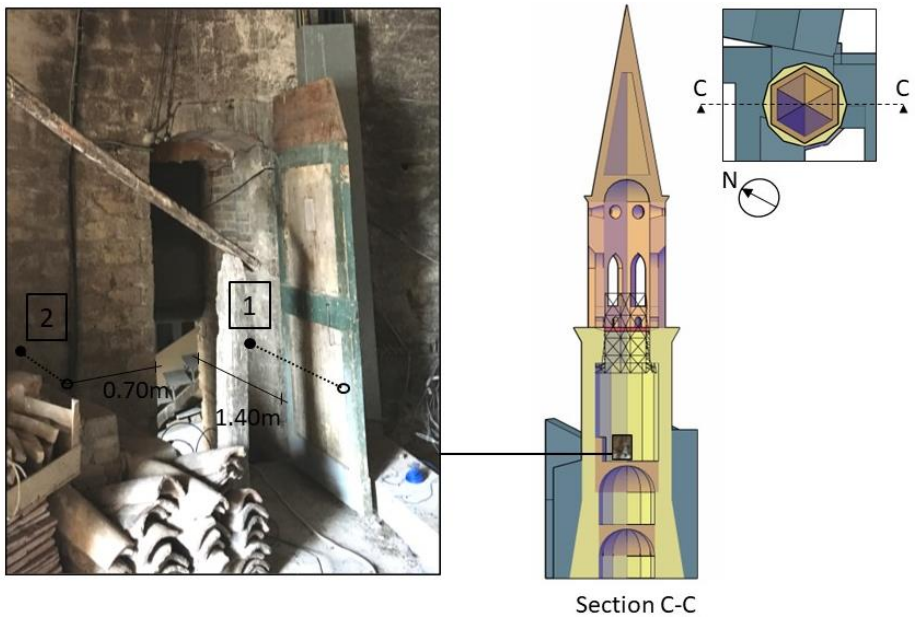

Figure 4-26 Door: investigated area and its localization in the bell tower

Table 4-16 Window: sonic test results

Point 1	Mean velocity, Wp [m/s]	Coefficient of variation [%]
1	2882.3	2.96

Table 4-17 Door: sonic test results

Point	Mean velocity, Wp [m/s]	Coefficient of variation [%]
1	2526.6	3.6
2	2085.2	2.3
Average	2305.9	10.1

4.4.3 Estimation of masonry mechanical properties

The values of wave velocities are used to estimate the elastic moduli of materials by means of the relations shown in paragraph 2.8. The ratio between the static and dynamic moduli of elasticity of the leaf is assumed equal to 0.8. The ratio between the dynamic modulus of the leaf and the static modulus of the entire wall is assumed equal to 0.5. The results are shown in Table 4-18.

Table 4-18: Estimated material properties

	Wr/Wp	Poisson's modulus, v	Density [kg/m^3]	Dynamic elastic modulus, E_d [GPa]	Static elastic modulus, E_s [GPa]	Masonry elastic modulus, E [GPa]
Interior stone masonry – 0.60m	0.49	0.31	2200	12.68	10.14	6.34
Interior stone masonry – 1.00m	0.41	0.39	2200	12.68	10.14	6.34
Interior brick masonry	0.40	0.39	1800	1.67	1.33	/
Exterior stone masonry – 0.60m	0.54	0.22	2200	9.29	7.43	4.65
Exterior stone masonry – 1.00m	0.39	0.40	2200	9.78	7.83	4.89
Exterior brick masonry	0.40	0.39	1800	1.78	1.42	/

Concerning the indirect tests on stairs and the exterior brick leaf, the estimated values of the elasticity modulus E_s are comparable to the masonry category "Solid brick masonry with lime mortar" (Muratura in mattoni pieni e malta di calce) found in the Italian code in Table C8A.2.1 [37], see Table 4-19. Therefore, the results of the sonic test on brick masonry con be considered reliable. Moreover, varying the distance between accelerometer and impact area of the hammer the results are almost coincident. The results are comparable with those obtained in previous works after the model calibration, see chapter 3.3.6. The high values of wave velocity found with the direct tests in proximity of the door confirm to some extend the good quality of the masonry of the shaft. In fact, the results indicate that the inner material of the three leaves masonry of the shaft presents high density and therefore good mechanical properties. The high values of wave velocity found in the masonry close to the window may be explained by the presence of bigger size stones in proximity of the opening. The estimated values of the Elastic modulus of the stone masonry of the shaft by means of indirect tests appear significantly higher than the values found with the MQI method. However, as previously explained, the results of the sonic test appear more trustworthy. The results of model calibration, reported in the following chapter, will provide additional information about material characterization.

Table 4-19 Extract from Table C8A.2.1. of Circ. NTC08

Masonry typology	f_m (N/mm2)	τ_0 (N/mm^2)	E (N/mm^2)	G (N/mm^2)	W (kN/m^3)
	min-max	min-max	min-max	min-max	
Solid brick masonry with lime mortar	2.4 4.0	0.060 0.090	1200 1800	400 600	18

4.5 Conclusion

The purpose of this chapter was to present the latest studies carried out on San Pietro bell tower, which consisted of visual survey, AVT, and sonic tests.

Generally, the monument appear in good state of conservation, at least from the structural point of view. It is now trivial to localize eventual damages caused by the last earthquakes. The only exception is constituted by some cracks that can be found in the lower portion of the belfry, in correspondence of the masonry arches above the six small windows. It is well known that the belfry is the most vulnerable part of this type of structures. The ordinary maintenance of the bell tower may be improved.

The MQI method applied on the masonry of the shaft provide low values of elastic modulus. Actually, this method was calibrated on ordinary Italian masonry walls. It may not be convenient using it on the circular walls of a masonry tower, of considerable thickness.

A survey was carried out on the metal structure supporting the four bells. The principal constitutive elements were identified and the geometrical features reported. This structure appears in contact with the bell tower only in proximity of the lower beams which are embedded in the masonry of the shaft. Indeed, it can been considered “a metal tower inside the masonry tower”. The estimated weight of the metal structure is in agreement with the results found in references.

Data from February 2015 AVT (AVT2) and from May 2017 AVT (AVT3) were analyzed and the results compared. The former corresponds to the pre-earthquakes condition, the latter to post-earthquakes condition. Four modes are found from AVT2: the first two bending modes, f_{x1} and f_{y1}, the torsional mode, f_{t1}, and the other mode in the X direction, f_{x2}. Six modes are found from AVT3: the first three modes (the bending modes f_{x1} and f_{y1} and the torsional mode f_{t1}), the second mode in Y direction, and the other two modes in the X direction (f_{x2} and f_{x3}). The higher number of modes found in AVT3 may be attributed neither to the higher number of sensor used or to the higher level of excitation of the tower, with respect to AVT2. The first two modes found in the two OMA are in great agreement, under the frequency and MAC point of view. The first torsional mode and the second mode in X direction present more significant modifications. They may be caused by the occurrence of damages or by the effects of environmental factors.

Both indirect and direct sonic tests were performed to characterize materials. The materials studied belong to the shaft of the tower: interior stone masonry, interior brick masonry, exterior stone masonry, and exterior brick masonry. The direct tests were conducted in proximity of the entrance door and the window of the shaft, where both sides of the wall could be reached. The values of wave velocities are used to estimate the elastic moduli of materials. Concerning the indirect tests on stairs and the exterior brick leaf, the estimated values of the elasticity modulus are comparable to the masonry category “Solid brick masonry with lime mortar found in the Italian code in Table C8A.2.1. The estimated values of the Elastic modulus of the stone masonry of the shaft are in agreement with the values estimated in previous works. The direct tests confirm the results obtained.

This page is left blank on purpose.

5. Numerical model

5.1 Introduction

This chapter is dedicated to the numerical model of San Pietro bell tower. The aim is to create a model which is able of representing the actual structural behavior of the monument. Numerical modeling of historic masonry buildings is not trivial. Their behavior is governed by innumerable variables, which are difficult to model and measure. In fact, these structures are made of composite materials, generally stone and mortar, whose characterization is affected by considerable uncertainty, both from the mechanical and geometrical point of view. For this reason, modeling of such structures is still a topic of discussion, for which different strategies exist. The choice between the different types of approach essentially depends on the purpose of the analysis. In this work, masonry is modelled by considering a homogeneous and equivalent material (macro-modeling), while the analysis is performed using the Finite Element (FE) method.

The implementation of the numerical model and the assumption made are described in the first part of this chapter. The methodology used is the following. First of all, the geometrical model was built with the software AutoCAD v.2015. Then, it was imported in the Pre-Processor environment FX+ v.3.3.0 [39] in order to create the Finite Element mesh and to assign the mechanical properties to materials. The analysis was carried out with the software DIANA v.10.1 [40] where Structural eigenvalue analyses are performed. The results are visualized in FX+ that serves also as Post-Processor.

Following, a sensitivity analysis is executed with the purpose of evaluating the influence of material properties on numerical outcomes. The results of the sensitivity analysis are used for model calibration. The mechanical parameters of masonry are updated until the dynamic behavior of the model is consistent with the experimental data. Not only the natural frequencies are compared but also the mode shapes by means of the MAC values. The model is calibrated twice, with the dynamic results obtained in both February 2015 AVT and May 2017 AVT.

An additional topic of this chapter is the study of the influence of the metal structure on the dynamic properties of the bell tower. In fact, it has been always neglected in previous works. Two models are built and their outcomes of the eigenvalue analyses are compared: a simplified model of the bell tower and a simplified model of bell tower plus metal structure.

The chapter is ended with conclusions

5.2 Implementation of the numerical model

A three dimensional representation of the bell tower is realized in AutoCAD v.2015 by means of solid elements, see Figure 5-1. The initial model is composed of cusp, belfry, shaft (with comprise also the basement), vaults, concrete floor, and stairs. Concerning the metal structure, it was taken into account by a rigid floor simulating the effect of the lower beams embedded in the masonry. The action of the adjacent buildings is modeled by considering a portion of them, as it was done in previous studies. Exterior masonry insertions, tie rods, confinement elements, FRP materials in the cusp, and small openings are neglected. The different elements forming the model are shown in Figure 5-2.

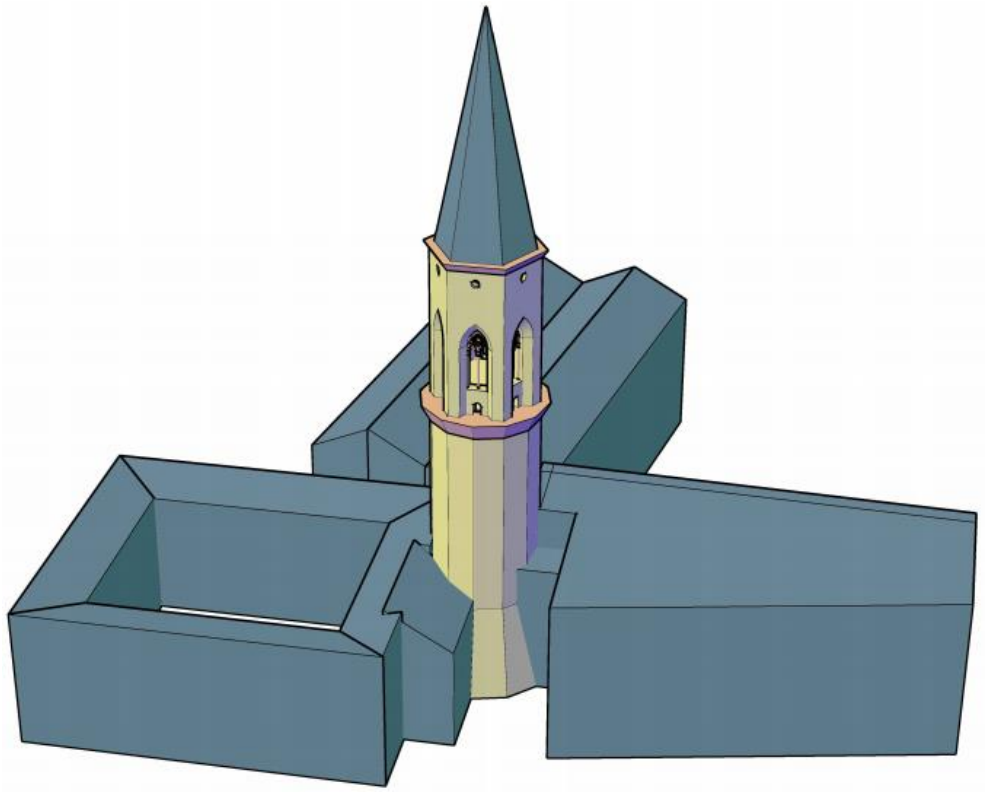

Figure 5-1 3D AutoCAD model of the bell tower

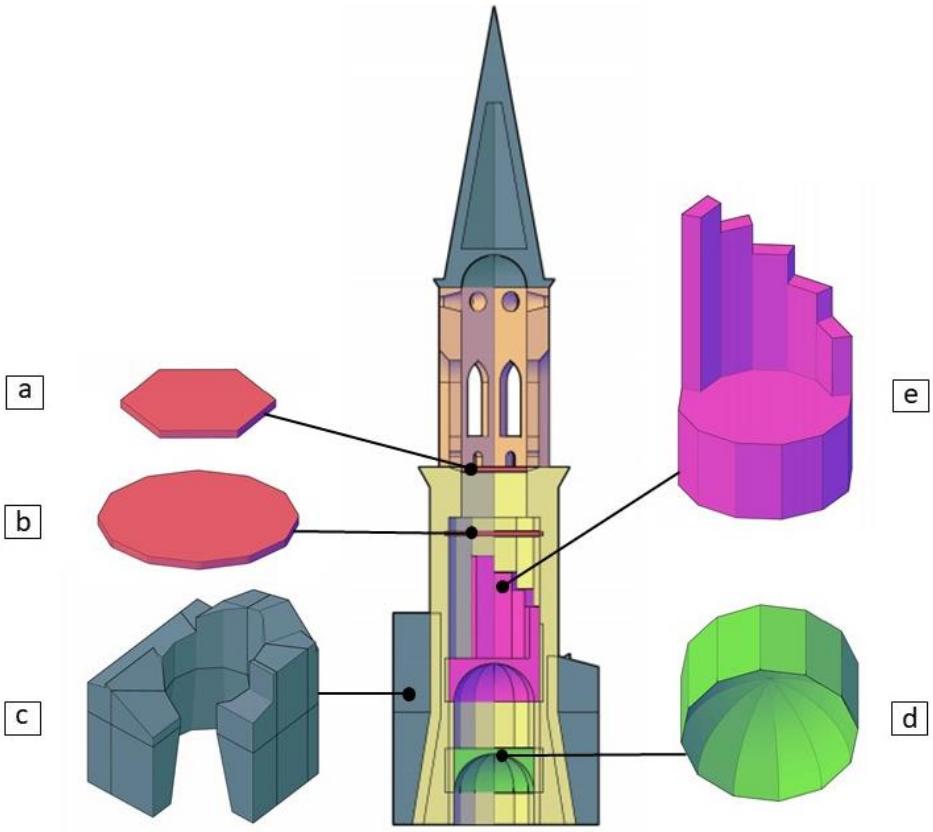

Figure 5-2 Section of the 3D AutoCAD model: (a) concrete floor, (b) rigid floor simulating the effect of the metal structure, (c) adjacent buildings, (d) lower vault of the shaft, (e) second vault of the shaft and stairs.

The solid elements are imported in FX+ in order to create the FE mesh and to assign the mechanical properties to materials. The Auto Mesh function of the software is used. The mesh is formed of 126 543 tetrahedral elements. The element size is set equal to 0.60 m. Details of the numerical model are shown in Figure 5-3.

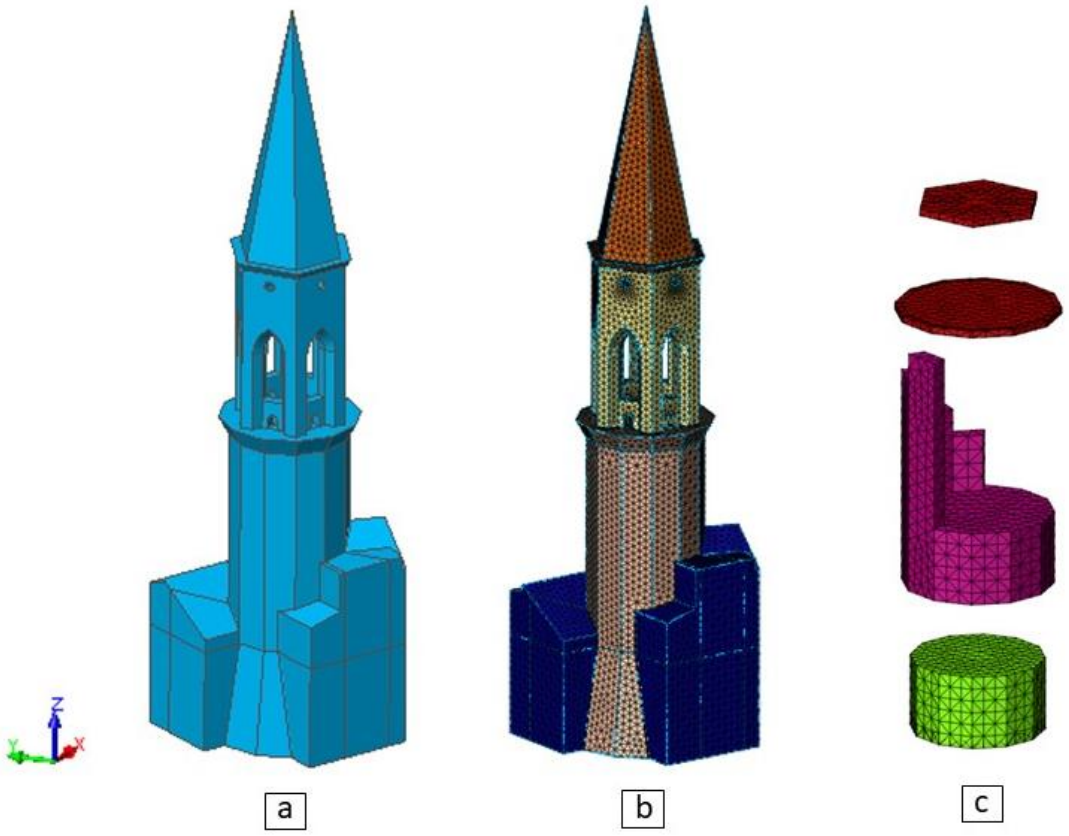

Figure 5-3 Numerical FEM model of the bell tower: (a) solid elements imported by AutoCAD, (b) FEM mesh, (c) particular of interior elements of the model.

Concerning material properties, the initial values were taken from Table C8A.2.1 of the Italian code [37]. The category "Dressed rectangular (ashlar) stone masonry" was assigned to the shaft whereas the category "Solid brick masonry with lime mortar" was assigned to cusp, belfry, vaults and stairs. However, the visual inspection on shaft and belfry highlight the good quality of the masonry of these structural elements. Therefore the multiplicative coefficient of Table C8A.2.2 [37] are applied, according to the code. The multiplicative coefficient are shown in Table 5-1. As far as concern the adjacent buildings, an equivalent homogeneous material is considered. The initial mechanical properties of materials are shown in Table 5-2. An elastic orthotropic model is assumed for masonry, whereas an elastic isotropic model is assumed for concrete. In the case study, the elasticity moduli are assumed equal in the three directions ($E_1 = E_2 = E_3, G_{12} = G_{23} = G_{13}$).

Table 5-1 Multiplicative coefficients from Table C8A.2.2 [37] considered for the case study

Structural element	Masonry typology	Good quality mortar	Thin mortar layers
Belfry	Solid brick masonry with lime mortar	1.5	/
Shaft	Dressed rectangular (ashlar) stone masonry	1.2	1.2

Table 5-2 Initial model: material properties

Element	Young's modulus [GPa]	Shear modulus [GPa]	Poisson modulus	Mass [kg]
Cusp	1.500	0.500	0.25	1800
Belfry	2.840	1.094	0.25	1900
Shaft	4.032	1.238	0.25	2200
Vaults and stairs	1.500	0.500	0.25	1800
Concrete floor	20.000	8.333	0.20	2500
Adjacent buildings	1.000	0.500	0.25	500

5.3 Sensitivity analysis

With the aim of performing a calibration of the EF model, a sensitivity analysis of natural frequencies was executed, varying the mechanical properties of the materials. Table 5-3 and Graph 5-1 summarize the results of this analysis expressed in terms of the coefficients of sensitivity calculated as:

$$S_{ik} = 100 \frac{X_k}{f_i^{FEM}} \frac{\Delta f_i^{FEM}}{\Delta X_k} \qquad 5\text{-}1$$

where X_k is the initial value of the mechanical property that is varied, f_i^{FEM} is the initial natural frequency, Δf_i^{FEM} is the variation in frequencies, ΔX_k is the variation of the mechanical properties assumed equal to the 100%. The coefficient is computed for variations in Young's modulus, Shear modulus and mass of cusp, belfry, shaft, vaults and stairs, and adjacent buildings.

The results show that variations in the mechanical parameters of vaults, stairs and adjacent buildings are not significant. Therefore they are not taken into account in the calibration phase. The first two natural frequencies are strongly dependent on the Young's moduli of belfry and shaft. The third frequency strongly depends on the stiffness of the belfry. The fourth and fifth frequencies are influenced mostly by the Young's modulus of the belfry. The sixth and seventh frequencies are mainly influenced by the Young's modulus of the cusp. The mass of the structural elements has strong impact on all frequencies.

Table 5-3 Sensitivity analysis coefficients

	Cusp			Belfry			Shaft			Vaults and stairs			Adj. buildings		
Mode	E	G	m	E	G	m	E	G	m	E	G	m	E	G	m
1	0.4	0.2	-21.7	6.8	2.0	-13.4	16.0	1.2	-2.3	0.3	0.1	0.0	3.6	1.1	0.0
2	0.4	0.2	-21.8	7.1	2.1	-13.4	15.0	1.2	-2.2	0.4	0.1	0.0	4.1	1.1	0.0
3	0.1	0.2	-13.6	12.1	15.2	-22.0	0.4	4.3	-1.0	0.0	0.1	0.0	0.2	0.7	-0.1
5	5.6	1.5	-16.4	9.3	0.3	-8.4	3.7	3.5	-14.4	0.1	0.3	-0.4	3.3	1.2	-0.7
4	5.4	1.5	-16.2	9.0	0.4	-8.4	3.5	4.1	-14.7	0.1	0.3	-0.4	3.3	1.1	-0.8
6	9.4	1.6	-11.7	6.4	4.2	-7.8	2.9	3.1	-9.6	0.1	0.3	-0.7	2.8	1.3	-1.5
7	9.5	1.6	-11.7	6.2	4.2	-7.7	2.4	3.5	-9.5	0.1	0.3	-0.8	3.0	1.0	-1.6

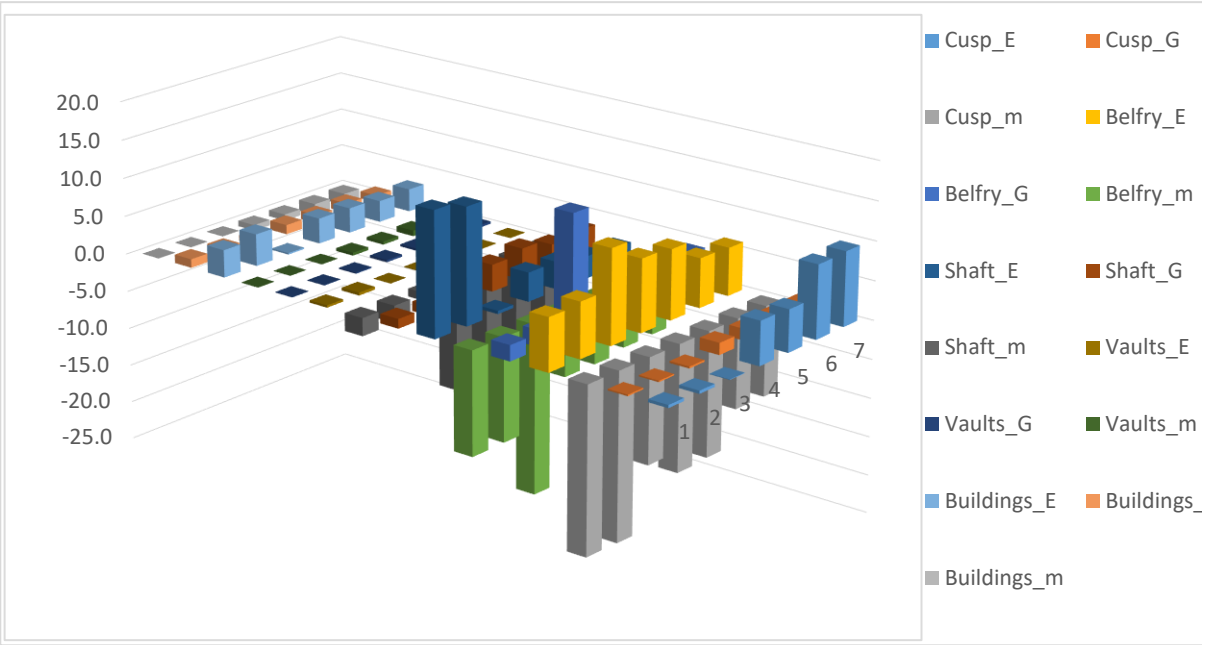

Graph 5-1 Plot of sensitivity coefficients

5.4 Calibration

The calibration of the numerical model was carried out manually on the basis of the results of the sensitivity analysis. The mechanical properties of cusp, belfry and shaft are variated by step until the natural frequencies obtained by structural eigenvalue analysis are similar enough to the experimental results. The initial model showed low values of natural frequencies. In order to increase frequencies, two strategies are possible: increase the stiffness or reducing the mass of the materials. However, exceeding in reducing the mass would bring to unrealistic results. For this reason, most of the modifications interested the stiffness of materials. The calibration is performed considering both the pre-earthquakes (February/2015 AVT) and post-earthquake conditions (18/05/2017 AVT).

5.4.1 Pre-Earthquakes condition

The model is calibrated manually considering the frequencies estimated during the February/2015 AVT. The updated material properties are shown in Table 5-4. It is interesting noticing that the final values of the mechanical properties are significantly higher than the initial ones. Moreover, the tuned Young modulus of the shaft is almost coincident with the values provided by sonic tests, see Table 4-18. Once the model is tuned on frequencies, the MAC values between the mode shapes given by the software ARTeMIS and the FE model are computed taking into account only the nodes and the degrees of freedom corresponding to the uniaxial accelerometers used in the AVT. In this way, the correspondence between the mode shapes estimated with numerical and experimental approach are compared quantitatively. The comparison between numerical and experimental frequencies and the MAC values are shown in Table 5-5. In Figure 5-5 and Figure 5-6, the first seven mode shapes computed with the FEM model are visualized. Graph 5-2 confirms the good agreement between numerical and experimental data.

Table 5-4 Pre-earthquakes model calibration: material properties

Element	Young's modulus [GPa]	Shear modulus [GPa]	Mass [kg]
Cusp	2.250	0.500	1700
Belfry	4.253	1.094	1900
Shaft	6.048	1.362	2200
Vaults and stairs	1.500	0.500	1800
Adjacent buildings	1.000	0.500	500

Table 5-5 Comparison between numerical and experimental frequencies (February 2015 AVT) (the missing experimental frequencies are indicated in blue were found in literature)

Mode	Num. freq. (Hz)	Mode type	SSI-PC (Hz)	Δ(%)	MAC	EFDD (Hz)	Δ(%)	MAC
1	1.47476	Fx1	1.455	1.4	0.935	1.458	1.2	0.951
2	1.51745	Fy1	1.525	-0.5	0.962	1.526	-0.6	0.908
3	4.50572	T1	4.376	3.0	0.848	4.357	3.4	0.793
4	4.71726	Fx2	4.620	2.1	0.598	4.617	2.2	0.441
5	4.77999	Fy2	4.889	-2.2	/	4.889	-2.2	/
6	6.98196	Fx3	7.245	-3.6	/	7.245	-3.6	/
7	7.02631	Fy3	7.263	-3.3	/	7.263	-3.3	/

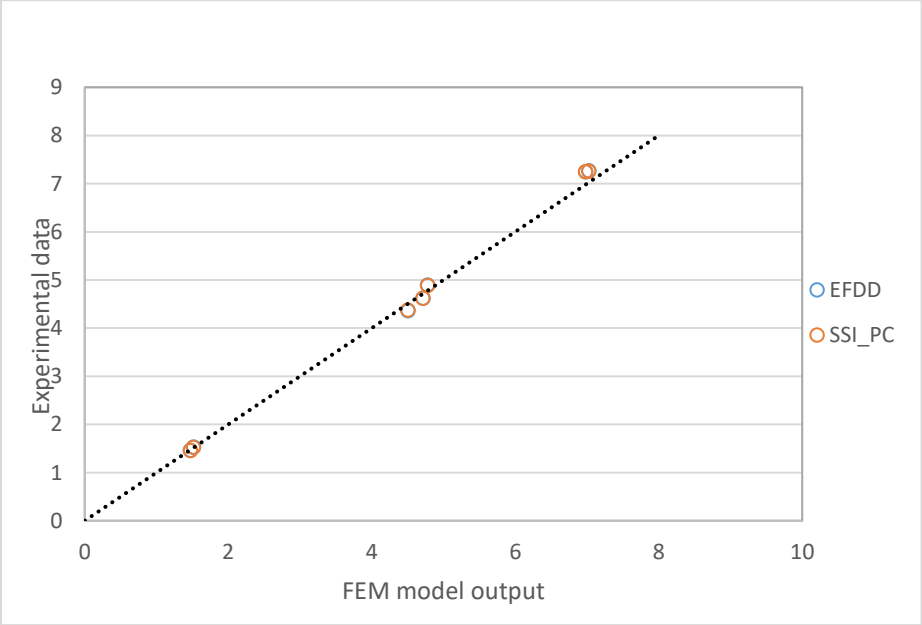

Graph 5-2 Pre-earthquakes condition: numerical frequencies VS experimental data: the data almost lie on the bisect of the first quadrant

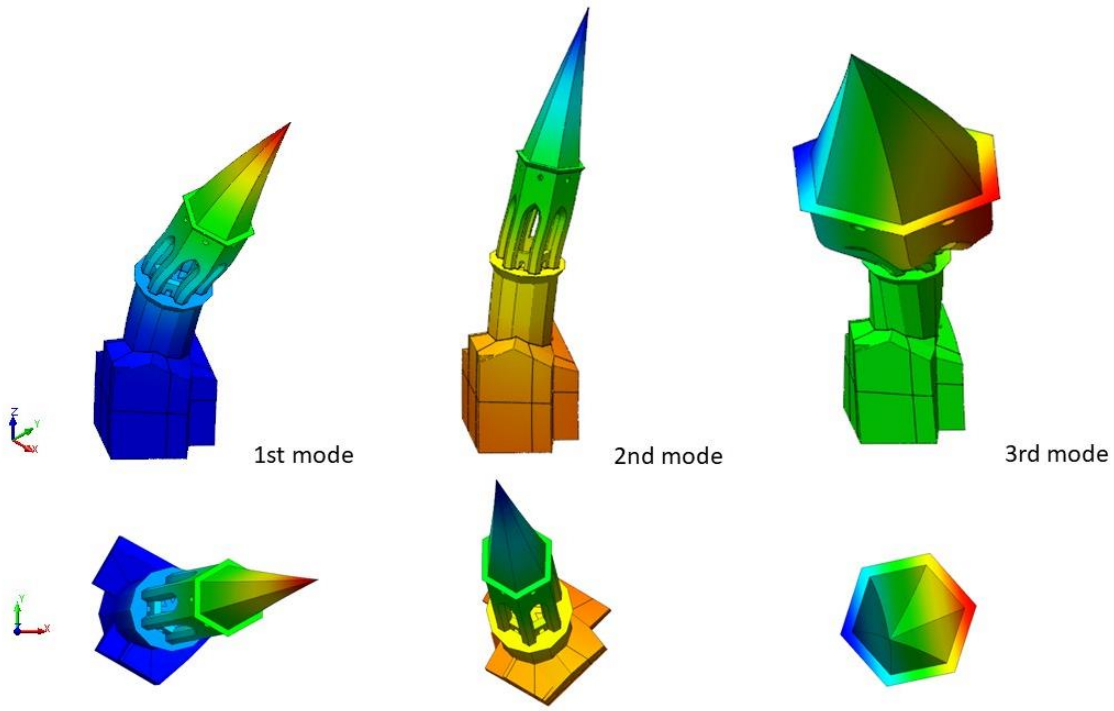

Figure 5-4 Pre-earthquakes model: first three mode shapes

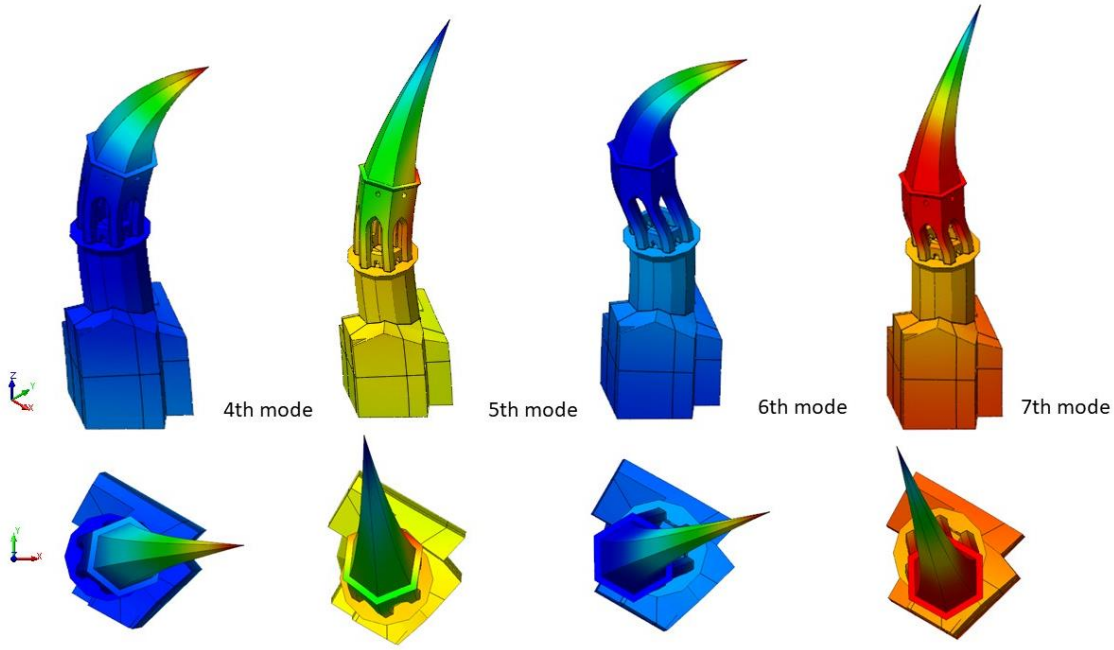

Figure 5-5 Pre-earthquakes model: from 4th to 7th mode shapes

5.4.1 Post-Earthquakes condition

The calibration is performed considering the data of the most recent AVT as well. The same procedure above described is applied. The updated material properties are shown in Table 5-6Table 5-6. A 10% reduction of the stiffness of the belfry was estimated with respect to the previous calibration. The comparison between numerical

and experimental frequencies and the MAC values are shown in Table 5-7. Visually, the mode shapes computed with the FE do not present significant alterations with respect to Figure 5-5 and Figure 5-6 and therefore they are not shown. Graph 5-3 confirms the good agreement between numerical and experimental data even if the quality of the calibration appears slightly lower, especially with respect to higher modes.

Table 5-6 Model calibration: post-earthquakes material properties

Element	Young's modulus [GPa]	Shear modulus [GPa]	Mass [kg]
Cusp	2.250	0.500	1700
Belfry	3.827	0.985	1900
Shaft	6.048	1.362	2200
Vaults and stairs	1.500	0.500	1800
Adjacent buildings	1.000	0.500	500

Table 5-7 Comparison between numerical and experimental frequencies (18/05/2017 AVT) (the missing experimental frequencies are indicated in blue are found in literature)

Mode	Num. freq. (Hz)	Mode type	SSI-PC (Hz)	Δ(%)	MAC	EFDD (Hz)	Δ(%)	MAC
1	1.45254	Fx1	1.458	-0.4	0.862	1.46	-0.5	0.834
2	1.4928	Fy1	1.526	-2.2	0.962	1.526	-2.2	0.960
3	4.33472	T1	4.176	3.8	0.911	4.169	4.0	0.848
4	4.63872	Fx2	4.983	-6.9	0.699	4.972	-6.7	0.828
5	4.69921	Fy2	4.487	4.7	0.434	4.500	4.7	0.325
6	6.84318	Fx3	7.116	-3.8	0.416	7.252	-5.6	0.665
7	6.81297	Fy3	7.263	-6.2	/	7.263	-6.2	/

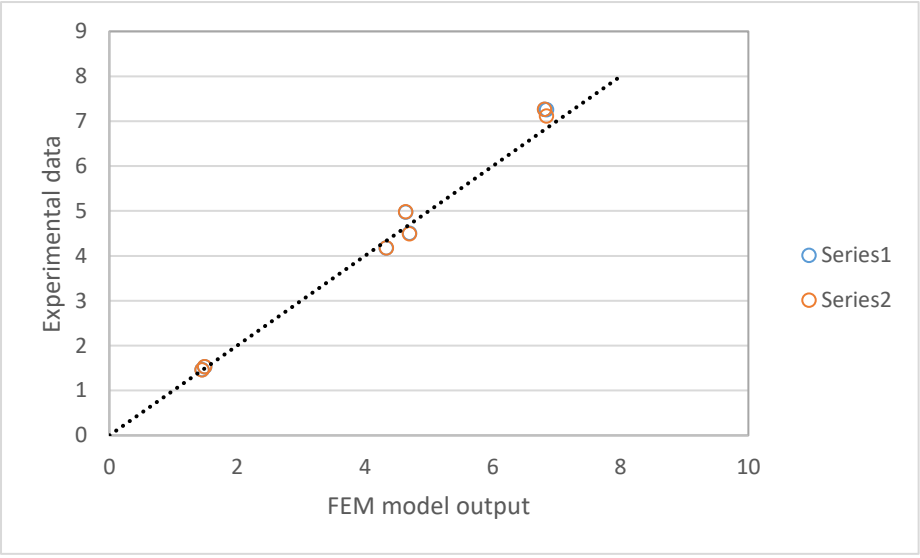

Graph 5-3 Post-earthquakes condition: numerical frequencies VS experimental data

5.5 Direct comparison between the conditions

For the sake of clarity, the results of the previous chapter are summarized in Table 5-8.

Table 5-8 Comparison between the two calibrations

Element	Young's modulus [GPa]			Shear modulus [GPa]		
	Before	After	Δ(%)	Before	After	Δ(%)
Cusp	2.250	2.250	0.0	0.500	0.500	0.0
Belfry	4.253	3.827	-10.0	1.094	0.985	-10.0
Shaft	6.048	6.048	0.0	1.362	1.362	0.0
Vaults and stairs	1.500	1.500	0.0	0.500	0.500	0.0
Adjacent buildings	1.000	1.000	0.0	0.500	0.500	0.0

Only the material corresponding to the belfry was modified with a reduction of the 10% of the Young's and shear moduli. The result obtained is consistent with the usual damages found in bell tower, see Section 2.2, and may be interpreted as an average damage parameter d=0.10, see Section 3.3.6.

5.6 Metal structure's effect

The influence of the metal structure on the tower is studied by means of a FEM model. The bell tower is modelled in a simplified way, coherently with the objective of the analysis. Solid elements are created in FX+ and the Auto Mesh function of the software is used. The mesh is formed of 12,755 tetrahedral elements. The element size is set equal to 1.00m. The metal structure is modelled with 1D elements representing the metal profiles described in paragraph 4.1.1. The mechanical properties of steel are found in literature [41]. The presence of the four bells is taken into account by adding the corresponding mass to node elements. The presence of metal plates in connections is considered by adding a mass of 20 kg on each node. The mechanical properties of materials and masses are shown in Table 5-9. The numerical model is presented in Figure 5-6. The structural eigenvalue analysis is performed twice. In the first part of the study, the metal structure is neglected. In the second part, it is considered. The comparison between results is showed in Table 5-10. It can be noticed that the natural frequencies do not differ significantly. Therefore, the metal structure can be considered negligible as for as concern the numerical global analysis.

Table 5-9 Mechanical properties of materials and masses

Element	Young's modulus [GPa]	Shear modulus [GPa]	Poisson's ratio [GPa]	Mass [kg]
Bell tower	5.645	1.238	0.25	2015
Steel	205	78.8	03	7500
Bell 1				1500
Bell 2				1200
Bell 3				1000
Bell 4				850
Connections/plates				20

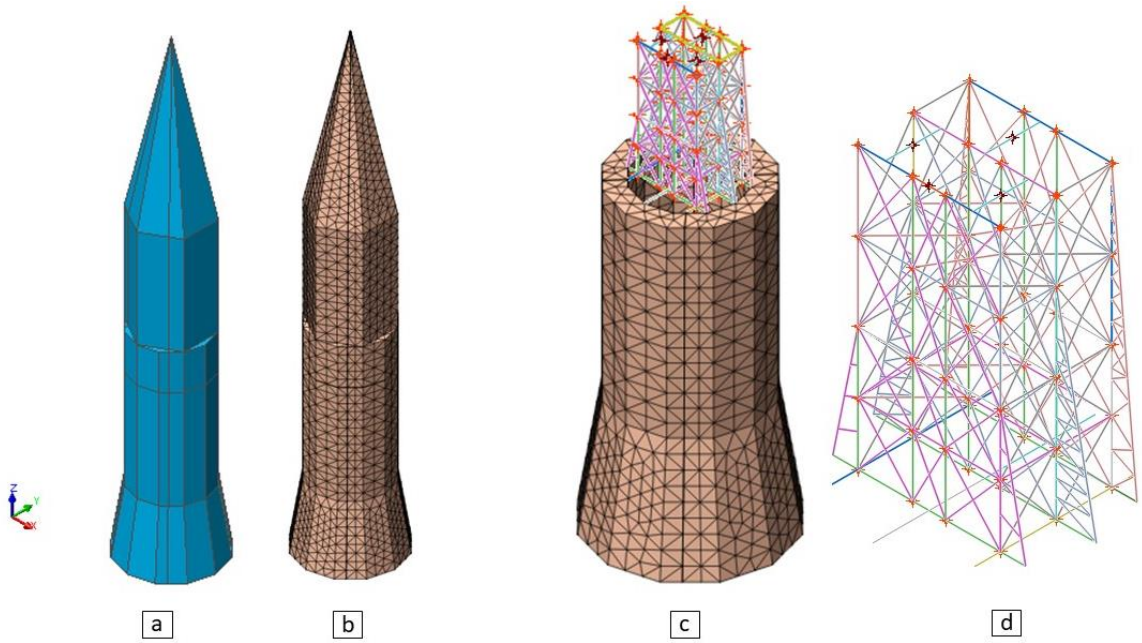

Figure 5-6 Bell tower's simplified model: (a) solid elements imported by AutoCAD, (b) FEM mesh, (c) position of the metal structure in the tower, (d) metal structure.

Table 5-10 Comparison between the frequencies of the two models

Tower		Tower + truss		
Mode	Frequency [Hz]	Mode	Frequency [Hz]	Δ[%]
1	1.251	1	1.250	0.098
2	1.251	2	1.250	0.103
		3	4.777 (local mode)	
3	5.127	4	5.110	0.328
4	5.129	5	5.196	-1.318
5	5.329	6	5.327	0.044
6	9.490	7	9.475	0.160
		8	10.212 (local mode)	
7	10.361	9	10.361	-0.007

5.7 Conclusion

This chapter was dedicated to the numerical modeling of San Pietro bell tower. A Finite Element model of the monument was build and analyzed with the software DIANA v.10.1. Following a sensitivity analysis that interested the natural frequencies, the model was calibrated according to the experimental results in pre-earthquakes and post-earthquakes conditions. Finally, the global effect of the metal structure on the bell tower was studied.

The sensitivity analysis showed that the model of the bell tower is particularly sensible to changing in the mechanical properties of cusp, belfry and shaft. Variations in the mechanical parameters of vaults, stairs and adjacent buildings are not significant. Therefore they are not taken into account in the calibration phase.

The initial mechanical properties assigned to materials did not allowed to obtain results consistent with the experimental data. Therefore a calibration of the model was carried out on the basis of the results of the sensitivity analysis. The calibration, allowed obtaining a satisfactory model, both in the pre-earthquakes and post-earthquakes conditions. In particular, little relative errors between experimental and numerical frequencies are obtained. Moreover, the MAC coefficient present elevate values, especially as far as it concerns the first three mode shapes. It is significant noticing that the tuned Young modulus of the shaft is almost coincident with the values provided by sonic tests.

An additional numerical model was built to study the influence of the metal structure on the global behavior of the tower. The structural eigenvalue analysis is performed twice. In the first part of the study, the metal structure is neglected. In the second part, it is considered. The results confirm that the metal structure may be neglected in the global analysis of the monument.

This page is left blank on purpose.

6. Monitoring analysis

6.1 Introduction

This chapter is focused on the presentation and preliminary elaboration of the long-term monitoring data recorded in San Pietro bell tower. In the first section, data related to natural frequencies and temperature are presented and the acquiring and processing methodology is described. Then, the correlation between data is studied separately in pre- and post-earthquakes conditions. In particular the correlation between natural frequencies themselves and between natural frequencies and temperature is investigated. The results are useful to figure out which variables present the highest dependency. On the basis of the correlation analysis, the dynamic response of the monument is modelled by means of ARX models [12].

6.2 Long-term monitoring data

The long-term monitoring data concern natural frequencies and environmental temperatures. Five modes are continuously tracked in operational conditions by means of the fully automated stochastic subspace identification (SSI) technique described in section 3.3.4: the first two bending modes f_{x1} and f_{y1}, the first torsional mode f_{t1} and the other two modes in the y direction, f_{y2} and f_{y3}. Moreover, since April 5th 2016, two thermocouples are installed in proximity of sensors T5 and T7, respectively see Figure 3-17. As previously described, the frequencies corresponding to the five modes are estimated each 30 minutes. Temperatures are acquired with a sampling rate of 1 Hz. For this reason, they are averaged on time windows of 30 minutes each corresponding to those of the frequencies. Here, data are analyzed until July 4th 2017. The series of data recorder by the thermocouples and the Tinytag sensors in the two locations, respectively, present correlation coefficients close to one, as it is possible to see in Table 6-1. Therefore, the series of data recorded by the two different sensors can be considered equivalent. In Figure 6-1 and Figure 6-2 the time histories of the identified natural frequency and of the temperatures, respectively, are presented. The very evident picks visible in the plot are attributable to freezing conditions. In Annex B, a time history plots of frequencies and temperature are provided.

Table 6-1 Correlation coefficients between data series

	T5-Thermocouple	T7-Thermocouple	T5-Tinytag	T7-Tinytag
T5-Thermocouple	1	0.8403	0.9920	0.8722
T7-Thermocouple		1	0.8466	0.9902
T5-Tinytag			1	0.8791
T7-Tinytag				1

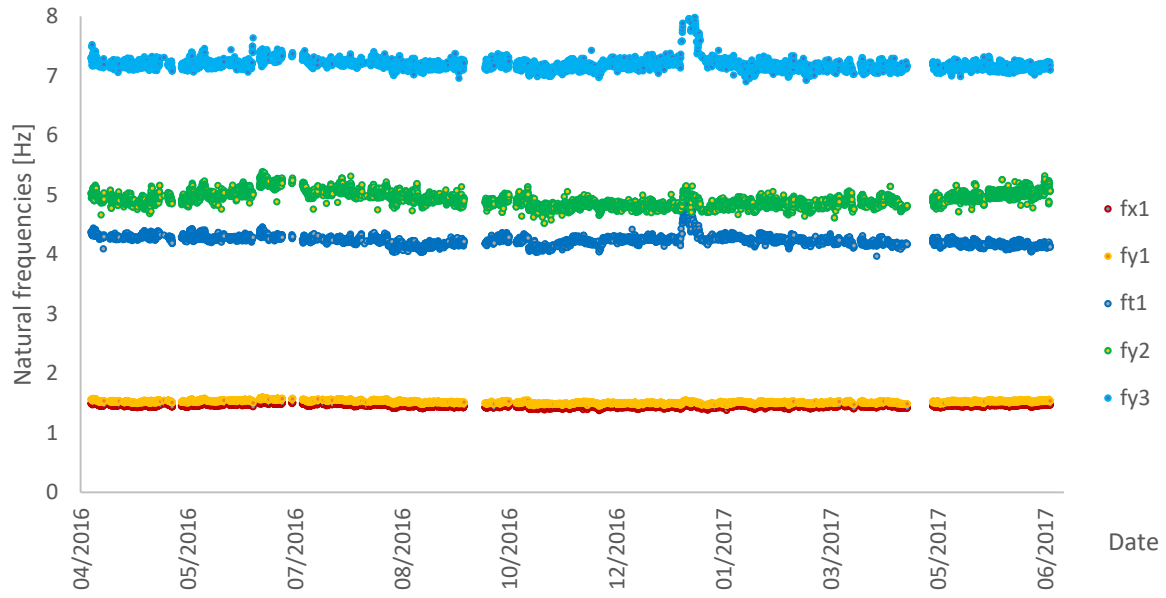

Figure 6-1 Identified natural frequencies of the bell tower versus time

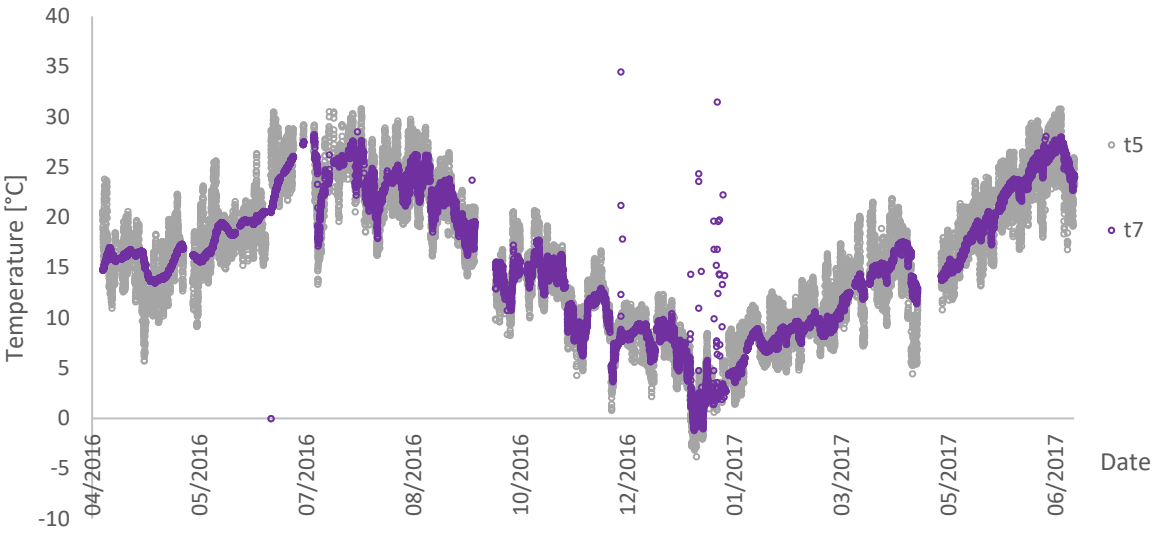

Figure 6-2 Time history plots of temperature

6.3 Results of long-term monitoring

The correlation between the variables is studied in this section. Data recorder between April 5th 2016 and August 23th are considered related to pre-earthquakes conditions. Data recorded between January 19th and July 4th are considered related to post-earthquakes conditions. Data recorder in between are not analyzed since seismic events were occurring.

6.3.1 Pre-earthquakes condition

Correlation coefficients between natural frequencies are presented in Table 6-2. High degree of correlation is observed between the natural frequencies of the modes f_{x1}, f_{y1}, f_{y2}. The correlation between the over mentioned and the modes and the mode f_{y3} is less significant. The torsional mode f_{t1} shows low correlation with all other modes. The high correlation coefficients may indicate a dependency on the same environmental parameter. In fact, the correlation between the temperature T5 and modes f_{x1}, f_{y1}, f_{y2} is significant. A negative correlation between the torsional model and temperature is noticed. The correlation between the temperature T7 and the other quantities is minor, with the only exception represented by the torsional mode. Correlation coefficients between natural frequencies and temperature are presented in Table 6-3. The plot showing the correlation between natural frequencies and temperature are provided in Annex B. Frequency-temperature relations are almost linear, with equation:

$$f_i = f_{i,0} + \kappa_{i,T} Tsi \qquad 6\text{-}1$$

where $i = x1, x2, T, y2, y3$ indicated the mode, si the number of the temperature sensors presenting the highest correlation with the mode i, $f_{i,0}$ is the frequency at 0°C and $\kappa_{i,T}$ are the frequency–temperature sensitivity coefficients. The last square estimates are show in Table 6-4. The corresponding plots are shown in . In general, the results obtained are in agreement with previous study, see 3.3.5.

Table 6-2 Pre-earthquakes conditions: correlation coefficients between frequencies

	f_{x1}	f_{y1}	f_{t1}	f_{y2}	f_{y3}
f_{x1}	1	0.98	0.42	0.88	0.71
f_{y1}		1	0.37	0.88	0.71
f_{t1}			1	0.22	0.47
f_{y2}				1	0.67
f_{y3}					1

Table 6-3 Pre-earthquakes conditions: correlation coefficients between frequencies and environmental parameters

	f_{x1}	f_{y1}	f_{t1}	f_{y2}	f_{y3}
T5	0.82	0.85	-0.02	0.81	0.54
T7	0.57	0.61	-0.38	0.67	0.37

Table 6-4 Pre-earthquakes conditions: parameters of best fitting lines between frequencies and temperature data

f_i	Tsi	$f_{i,0}$ [Hz]	$\kappa_{i,T}$ (mHz/°C)	R^2
f_{x1}	T5	1.41	3.1	0.67
f_{y1}	T5	1.48	3.1	0.71
f_{t1}	T7	4.36	-4.0	0.14
f_{y2}	T5	4.66	18.3	0.65
f_{y3}	T5	7.09	7.3	0.30

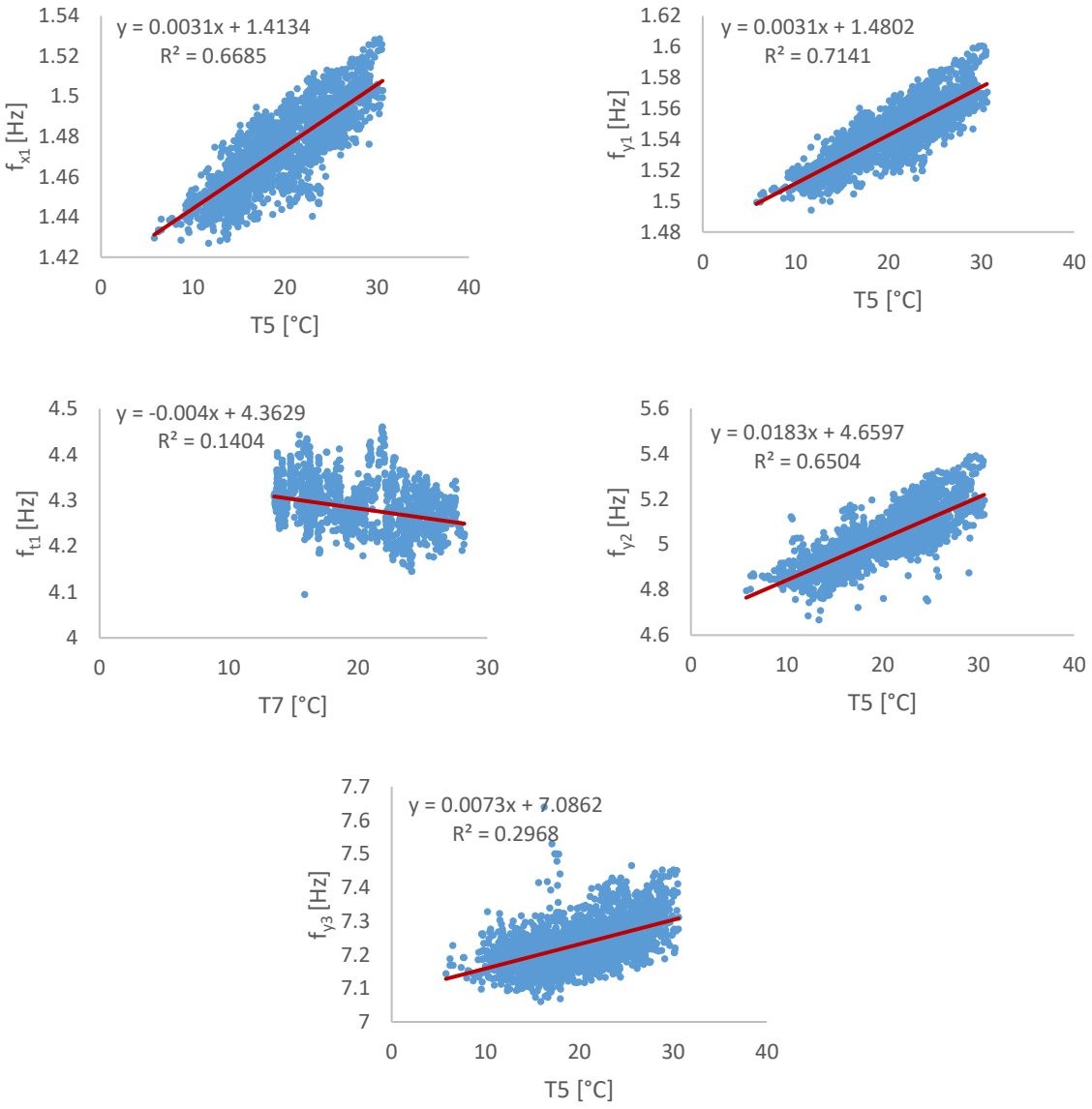

Graph 6-1 Pre-earthquakes conditions: correlation between frequencies and temperature data

6.3.2 Post earthquake condition

Post-earthquakes data are processed with the same methodology of the previous ones. Correlation coefficients between natural frequencies are presented in Table 6-6. Correlation coefficients between natural frequencies and temperature are presented in Table 6-5. The last square estimates are show in Table 6-7. It is worth noticing that the correlation between correlation between the two modes f_{t1} and f_{y3} and the other modes has decreased and, in turn, the dependency between modes f_{t1} and f_{y3} has increased. The correlation between the torsional mode f_{t1} and the temperature is negative and it has increased in absolute value. The correlation between the mode f_{y3} and the temperature T7 has become slightly negative. The results may indicate a stronger dependency in post-earthquake condition between the modes f_{t1} and f_{y3} and the behavior of the fiber reinforcements which are widely present in the

belfry, see 3.3.5. Indeed, the two modes are the ones that imply the larger deformations in the belfry. In Table 6-8,**Error! Reference source not found.** a comparison between the average frequencies before and after the earthquakes is reported. Confidence limits are fixed multiplying the standard deviations by the factor 1.96, found in statistical t-distribution tables. In general, the average frequencies decreased after the seismic events. However, the values do not exceed the fixed confidence interval meaning that major damages did not occur.

Table 6-5 Post-earthquakes conditions: correlation coefficients between frequencies

	f_{x1}	f_{y1}	f_{t1}	f_{y2}	f_{y3}
f_{x1}	1	0.96	-0.10	0.82	0.39
f_{y1}		1	-0.17	0.88	0.31
f_{t1}			1	-0.34	0.50
f_{y2}				1	0.22
f_{y3}					1

Table 6-6 Post-earthquakes conditions: correlation coefficients between frequencies and environmental parameters.

	f_{x1}	f_{y1}	f_{t1}	f_{y2}	f_{y3}
T5	0.74	0.84	-0.6121	0.85	0.02
T7	0.62	0.73	-0.75	0.80	-0.09

Table 6-7 Post-earthquakes conditions: parameters of best fitting lines between frequencies and temperature data

f_i	Tsi	$f_{i,0}$ [Hz]	$\kappa_{i,T}$ (mHz/°C)	R^2
f_{x1}	T5	1.43	1.7	0.55
f_{y1}	T5	1.49	2.1	0.71
f_{t1}	T7	4.29	-5.8	0.56
f_{y2}	T5	4.73	12.6	0.72
f_{y3}	T7	7.17	-0.8	0.01

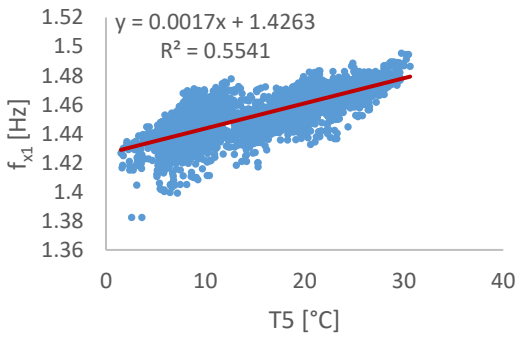

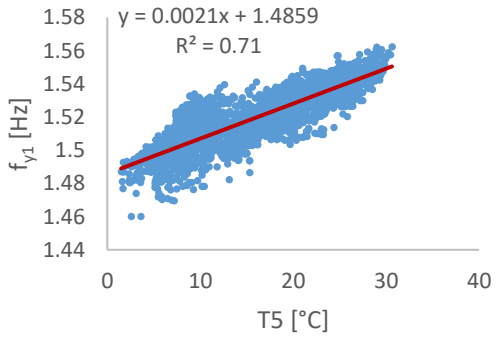

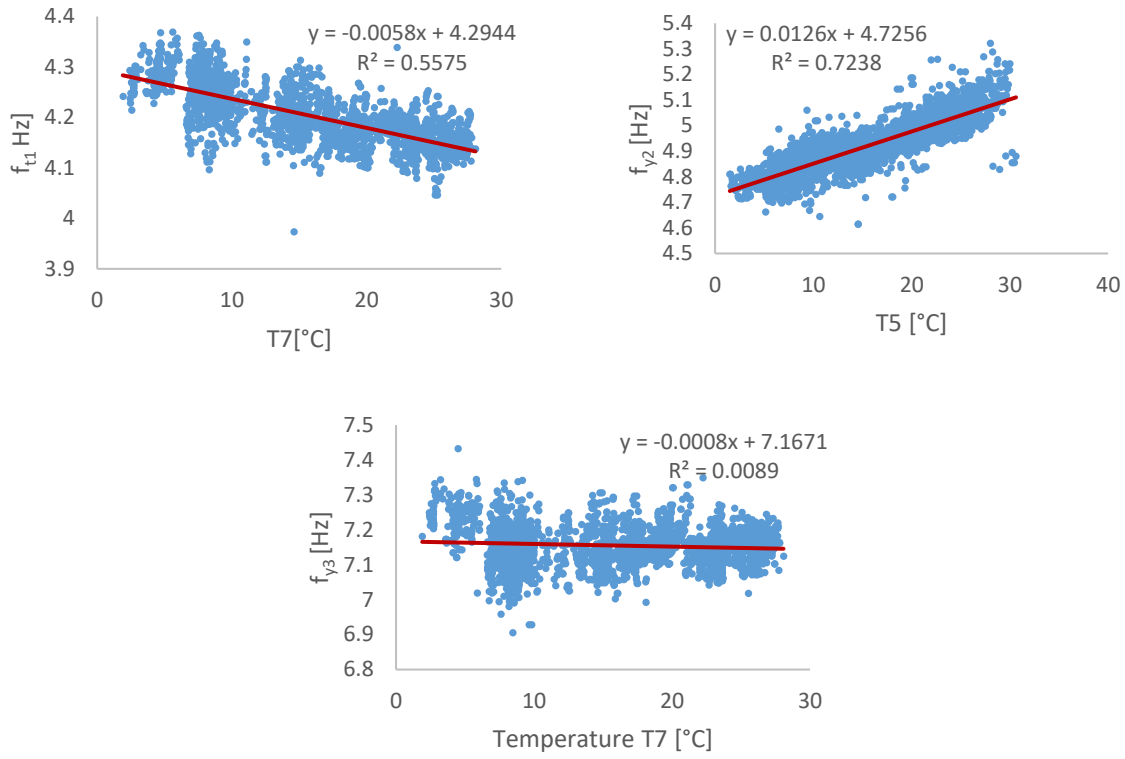

Graph 6-2 Post-earthquakes conditions: correlation between frequencies and temperature data

Table 6-8 Comparison between frequencies in pre- and post-earthquake conditions

Mode	Average frequency [Hz]		Δf [%]	Freq. s.dev, σ	Confidence interval [Hz]	
	Before	After			Lower Bound	Upper Bound
f_{x1}	1.473	1.455	-1.26	0.019	1.436	1.510
f_{y1}	1.541	1.520	-1.34	0.019	1.504	1.578
f_{t1}	4.284	4.201	-1.93	0.044	4.199	4.369
f_{y2}	5.014	4.930	-1.66	0.114	4.789	5.238
f_{y3}	7.227	7.155	-0.99	0.067	7.095	7.358

6.4 ARX model

ARX model are applied on the modes that show the higher correlation with the temperature. The function arx of the software Matlab [16] is used. Several ARX models are estimated, changes the parameters na, nb, nk and the selection of the "best" model was based on quality criteria, such as FPE and MSE, see2.5.3. The model is calibrated on a training period corresponding to pre-earthquakes condition. After that, the response of the structure is simulated in post-earthquakes condition with the previous selected model. The simulation error and its statistics are computed and the confidence interval is established. The detection of damage is carried out observing

frequency shifts that significantly go out the interval. The best fitting models are shown in Table 6-9. In Annex B, the fitting models through the normalized frequency and simulated errors with 95% confidence interval are presented.

Table 6-9 Comparison between ARX and linear regression model on the training period

	ARX Model				Static Regression Model			
Mode	na, nb, nk	FPE	MSE	Correlation, R^2	na, nb, nk	FPE	MSE	Correlation, R^2
f_{x1}	2, 5, 0	0.039	0.039	0.676	0, 1, 0	0.331	0.331	0.669
f_{y1}	1, 4, 0	0.037	0.037	0.721	0, 1, 0	0.286	0.286	0.714
f_{y2}	1, 4, 0	0.128	0.127	0.679	0, 1, 0	0.350	0.350	0.650

The results with the ARX models are only slightly better than the results obtained with the static ones. In general, the models do not seem able to fully represent the behavior of the structure. The reason is possibly due to a lack of information about additional variable that may influence the frequency variation, such as: additional temperatures air humidity, water absorption, wind, excitation level. Furthermore, the training period may be insufficient to properly calibrate the model for frequency prediction.

6.5 Conclusion

In this chapter, a preliminary study about the correlation between natural frequencies variations and environmental parameters is presented. Data studied included temperatures provided by two thermocouples and the five continuously-tracked natural frequencies. The correlation between data is studied separately in pre- and post-earthquakes conditions.

It was demonstrated that the data provided by the thermocouples are equivalent to those provided by the Tinytag sensors can be considered equivalent. The fluctuations of the modes are associate to daily and seasonal variations of environmental parameters and freezing conditions.

In pre-earthquakes conditions, the frequencies exhibit correlation with temperature data with exception of the torsional mode, in accordance with previous studies. It is noticed that the correlation between the mode fy3 and the temperature T7 has become slightly negative. The results may indicate a stronger dependency in post-earthquakes condition between the modes f_{t1} and f_{y3} and the behavior of the fiber reinforcements which are widely present in the belfry. The average values of the frequencies in post-earthquakes condition do not exceed the fixed confidence interval meaning that major damages did not occur.

ARX models do not seem able to fully represent the behavior of the structure. The reason is possibly due to a lack of information about additional variable that may influence the frequency variation, such as: additional temperatures air humidity, water absorption, wind, excitation level. Furthermore, the training period may be insufficient to properly calibrate the model for frequency prediction.

This page is left blank on purpose.

7. Conclusion and future works

The most recent investigations carried out on the monumental San Pietro bell tower are presented in this work. The main objective was to detect any change in the structural behavior following the 2016-2017 Central Italy earthquakes. In this chapter, the major results that were obtained are reported and commented. Moreover, suggestions for future studies are provided.

7.1 General outcomes

The actual aspect of the bell tower is the result of its complex history. It has been subject to numerous repair interventions over time following damages caused by earthquakes and, especially, lightning. The structural works carried out in the years 1929-1933 have revealed to be particularly deleterious. More respectful restoration works were performed in 2002 after the 1997 Marche-Umbria earthquake. New techniques and modern materials were used to repair and consolidate the structure.

Starting from 2013, several investigations have been carried out aiming at installing a permanent vibration-based structural health monitoring (SHM) system able to detect anomalies in the structural behavior by means of statistical process control tools. The SHM is based on the continuous identification of the natural frequencies of the bell tower and on the analysis of their variations. Environmental parameters, i.e. temperature and humidity, are monitored as well. In particular, it is possible to track five modes among the seven identified.

Concerning the visual survey, the monument appear in good state of conservation. The cracks that are found in the lower portion of the belfry are the only damage clearly attributable to the last earthquakes. The geometrical survey of the metal structure supporting the bells was carried out. The ordinary maintenance of the bell tower may be improved.

Data from two different Ambient Vibration Tests (AVT) were analyzed and the results compared, namely AVT2 and AVT3. The former corresponds to the pre-earthquakes condition, the latter to post-earthquakes condition. Four modes are found from AVT2: the first two bending modes, f_{x1} and f_{y1}, the torsional mode, f_{t1}, and the other mode in the X direction, f_{x2}. Six modes are found from AVT3: the first three modes (the bending modes f_{x1} and f_{y1} and the torsional mode f_{t1}), the second mode in Y direction, and the other two modes in the X direction (f_{x2} and f_{x3}). The higher number of modes found in AVT3 may be attributed neither to the higher number of sensor used or to the higher level of excitation of the tower, with respect to AVT2. The first two modes found in the two operational modal analyses are in great agreement, under the frequency and Modal Assurance Criterion (MAC) point of view. The first torsional mode and the second mode in X direction present more significant modifications. They may be caused by the occurrence of damages or by the effects of environmental factors.

Both indirect and direct sonic tests were performed to characterize materials. The materials studied belong to the shaft of the tower: interior stone masonry, interior brick masonry, exterior stone masonry, exterior brick masonry. The direct tests were conducted in proximity of the entrance door and the window of the shaft, where both sides of the wall could be reached. The values of wave velocities are used to estimate the elastic moduli of materials. The results are in agreement with the values estimated in previous works. The direct tests confirm the results obtained.

A Finite Element model of the monument was implemented and analyzed. The sensitivity analysis showed that the model of the bell tower is particularly sensible to changing in the mechanical properties of cusp, belfry and shaft. Variations in the mechanical parameters of vaults, stairs and adjacent buildings are not significant. After the calibration, little relative errors between experimental and numerical frequencies are obtained. Moreover, the MAC coefficient present significant values, especially as far as it concerns the first three mode shapes. It is worth noticing that the tuned Young modulus of the shaft is almost coincident with the values provided by sonic tests. It was demonstrated that the metal structure may be neglected in the global analysis of the monument.

It was shown that the data provided by the thermocouples are equivalent to those provided by the Tinytag sensors can be considered equivalent. The fluctuations of the modes are associate to daily and seasonal variations of environmental parameters and freezing conditions. In pre-earthquakes conditions, the frequencies exhibit correlation with temperature data with exception of the torsional mode, in accordance with previous studies. It is noticed that the correlation between the mode f_{y3} and the temperature T7 has become slightly negative. The results may indicate a stronger dependency in post-earthquakes condition between the modes f_{t1} and f_{y3} and the behavior of the fiber reinforcements which are widely present in the belfry. The average values of the frequencies in post-earthquakes condition do not exceed the fixed confidence interval meaning that major damages did not occur. ARX models do not seem able to fully represent the behavior of the structure. The reason is possibly due to a lack of information about additional variable that may influence the frequency variation, such as: additional temperatures air humidity, water absorption, wind, excitation level. Furthermore, the training period may be insufficient to properly calibrate the model for frequency prediction.

7.2 Future works

The geometrical and material knowledge of the bell tower could be improved. Aerial photographic survey, photogrammetry and 3D laser scanner may be used. An accurate crack mapping should be carried out. Sonic tests may be executed more extensively to detect structural differences and irregularities. In particular, the area corresponding to the bell fry may the investigated. Flat-jack and double flat-jack tests may be applied to determine the compressive stress levels of masonry walls and to determine the mechanical properties of materials, respectively. Boroscopy may be useful to better characterize the internal structure of three leaves masonry walls. Additional geometrical survey on the metal structure may be useful characterize its details, deformations and material degradation.

The results of complementary visual survey, NDT and MDT may be used to realize a more accurate numerical model of the structure. Possible improvements may concern the effects of: (1) adjacent buildings; (2) masonry insertions; (3) tie rods and confinement elements; (4) concrete elements and composite materials in the belfry; and (5) dynamic effects of bells. The results obtained with models of different complexity may be compared.

Numerical analysis should be carried out in order to simulate the structural behavior of the bell tower under different conditions and actions. In particular the ultimate capacity of the structure and the effects of the recent earthquakes may be investigated. Push over analyses may simulate the evolution of the state of the structure under seismic force. Linear and non-linear dynamic analysis in time domain may be performed once the accelerograms of the earthquakes are conveniently scaled. Kinematics analyses may be performed as well to establish the most

concerning rigid mechanisms. The analyses may indicate the need of strengthening interventions. The results may be compared with those of previous studies.

As far as the monitoring system, it may be complemented with additional types of sensors, namely tiltmeters, water absorption and wind sensors. The data obtained may complement the long term monitoring system and help to better interpret the structural behavior of the tower. In particular, the exogenous factors that influence the modes with low level of correlation with temperature may be identified. In this way, the automatic damage detection system may be improved. ARX models may be improved using data provided be the additional sensors present in the tower that were not processed (because still not available).

This page is left blank on purpose.

8. References

[1] L. F. Ramos, L. Marques, P. B. Lourenço, G. De Roeck, A. Campos-Costa and J. Roque, "Monitoring of Historical Masonry Structures with Operation Modal Analysis: Two case studies," *Mechanical Systems and Signal Processing,* 2010.

[2] A. Giuffè, Sicurezza e conservazione dei centri storici : il caso Ortigia : codice di pratica per gli interventi antisismici nel centro storico, Roma: Laterza, 1993.

[3] S. Podestà, Verifica sismica di edifici in muratura, Palermo: Dario Flaccovio, 2012.

[4] Presidenza del Consiglio dei Ministri, Manuale per la compilazione della scheda per il rilievo del danno ai beni culturali, Chiese (Modello A-DC), Roma: Dipartimento della Protezione Civile, 2011.

[5] Presidenza del Consiglio dei Ministri, Direttiva del Presidente del Consiglio dei Ministri del 9 febbraio 2011: Valutazione e riduzione del rischio sismico del patrimonio culturale, G.U. n. 47 del 26/2/2011 S.O. n. 54.

[6] D. Balageas, C.-P. Fritzen and A. Güemes , Structural Health Monitoring, ISTE editions, 2006.

[7] C. Rainieri, G. Fabbrocino and E. Cosenza, "Structural Health Monitoring systems as a tool for seismic protection," in *The 14th World Conference on Earthquake Engineering*, Beijing, China, 2008.

[8] M.-G. Masciotta, L. F. Ramos and P. B. Lourenço, "The importance of structural monitoring as a diagnosis and control tool in the restoration process of heritage structures: a case-study in Portugal," *Journal of Cultural Heritage,* 2017.

[9] P. C. Chang, A. Flatau and S. C. Liu, "Review Paper: Health Monitoring of Civil Infrastructure," *Structural Health Monitoring,* vol. 2, no. 3, p. 257–267, 2003.

[10] ICOMOS/ISCARSAH, "Recommendations for the Analysis, Conservation and Structural Restoration of Architectural Heritage," 2005.

[11] A. Elyamani, O. Caselles, P. Roca and J. Clapes, "Dynamic Investigation of a Large Historical Cathedral," *Structural Control and Health Monitoring,* vol. 24, no. 3, 2017.

[12] L. F. Ramos, *Damage Identification on Masonry Structures Based on Vibration Signatures, PhD Thesis,* Universidade do Minho, 2007.

[13] M. Pastor, M. Binda and . T. Harcarik, "Modal Assurance Criterion," *Procedia Engineering,* vol. 48, pp. 543-548, 2012.

[14] F. Lorenzoni, F. Casarin, C. Modena, M. Caldon, K. Islami and F. da Porto, "Structural health monitoring of the Roman Arena of Verona, Italy," *ournal of Civil Structural Health Monitoring,* vol. 3, p. 227–246, 2013.

[15] F. Ubertini, G. Comanducci, N. Cavalagli, A. L. Pisello, A. L. Materazzi and F. Cotana, "Environmental effects on natural frequencies of the San Pietro bell tower in Perugia, Italy, and their removal for structural performance assessment," *Mechanical Systems and Signal Processing ,* vol. 82, pp. 307-322, 2017.

[16] "MathWorks," [Online]. Available: https://www.mathworks.com. [Accessed July 2017].

[17] G. Comanducci, N. Cavalagli and F. Ubertini, "Vibration-based SHM for cultural heritage preservation: the case of the S. Pietro bell tower in Perugia," *MATEC Web of Conferences,* vol. 24, 2015.

[18] F. Ubertini, C. Gentile and A. L. Materazzi, "Automated modal identification in operational conditions and its application to bridges," *Engineering Structures,* vol. 46, pp. 264-278, 2013.

[19] S. Atamturktur and J. A. Laman, "Finite element model correlation and calibration of historic masonry monuments: review," *The Structural Design of Tall and Special Buildings,* vol. 21, no. 2, pp. 96-113, 2012.

[20] L. A. Binda and M. Lualdi, "Non-Destructive Testing Techniques Applied for Diagnostic Investigation: Syracuse Cathedral in Sicily, Italy," *International Journal of Architectural Heritage,* vol. 1, no. 4, pp. 380 - 402, 2007.

[21] E. Manning, L. F. Ramos and F. Fernandes, "Direct Sonic and Ultrasonic Wave Velocity in Masonry under Compressive Stress," in *9th International Masonry Conference*, Guimarães, 2014.

[22] D. McCann and M. Forde, "Review of NDT methods in the assessment of concrete and masonry structures," *NDT&E International,* vol. 34, pp. 71-84, 2001.

[23] A. Borri, M. Corradi and G. Castoldi, "A method for the analysis and classification of historic masonry," *Bulletin of Earthquake Engineering,* 2015.

[24] M. Tiritiello, *Analisi e modellazione numerica del campanile della Basilica di S. Pietro in Perugia, Master's thesis,* University of Perugia, 2013.

[25] *Archivio storico dell'abbazia San Pietro in Perugia,* Collocazione archivistica: Cronache di Don Mauro Bini, C.M. 439 IV, C.M. 439 V; Libri Diversi 111, 31, 38, 89, 9; Mazzi ,LXXI, LXVIII, XXXVIII; Libri dei contratti, 121; Libri economici, Giornali, 96,150.

[26] *Archivio privato della Fondazione per l'istruzione agraria,* Verbali dei consigli di amministrazione, Collocazione archivistica: 1928-1932; 1949-1951.

[27] *Biblioteca archivistica della Soprintendenza ai beni architettonici e paesaggistici per l'Umbria,* Collocazione archivistica: A.s.c. 37, p.39; A.s. 59, fasc. 1-4.

[28] Abate Pietro Elli O.S.B., Cronotassi degli Abbati del Monastero di San Pietro in Perugia conforme alla cronaca ms. dell'Abate Don Mauro Bini, Abbazia S.Pietro in Perugia, 1994.

[29] F. Cotana, Vibio Treboniano Gallo e la sua Terra, 2012.

[30] R. Vetturini, "DIVISARE," 9 January 2014. [Online]. Available: https://divisare.com/projects/247982-riccardo-vetturini-campanile-del-complesso-monumentale-di-s-pietro-in-perugia. [Accessed June 2017].

[31] "Protezione Civile ufficial webpage," [Online]. Available: http://www.protezionecivile.gov.it. [Accessed June 2017].

[32] "Blog INGVterremoti," [Online]. Available: https://ingvterremoti.wordpress.com/. [Accessed June 2017].

[33] C. Gentile, F. Ubertini, N. Cavalagli, M. Guidobaldi, A. L. Materazzi and A. Saisi, "Dynamic investigation of the "San Pietro" bell-tower in Perugia," in *Proceedings of the 9th International Conference on Structural Dynamics, EURODYN 2014*, Porto, Portugal, 2014.

[34] F. Ubertini, N. Cavalagli, G. Comanducci and A. L. Materazzi, "Campanile di San Pietro," *L'Ingegnere Umbro,* pp. 7-13, June 2014.

[35] F. Ubertini, G. Comanducci, N. Cavalagli, A. L. Materazzi, A. L. Pisello and F. Cotana, "Automated post-earthquake damage detection in a monumental bell tower by continuous dynamic monitoring," in *Proceedings of the 10th International Conference on Structural Analysis of Historical Constructions, SAHC 2016*, Leuven, Belgium, Koen Van Balen & Els Verstrynge, 2016, pp. 812-819.

[36] F. Ubertini, G. Comanducci and N. Cavalagli, "Vibration-based structural health monitoring of a historic bell-tower using output-only measurements and multivariate statistical analysis," *Structural Health Monitoring,* vol. 15, no. 4, pp. 438 - 457, 2016.

[37] "Istruction document to the Italian Code for Structural Design, G.U. no. 47 del 26/2/09 suppl. ord. n. 27," *Official Bulletin no.617 of February 2,* 2009.

[38] "Historical Weather Archive," [Online]. Available: http://www.ilmeteo.it. [Accessed June 2017].

[39] D. -. F. E. Analysis, User's Manual release 10.1 - FX+ for DIANA, Delft, The Netherlands: DIANA FEA BV .

[40] D. -. F. E. Analysis, User's Manual release 10.1, Delft, The Netherlands: DIANA FEA BV.

[41] M. N. Bussell, Appraisal of existing iron and steel structures, Berkshire : Steel Construction Institute, 1997.

[42] A. C. Núñez García, *Evaluation of structural intervention in the Quartel das Esquadras, Almeida (Portugal), Master's Thesis,* SAHC, 2015.

[43] C. A. Arce Campos, *The São Francisco portal in Almeida: modelling, analysis and conservation, Master's Thesis,* SAHC, 2016.

[44] B. Peeters and G. De Roeck, "Stochastic System Identification for Operational Modal Analysis: A Review," *Journal of Dynamic Systems, Measurement, and Control,* vol. 123, pp. 659-667, 2001.

[45] "Italian Code for Structural Design, D.M. 14/1/2008," *Official Bulletin no. 29 of February 4 2008,* 2008.

This page is left blank on purpose.

Annex A

Additional geometrical details of the metal structure are provided in this section of the work.

Plant

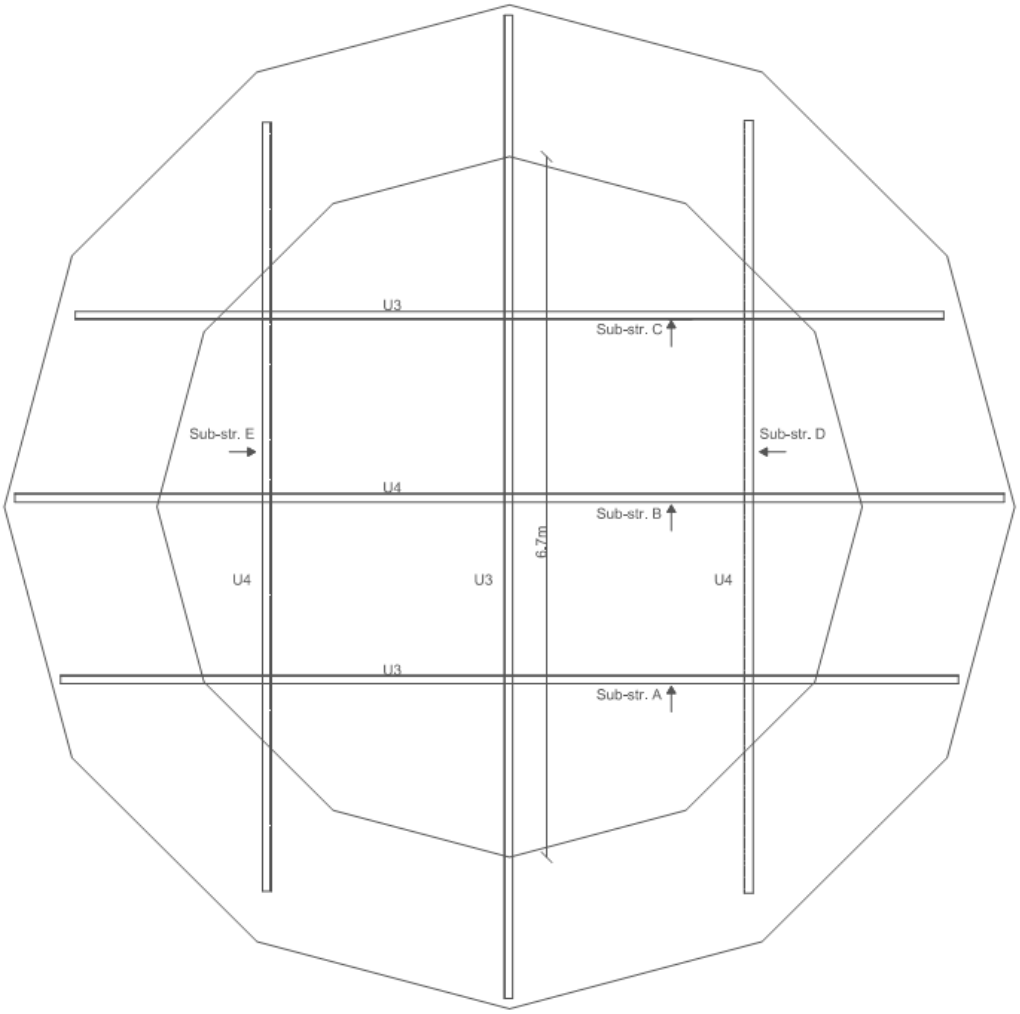

Details

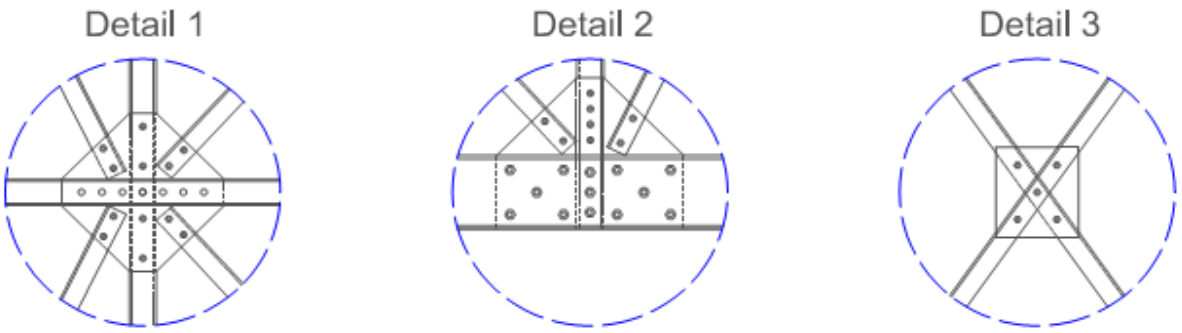

Sub-structure A

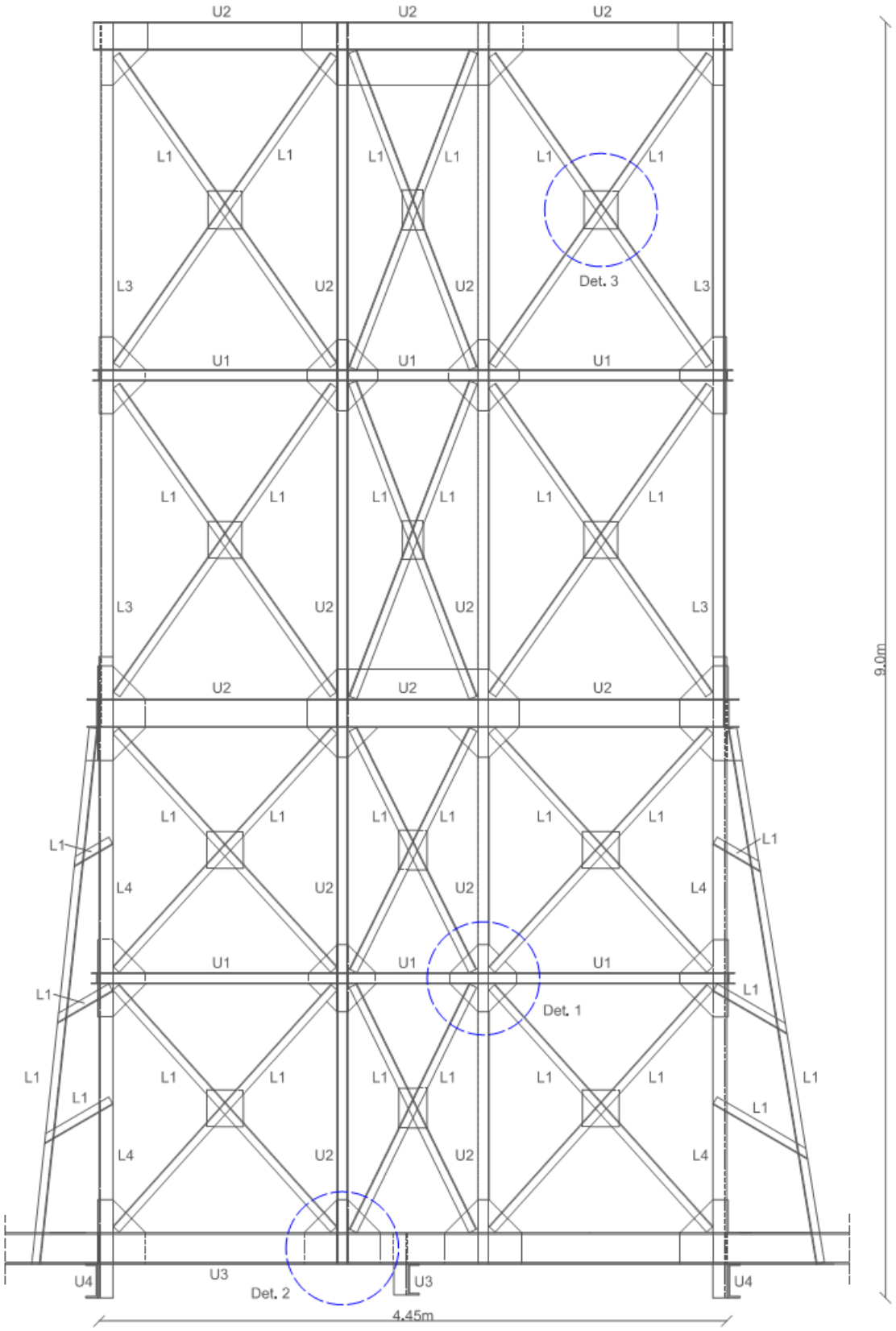

Sub-structure B

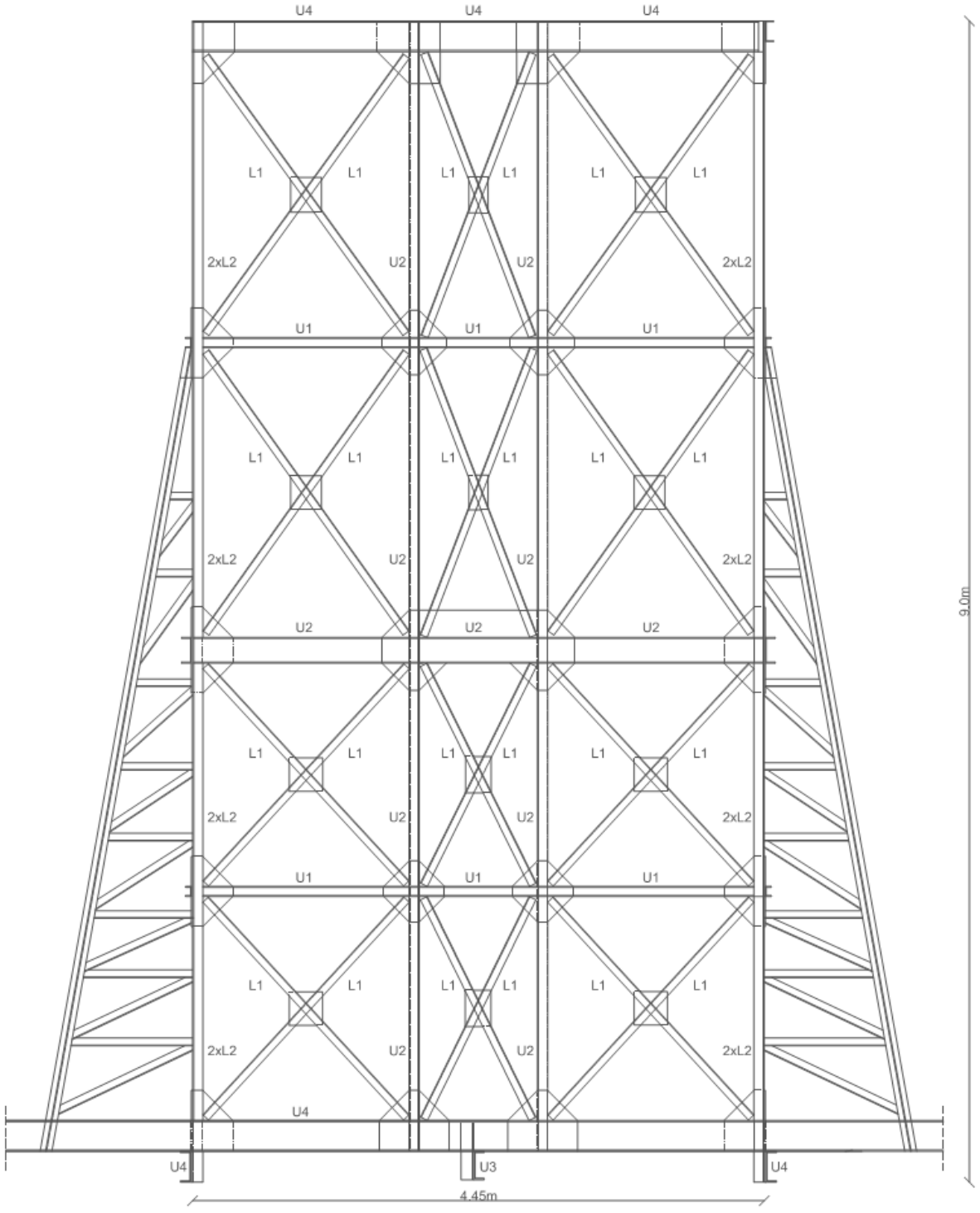

Sub-structure C

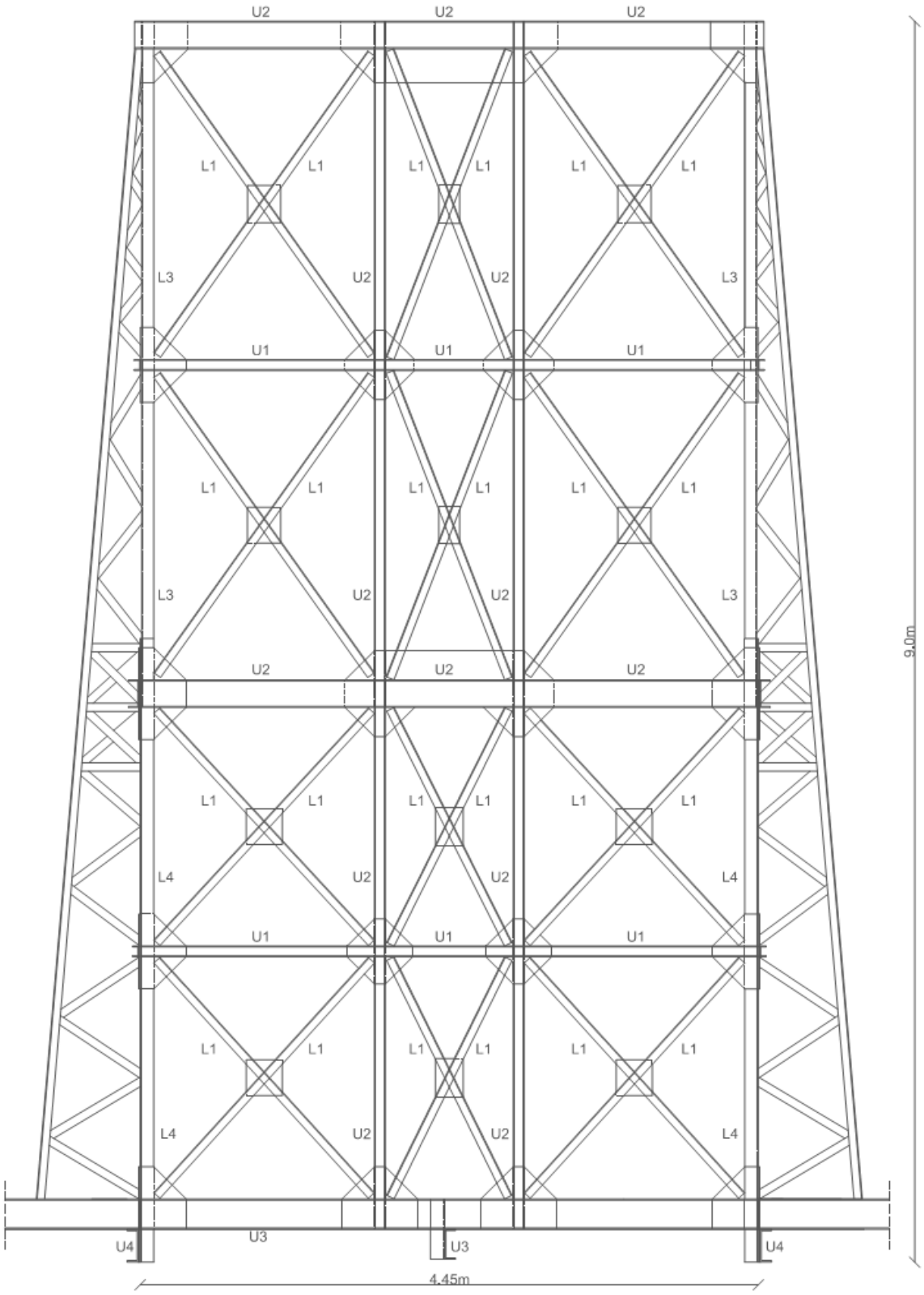

Sub-structure D

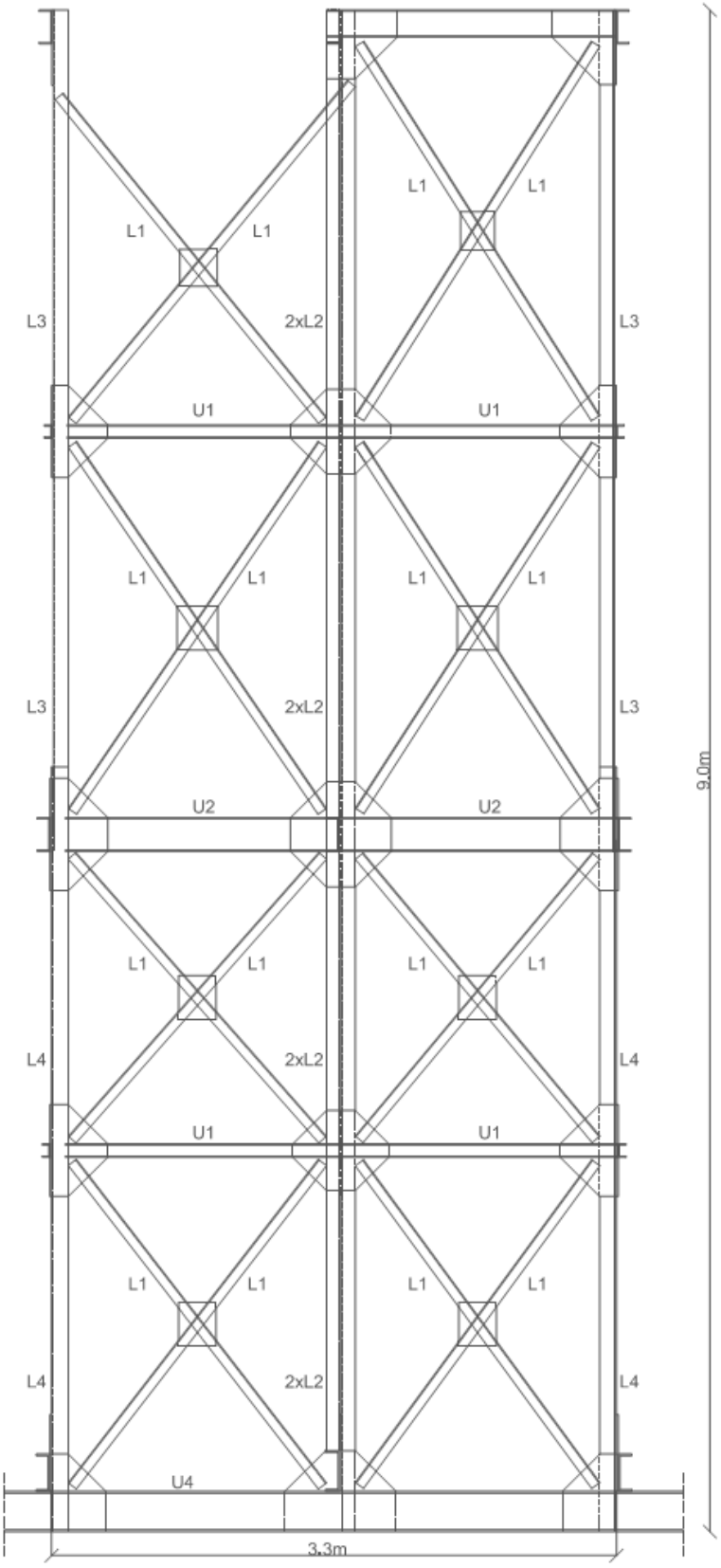

Sub-structure E

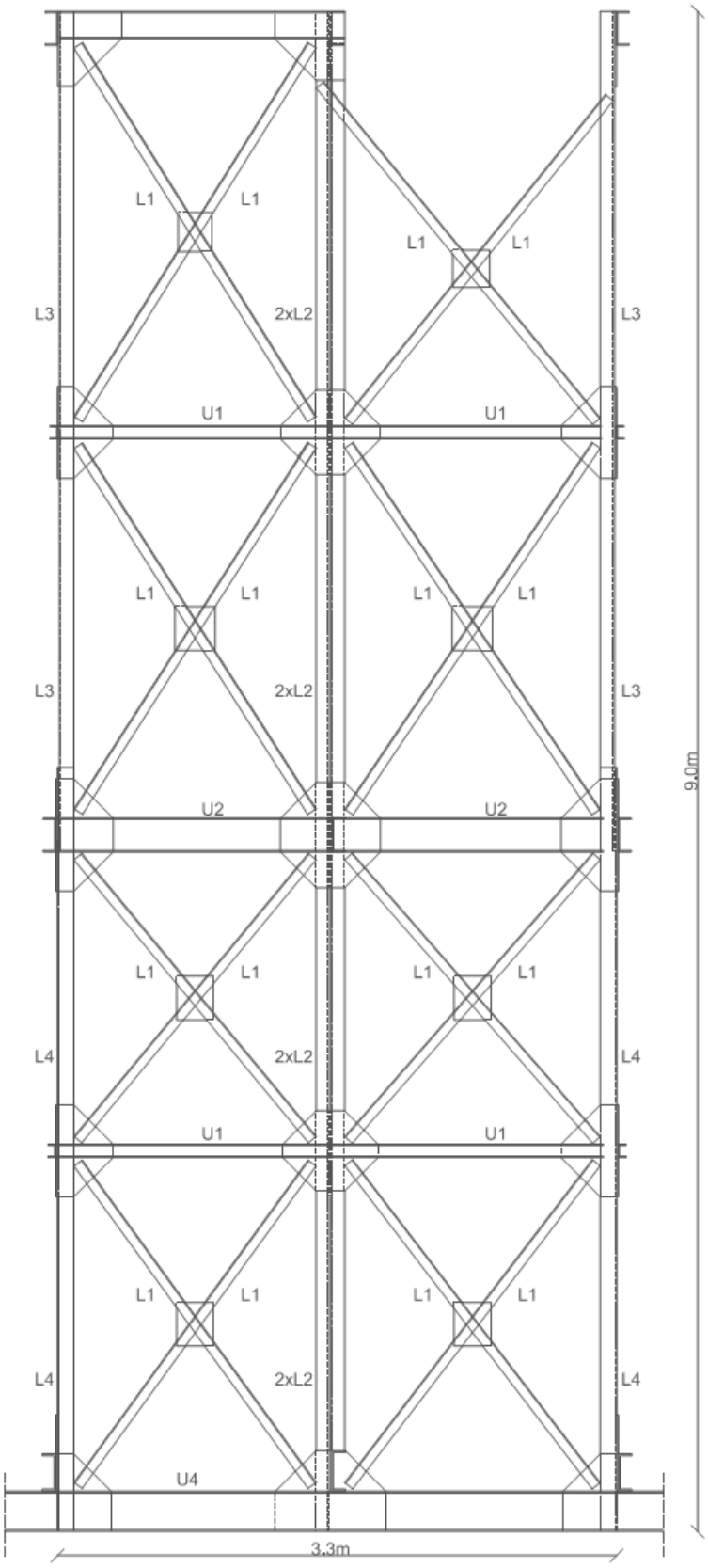

Annex B

In this section relevant plots related to Chapter 6 are presented. In particular, they are shown: time history of frequencies and temperature; correlation between natural frequencies and temperatures; ARX fitting models through the normalized frequency and simulated errors with 95% confidence interval.

Long-term monitoring data - time history of frequencies and temperature

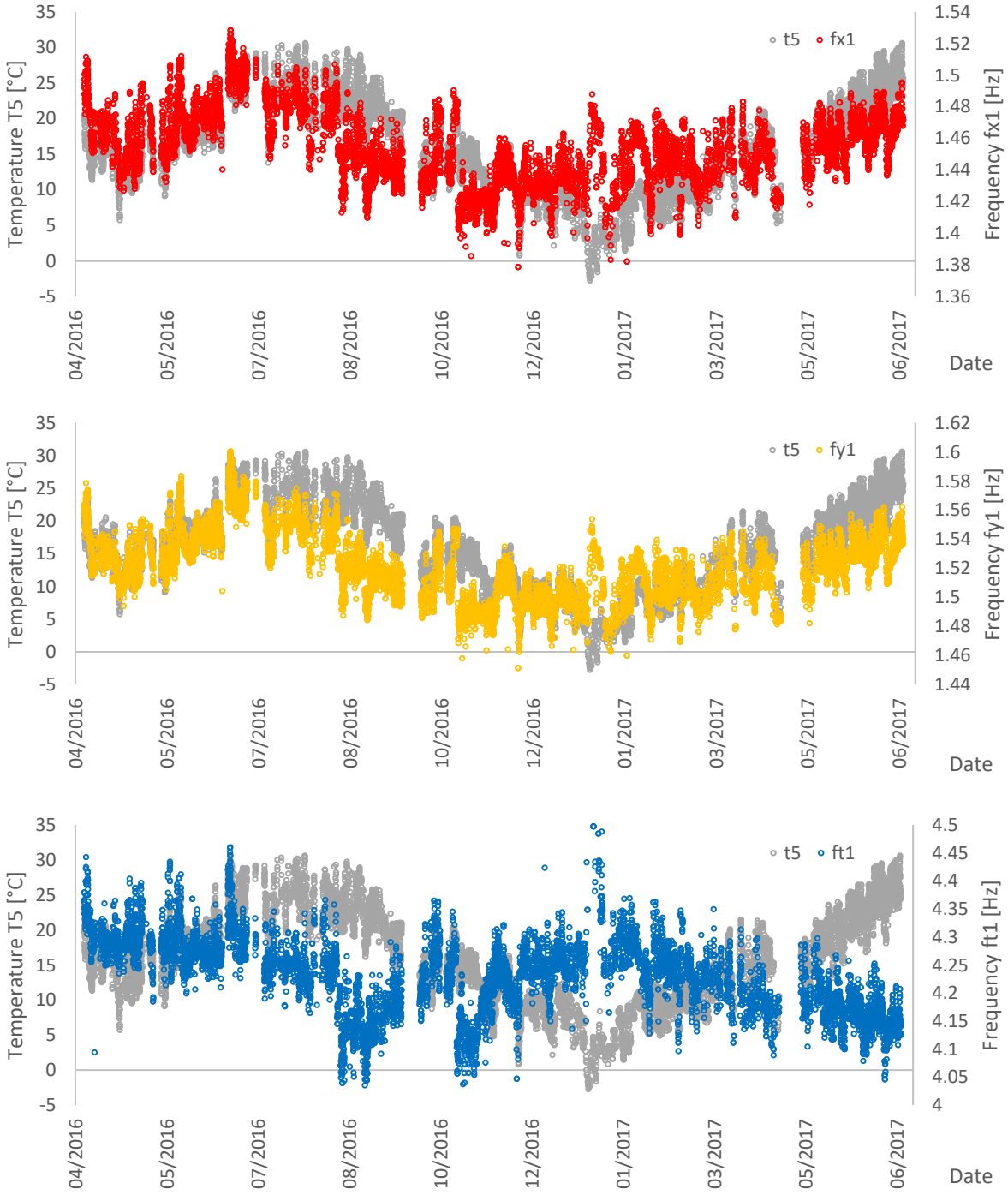

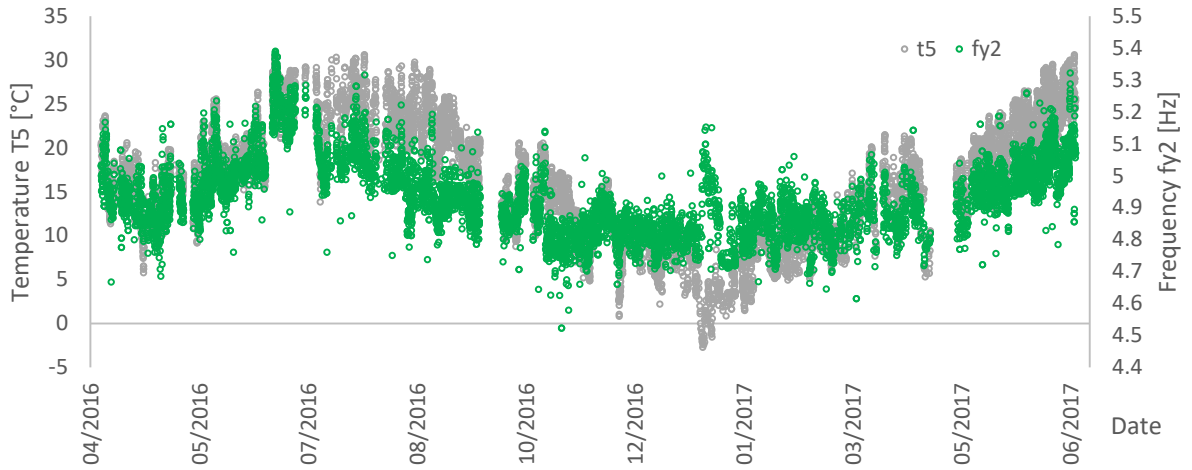
t5
fy2
Temperature T5 [°C]
Frequency fy2 [Hz]
Date
35
30
25
20
15
10
5
0
-5
5.5
5.4
5.3
5.2
5.1
5
4.9
4.8
4.7
4.6
4.5
4.4
04/2016
05/2016
07/2016
08/2016
10/2016
12/2016
01/2017
03/2017
05/2017
06/2017

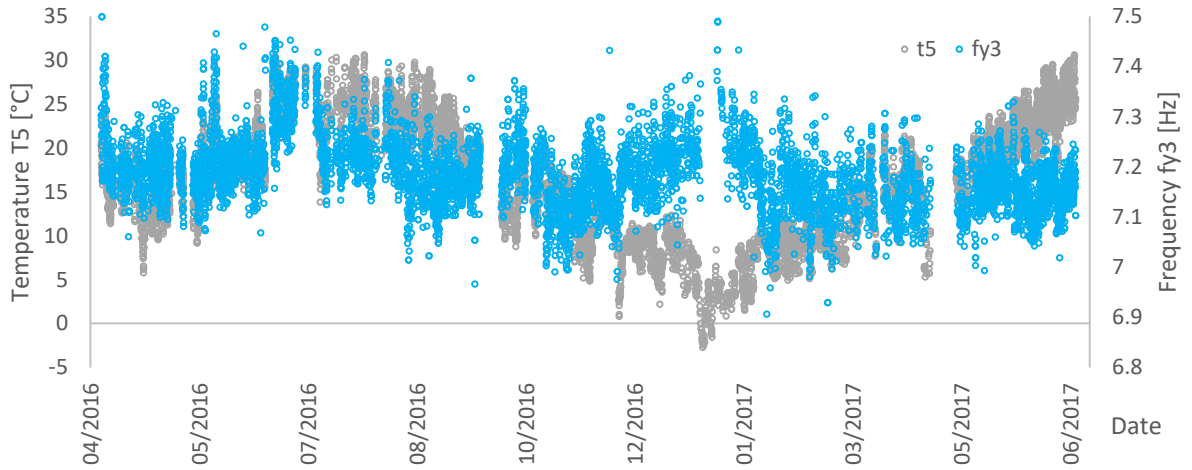
t5
fy3
Temperature T5 [°C]
Frequency fy3 [Hz]
Date
35
30
25
20
15
10
5
0
-5
7.5
7.4
7.3
7.2
7.1
7
6.9
6.8
04/2016
05/2016
07/2016
08/2016
10/2016
12/2016
01/2017
03/2017
05/2017
06/2017

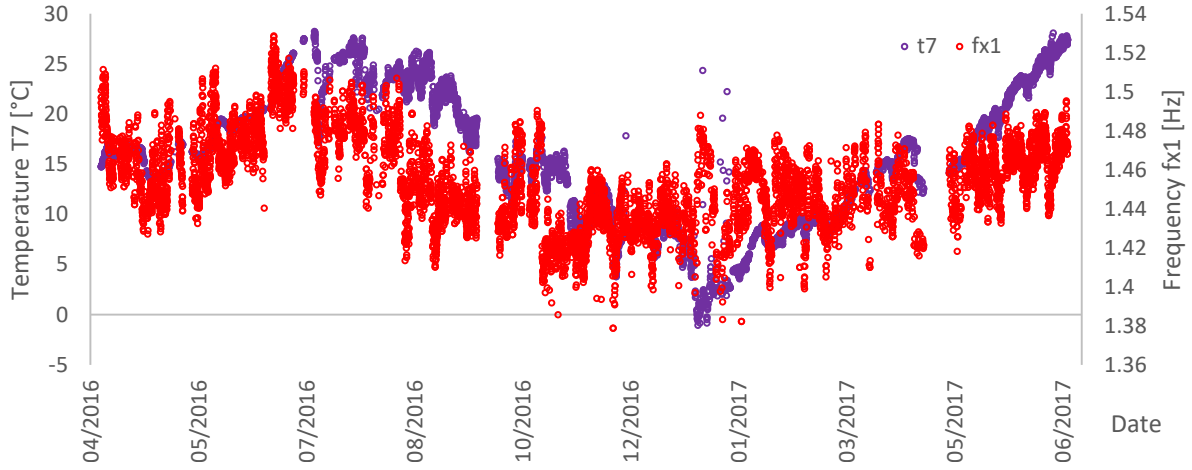
t7
fx1
Temperature T7 [°C]
Frequency fx1 [Hz]
Date
30
25
20
15
10
5
0
-5
1.54
1.52
1.5
1.48
1.46
1.44
1.42
1.4
1.38
1.36
04/2016
05/2016
07/2016
08/2016
10/2016
12/2016
01/2017
03/2017
05/2017
06/2017

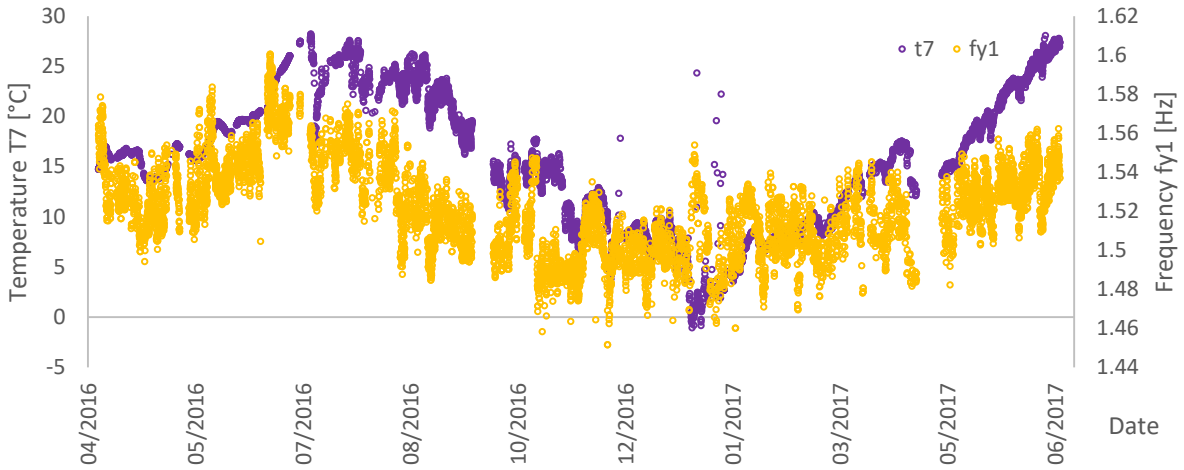
Temperature T7 [°C]
Frequency fy1 [Hz]
t7
fy1
Date
04/2016
05/2016
07/2016
08/2016
10/2016
12/2016
01/2017
03/2017
05/2017
06/2017

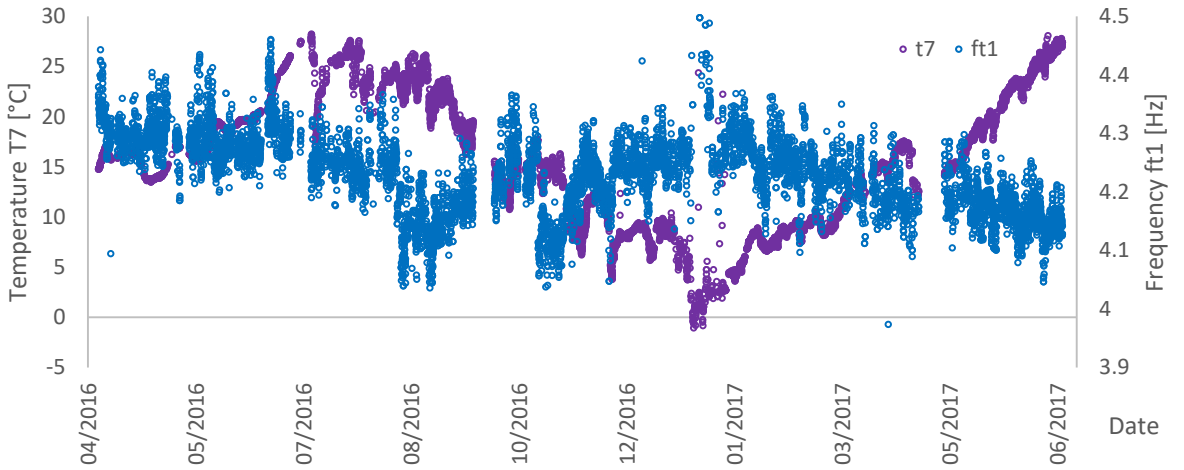
Temperature T7 [°C]
Frequency ft1 [Hz]
t7
ft1
Date
04/2016
05/2016
07/2016
08/2016
10/2016
12/2016
01/2017
03/2017
05/2017
06/2017

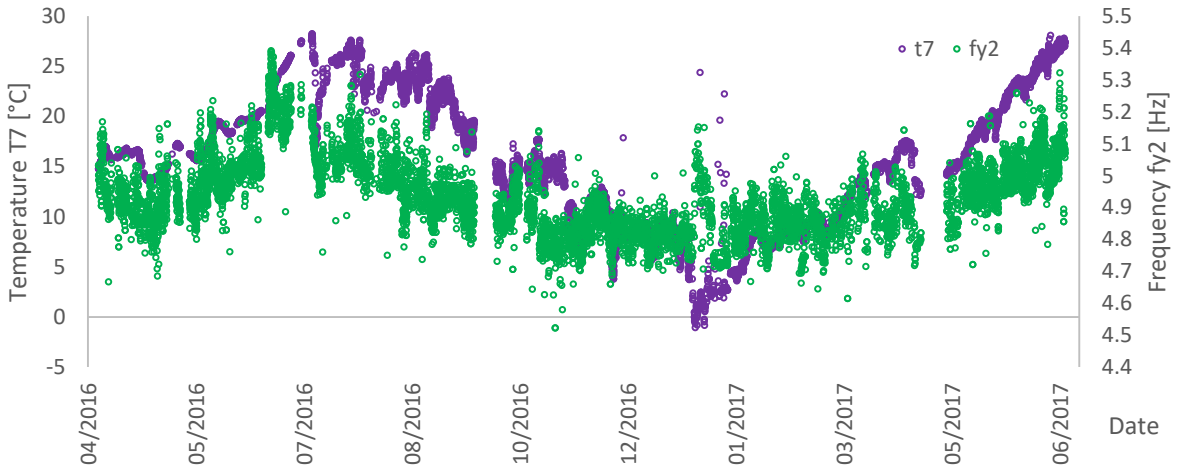
Temperature T7 [°C]
Frequency fy2 [Hz]
t7
fy2
Date
04/2016
05/2016
07/2016
08/2016
10/2016
12/2016
01/2017
03/2017
05/2017
06/2017

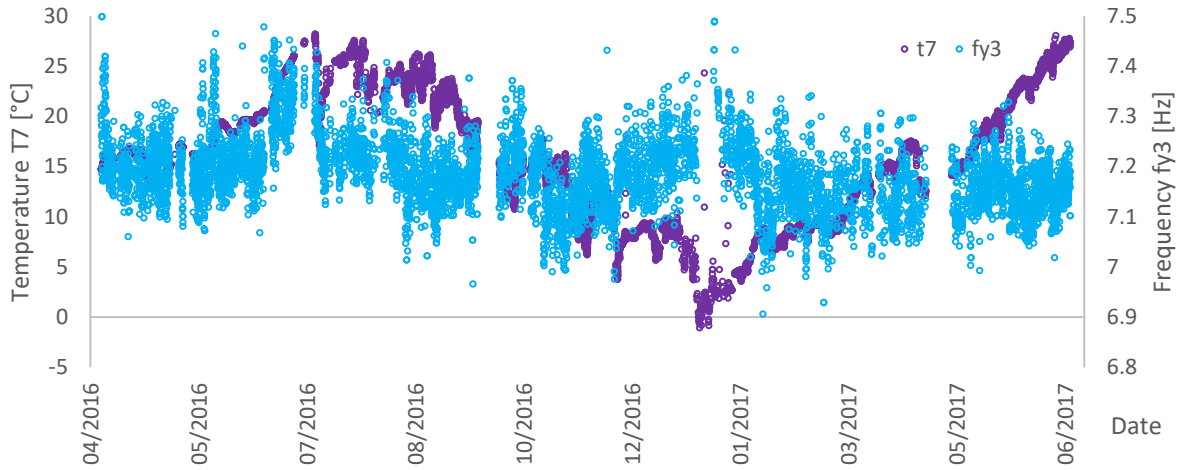

Correlation between natural frequencies and temperatures

Pre-earthquakes conditions

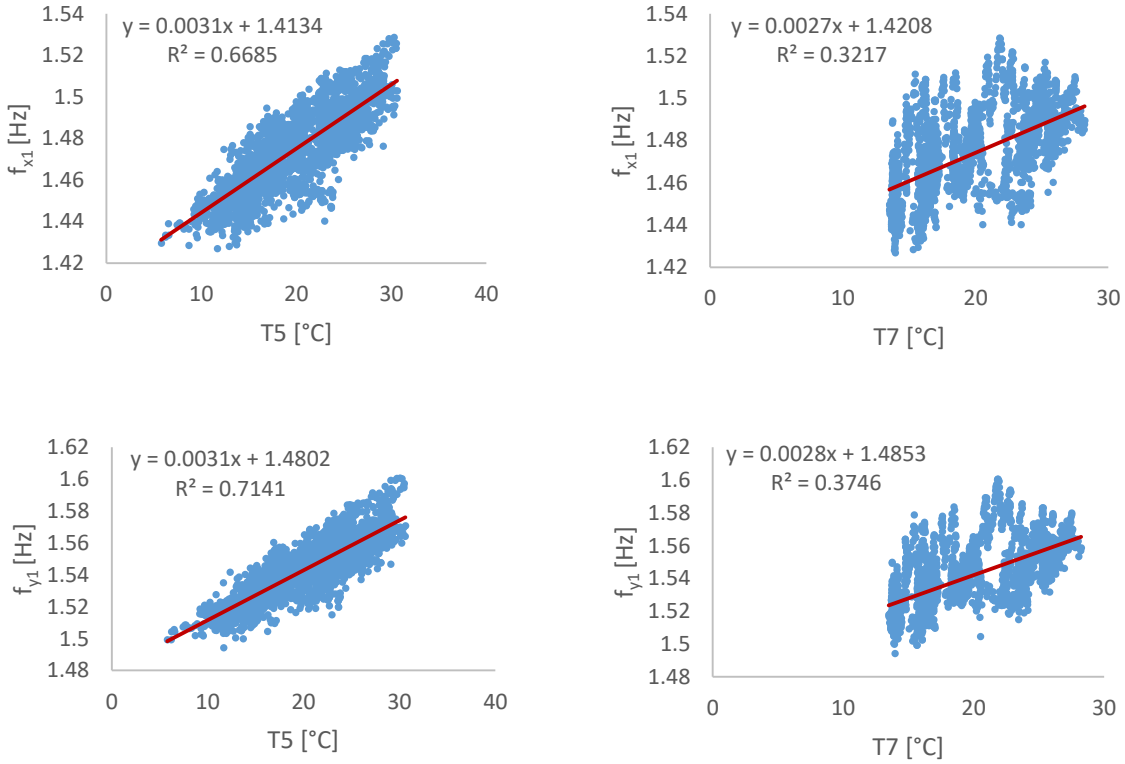

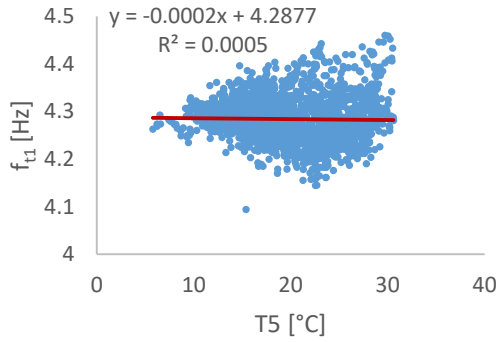

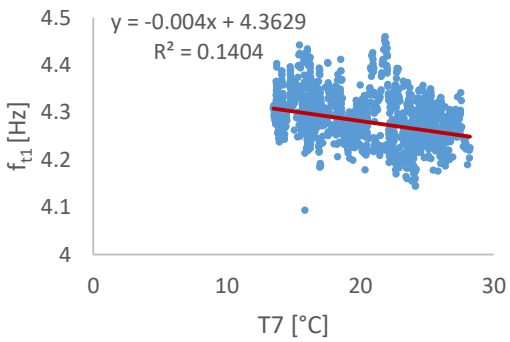

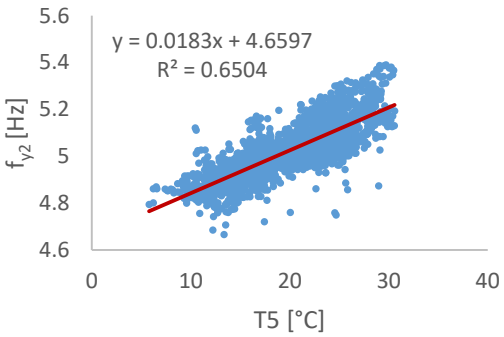

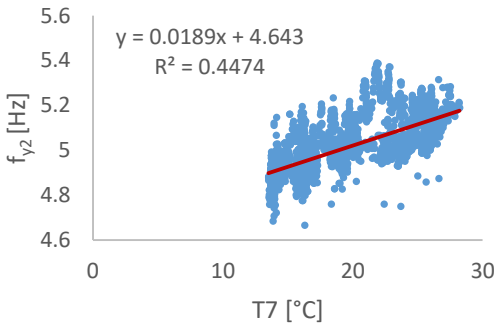

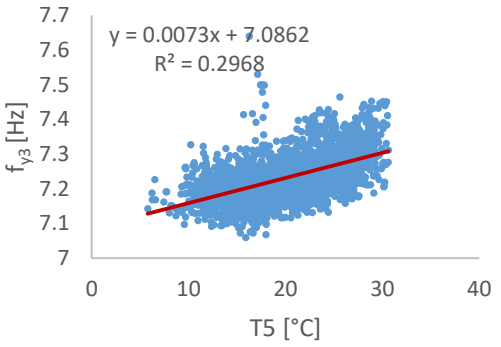

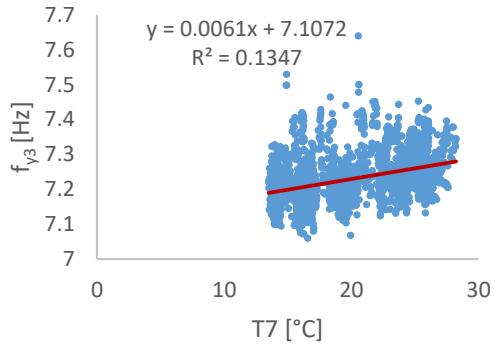

Post-earthquakes conditions

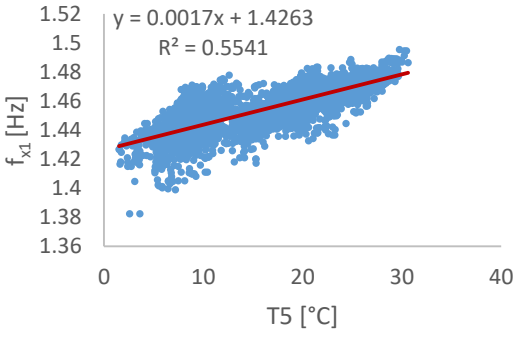

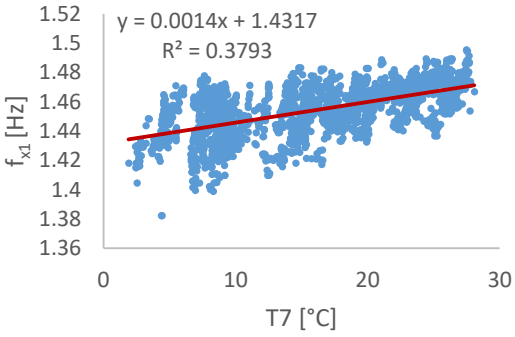

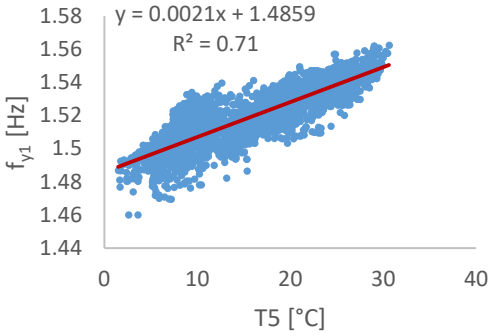
y = 0.0021x + 1.4859
R² = 0.71
f_y1 [Hz]
T5 [°C]

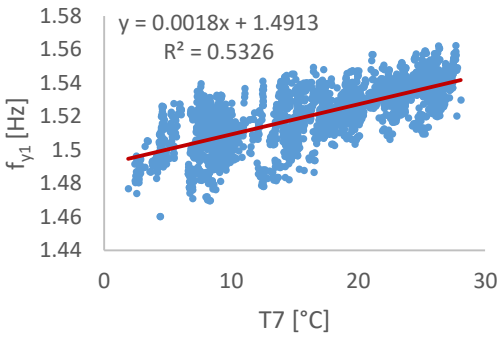
y = 0.0018x + 1.4913
R² = 0.5326
f_y1 [Hz]
T7 [°C]

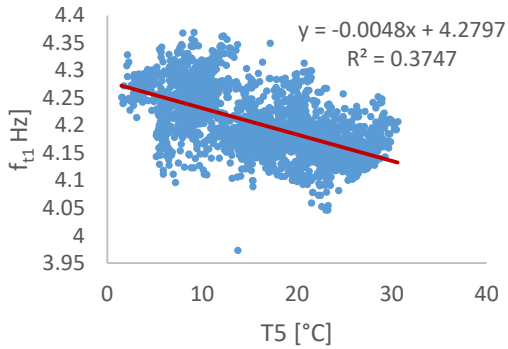
y = -0.0048x + 4.2797
R² = 0.3747
f_t1 Hz]
T5 [°C]

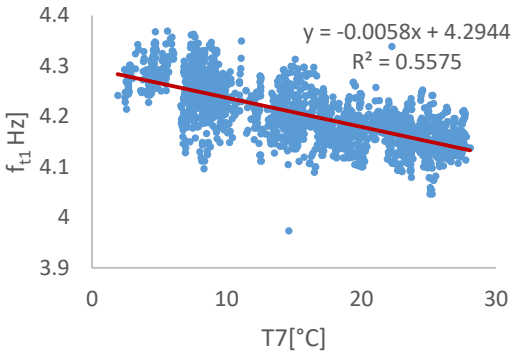
y = -0.0058x + 4.2944
R² = 0.5575
f_t1 Hz]
T7[°C]

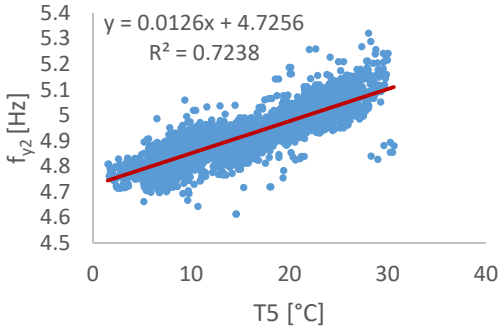
y = 0.0126x + 4.7256
R² = 0.7238
f_y2 [Hz]
T5 [°C]

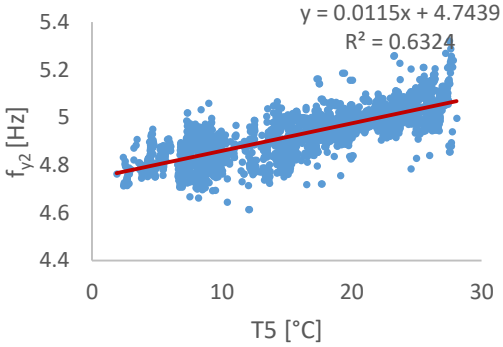
y = 0.0115x + 4.7439
R² = 0.6324
f_y2 [Hz]
T5 [°C]

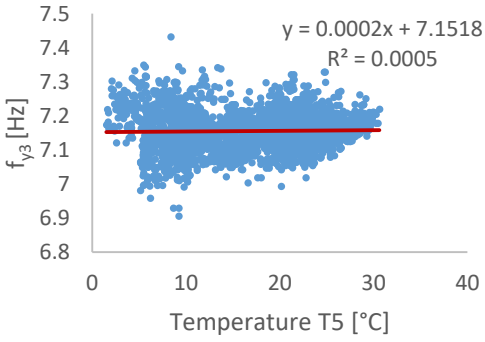
y = 0.0002x + 7.1518
R² = 0.0005
f_y3 [Hz]
Temperature T5 [°C]

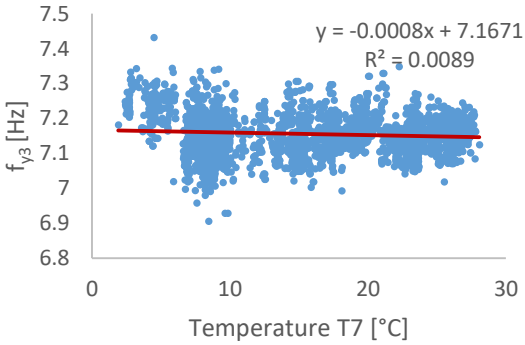
y = -0.0008x + 7.1671
R² = 0.0089
f_y3 [Hz]
Temperature T7 [°C]

ARX fitting models

Mode fx1 – Training period, pre-earthquakes

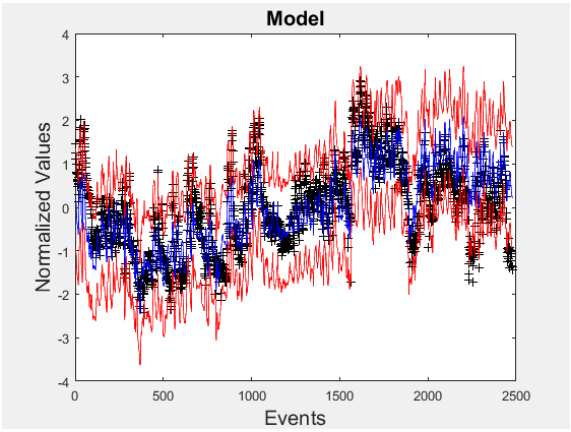

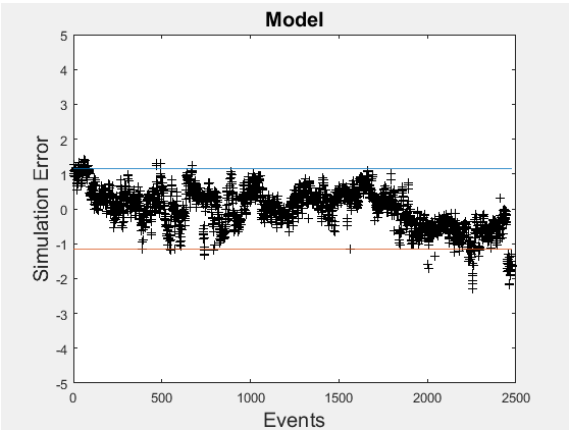

Mode fx1 – Simulation, post-earthquakes

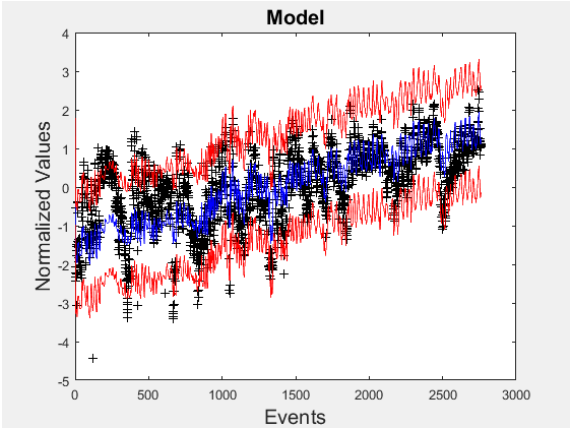

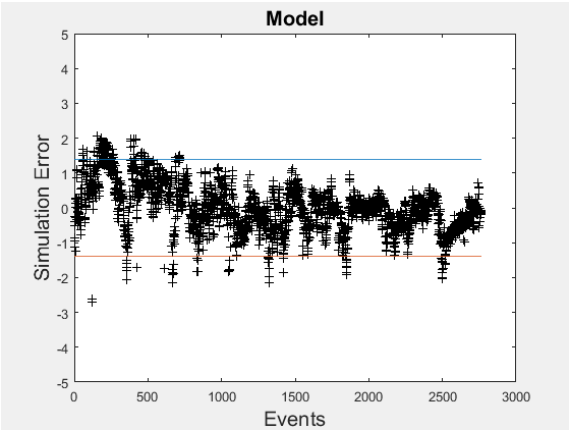

Mode fy1 – Training period, pre-earthquakes

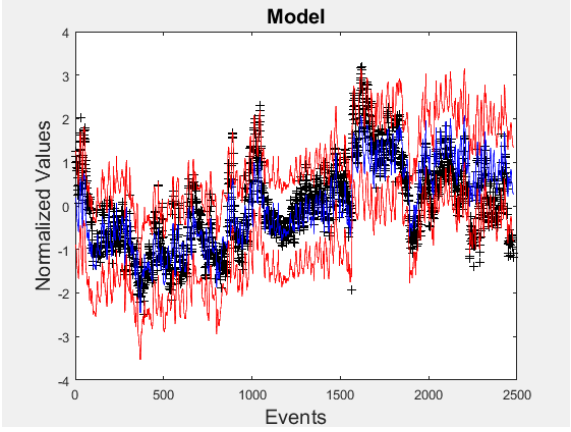

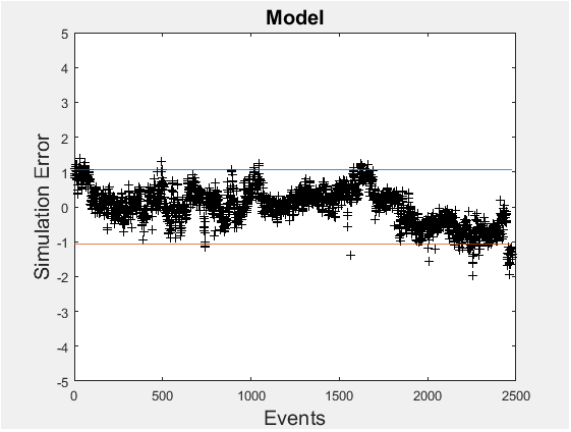

Mode fy1 – Simulation, post-earthquakes

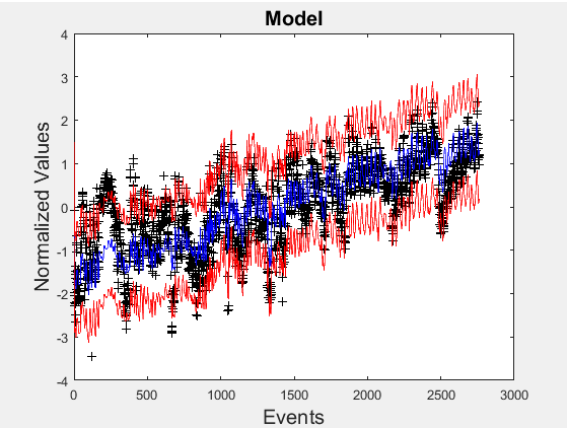

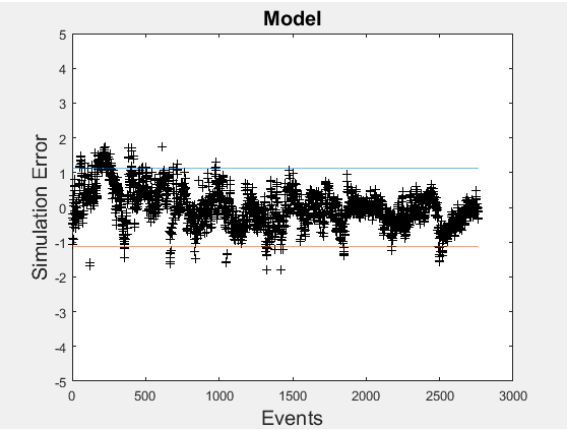

Mode fy2 – Training period, pre-earthquakes

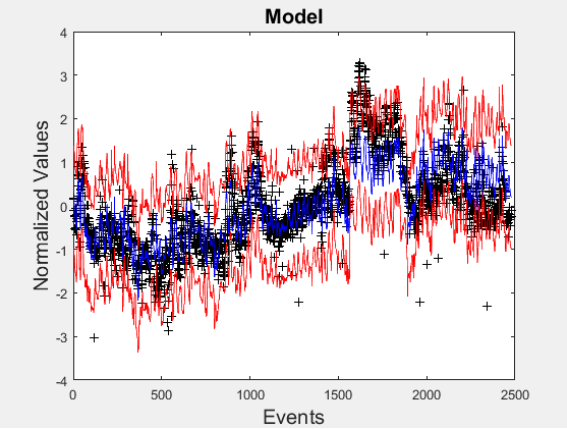

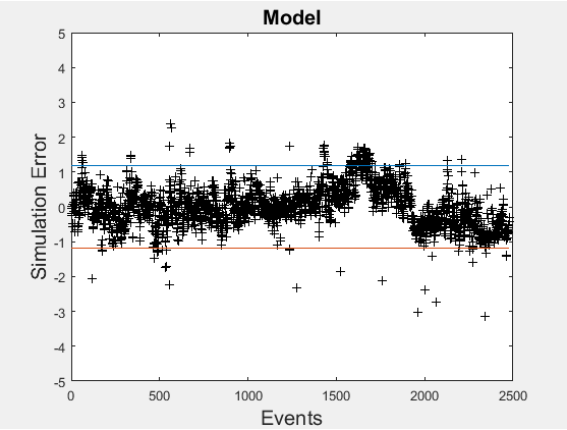

Mode fy2 – Simulation, post-earthquakes